8 8 7 4 *ERID#:* 88749

LOS ALAMOS NATIONAL LABORATORY
ENVIRONMENTAL RESTORATION (RRES-R)
Records Processing Facility
ER Records Index Form

Date Received: 6/8/2005 ***Processor:*** JR ***Page Count:*** 42

Privileged: (Y/N) N ***Record Category:*** P ***Administrative Record: (Y/N)*** Y

FileFolder: N/A

Miscellaneous Comments: N/A

Record Documents:

Start Pg	*Doc Type*	*Doc Date*	*Title*	*Box*	*Package*
1	REPORT	1/1/1985	NATHEMATICAL MODEL OF THE TESUQUE AQUIFER SYSTEM NEAR POJOAQUE, NEW MEXICO. UNITED STATES GEOLOGICAL SURVEY WATER SUPPLY PAPER 2205 N/A N/A N/A		

14260

Mathematical Model of The Tesuque Aquifer System Near Pojoaque, New Mexico

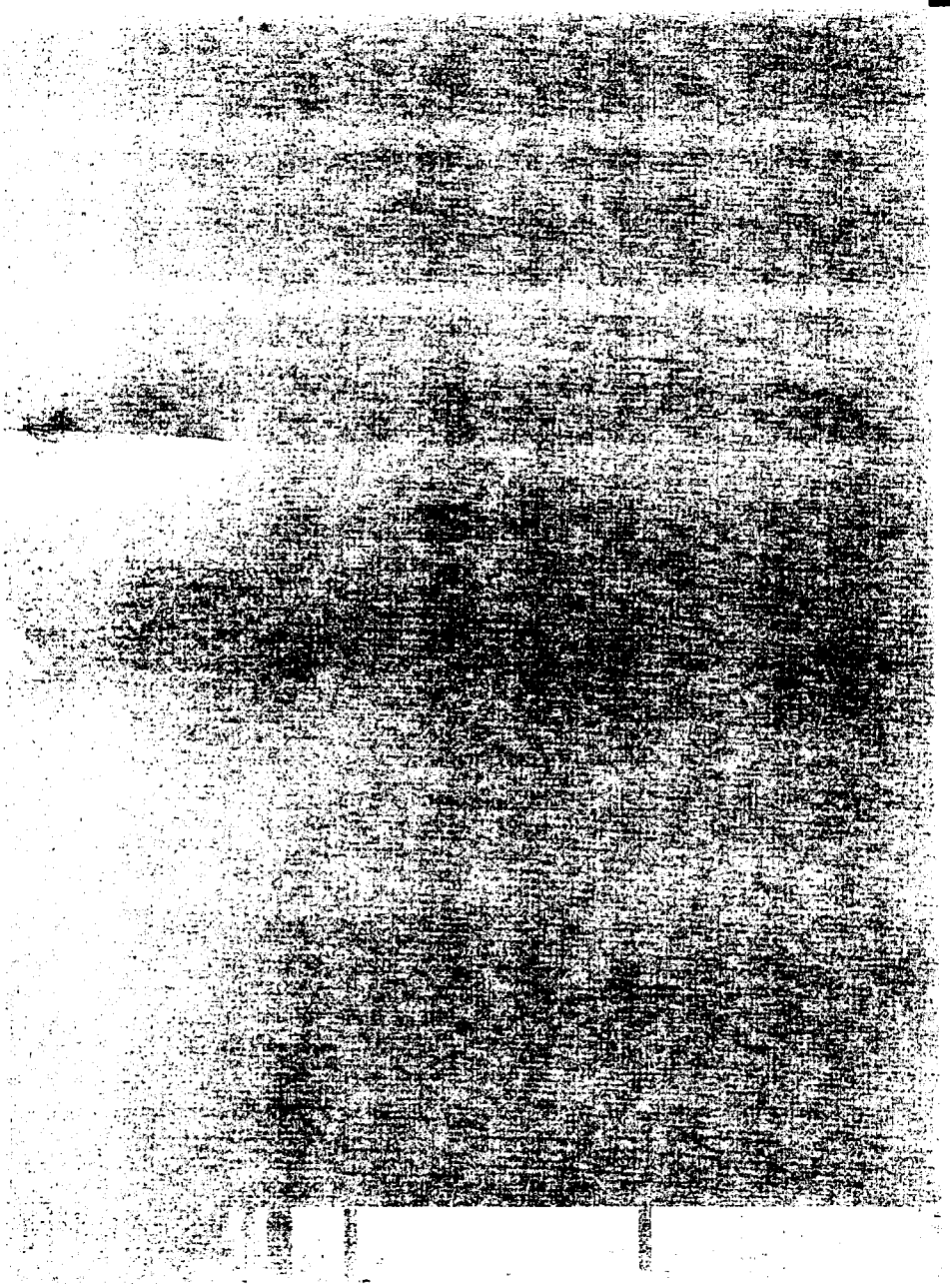

United States Geological Survey Water-Supply Paper 2205

Prepared in cooperation with the U.S. Bureau of Indian Affairs

RECEIVED
JUN 08 2005
By

Mathematical Model of The Tesuque Aquifer System Near Pojoaque, New Mexico

By GLENN A. HEARNE

Prepared in cooperation
with the U.S. Bureau
of Indian Affairs

U.S. GEOLOGICAL SURVEY WATER-SUPPLY PAPER 2205

DEPARTMENT OF THE INTERIOR
DONALD PAUL HODEL, Secretary

U.S. GEOLOGICAL SURVEY
Dallas L. Peck, Director

UNITED STATES GOVERNMENT PRINTING OFFICE: 1985

For sale by the Distribution Branch, U.S. Geological Survey,
604 South Pickett Street, Alexandria, VA 22304

Library of Congress Cataloging-in-Publication Data

Hearne, Glenn A.
Mathematical model of the Tesuque aquifer system near Pojoaque, New Mexico.
(Geological Survey water-supply paper ; 2205)
"January 1981."
Bibliography: p. 73
Supt. of Docs. no. : I 19.2.Aq5/4
1. Aquifers—New Mexico—Pojoaque Valley—Mathematical models. I. United States. Bureau of Indian Affairs. II. Title. III. Series: U.S. Geological Survey water-supply paper ; 2205.
GB1199.3.N6H4 551.49 81-607586

CONTENTS

Abstract 1
Introduction 1
Model description 3
Structure of the prototype 3
Structure represented in the model 4
Aquifer characteristics in the prototype 6
Hydraulic conductivity 8
Anisotropy 8
Specific storage 9
Specific yield 10
Aquifer characteristics represented in the model 10
Boundaries in the prototype 11
Adjacent ground-water systems 11
Rio Grande 11
Santa Cruz River 11
Pojoaque River and tributaries 11
Santa Fe River 12
Storm runoff 12
Native vegetation 12
Channel losses 13
Boundaries represented in the model 13
Adjacent ground-water systems 13
Rio Grande and Santa Cruz River 13
Pojoaque River and tributaries 13
Santa Fe River 17
Storm runoff 18
Native vegetation 18
Channel losses 18
Steady-state condition 18
Hydraulic-head distribution in the prototype 18
Hydraulic-head distribution simulated by the model 19
Flow between ground water and surface water in the prototype 21
Rio Grande 22
Santa Cruz and Santa Fe Rivers 24
Pojoaque River and tributaries 24
Flow between ground water and surface water simulated by the model 25
Rio Grande 25
Santa Cruz and Santa Fe Rivers 25
Pojoaque River and tributaries 26
Changes superimposed on steady-state condition 26
History in the prototype 26
Withdrawals 26
Change in hydraulic head 27
Change in flow between ground water and surface water 27
History represented in the model 28
Withdrawals 28
Change in hydraulic head 28
Change in flow between ground water and surface water 32
Projected withdrawals and diversions in the prototype 32
Projected withdrawals and diversions represented in the model 33

Simulated response to projected withdrawals and diversions 42
Simulated changes in water levels 44
Los Alamos Canyon well field 44
Guaje Canyon well field 45
Pajarito Mesa well field 46
Buckman well field 47
Pojoaque River basin 48
Simulated changes in flow between ground water and surface water 49
Rio Grande, Santa Cruz, and Santa Fe Rivers 49
Pojoaque River and tributaries 50
Simulated sources of water withdrawn from wells 50
Model sensitivity 52
Thickness of the Tesuque Formation 53
Simulated steady-state condition 53
Simulated transient response 53
Hydraulic conductivity 56
Simulated steady-state conditions 56
Simulated transient response 56
Anisotropy ratio 58
Simulated steady-state conditions 58
Simulated transient response 61
Specific storage: simulated transient response 66
Specific yield: simulated transient response 68
Uncertainty in predicted response 70
Summary 71
Selected references 73
Metric conversion factors 75

FIGURES

1. Map showing location of the modeled area 2
2. Generalized east-west geologic section near Pojoaque River basin 5
3-6. Diagrams showing:
3. Dip represented along row 10 of the model 6
4. Saturated thickness of the Tesuque Formation represented in the model 7
5. Boundary conditions represented in the model 14
6. Simplified geometry for an individual cell used to estimate the constant of proportionality (K_R) for hydraulic-head dependent boundaries 16
7-9. Maps showing contours of:
7. Prepumping water surface east of the Rio Grande 19
8. 1968 water surface east of the Rio Grande 20
9. Prepumping water surface west of the Rio Grande 21
10. Graph showing comparison between measured or reported water levels for selected wells and springs and water levels simulated by the model 22
11. Map showing contours of steady-state water surface simulated by the model 23
12-20. Graphs showing comparison between decline in hydraulic head simulated at:
12. Row 13, column 5, layer 19 of the mathematical model and declines in nonpumping water levels measured in wells LA-1, LA-1B, LA-2, and LA-3 29
13. Row 15, column 4, layer 20 of the mathematical model and decline in nonpumping water level measured in well LA-4 29

14. Row 14, column 4, layer 20 of the mathematical model and decline in nonpumping water level measured in well LA-5 **30**
15. Row 14, column 5, layer 19 of the mathematical model and decline in nonpumping water level measured in well LA-6 **30**
16. Row 13, column 4, layer 20 of the mathematical model and declines in nonpumping water levels measured in wells G-1 and G-1A **30**
17. Row 13, column 3, layer 21 of the mathematical model and declines in nonpumping water levels measured in wells G-2, G-3, G-4, G-5, and G-6 **31**
18. Row 16, column 3, layer 21 of the mathematical model and declines in nonpumping water levels measured in wells PM-1 and PM-3 **31**
19. Row 18, column 3, layer 21 of the mathematical model and decline in nonpumping water level measured in well PM-2 **31**
20. Row 17, column 7, layer 17 of the mathematical model and decline in water level measured in well B-7 **31**

21. Diagram showing representation of withdrawals and return flow in a typical cluster of cells representing the Tesuque aquifer system **33**

22-25. Maps showing:
22. Location of wells and canals of the irrigation development plan **34**
23. Contours of simulated water surface in 2030 assuming withdrawals as shown in table 12 **45**
24. Lines of equal simulated decline in water surface from 1980 through 2030 assuming withdrawals as shown in table 12 **46**
25. Lines of equal simulated decline in hydraulic head in the uppermost confined cells from 1980 through 2030 assuming withdrawals as shown in table 12 **47**

26-33. Graphs showing simulated decline in hydraulic head near:
26. Los Alamos Canyon well field (row 13, column 5, layer 19) **47**
27. Guaje Canyon well field (row 13, column 3, layer 21) **48**
28. Pajarito Mesa well field (row 16, column 3, layer 21) **48**
29. Buckman well field (row 17, column 7, layer 17) **48**
30. San Ildefonso Pueblo (row 11, column 7, layer 17) **48**
31. Pojoaque Pueblo (row 9, column 12, layer 12) **49**
32. Nambe Pueblo (row 8, column 16, layer 8) **49**
33. Tesuque Pueblo (row 14, column 18, layer 6) **49**

34. Graph showing simulated source of water withdrawn from Tesuque aquifer system without irrigation development **51**
35. Graph showing simulated source of water withdrawn from Tesuque aquifer system with irrigation development **51**
36. Diagram showing alternative saturated thickness used to test sensitivity of the model to represented thickness **54**
37. Graph showing comparision between measured or reported water levels for selected wells and springs and water levels simulated by assuming a greater saturated thickness **55**
38. Graph showing effect of variations in represented saturated thickness on steady-state flow rates **56**

39-43. Graphs showing effect of variations in represented saturated thickness on decline in hydraulic head near:
39. Buckman well field (row 17, column 7, layer 17) **56**
40. San Ildefonso Pueblo (row 11, column 7, layer 17) **57**
41. Pojoaque Pueblo (row 9, column 12, layer 12) **57**
42. Nambe Pueblo (row 8, column 16, layer 8) **57**
43. Tesuque Pueblo (row 14, column 18, layer 6) **57**

44. Graph showing effect of variations in represented saturated thickness on the source of water withdrawn from wells **58**
45. Graph showing effect of variations in hydraulic conductivity on steady-state flow rates **59**
46-53. Graphs showing effect of variations in hydraulic conductivity on decline in hydraulic head near:
46. Los Alamos Canyon well field (row 13, column 5, layer 19) **59**
47. Guaje Canyon well field (row 13, column 3, layer 21) **59**
48. Pajarito Mesa well field (row 16, column 3, layer 21) **59**
49. Buckman well field (row 17, column 7, layer 17) **59**
50. San Ildefenso Pueblo (row 11, column 7, layer 17) **60**
51. Pojoaque Pueblo (row 9, column 12, layer 12) **60**
52. Nambe Pueblo (row 8, column 16, layer 8) **60**
53. Tesuque Pueblo (row 14, column 18, layer 6) **60**
54. Graph showing effect of variations in hydraulic conductivity on the source of water withdrawn from wells **61**
55. Graph showing comparison between measured or reported water levels for selected wells and springs and water levels simulated by assuming a smaller anisotropy ratio **62**
56. Graph showing comparison between measured or reported water levels for selected wells and springs and water levels simulated by assuming a larger anisotropy ratio **63**
57. Graph showing effect of variations in anisotrophy ratio on steady-state flow rates **64**
58-65. Graphs showing effect of variations in anisotropy ratio on decline in hydraulic head near:
58. Los Alamos Canyon well field (row 13, column 5, layer 19) **64**
59. Guaje Canyon well field (row 13, column 3, layer 21) **64**
60. Pajarito Mesa well field (row 16, column 3, layer 21) **64**
61. Buckman well field (row 17, column 7, layer 17) **65**
62. San Ildefonso Pueblo (row 11, column 7, layer 17) **65**
63. Pojoaque Pueblo (row 9, column 12, layer 12) **65**
64. Nambe Pueblo (row 8, column 16, layer 8) **65**
65. Tesuque Pueblo (row 14, column 18, layer 6) **66**
66. Graph showing effect of variations in anisotropy ratio on the source of water withdrawn from wells **66**
67-71. Graphs showing effect of variations in specific storage on decline in hydraulic head near:
67. Buckman well field (row 17, column 7, layer 17) **67**
68. San Ildefonso Pueblo (row 11, column 7, layer 17) **67**
69. Pojoaque Pueblo (row 9, column 12, layer 12) **67**
70. Nambe Pueblo (row 8, column 16, layer 8) **67**
71. Tesuque Pueblo (row 14, column 18, layer 6) **68**
72. Graph showing effect of variations in specific storage on the source of water withdrawn from wells **68**
73-80. Graphs showing effect of variations in specific yield on decline in hydraulic head near:
73. Los Alamos Canyon well field (row 13, column 5, layer 19) **69**
74. Guaje Canyon well field (row 13, column 3, layer 21) **69**
75. Pajarito Mesa well field (row 16, column 3, layer 21) **69**
76. Buckman well field (row 17, column 7, layer 17) **69**
77. San Ildefonso Pueblo (row 11, column 7, layer 17) **69**
78. Pojoaque Pueblo (row 9, column 12, layer 12) **70**
79. Nambe Pueblo (row 8, column 16, layer 8) **70**
80. Tesuque Pueblo (row 14, column 18, layer 6) **70**

81. Graph showing effect of variations in specific yield on the source of water withdrawn from wells 71

TABLES

1. Most likely value and plausible range of aquifer characteristics 11
2. Specified hydraulic-head boundaries represented in the model 15
3. Hydraulic-head dependent boundaries represented in the model 16
4. Specified-flow boundaries represented in the model 17
5. Vertical hydraulic gradients 23
6. Water balance for the Pojoaque River and tributaries 24
7. Simulated steady-state flow rates at specified hydraulic-head boundaries 25
8. Simulated steady-state flow rates at hydraulic-head dependent boundaries 25
9. Water balance for the Pojoaque River and tributaries using simulated flows from the digital model 26
10. History of withdrawals from the Los Alamos Canyon, Guaje Canyon, Pajarito Mesa, and Buckman well fields 27
11. Measured depths to water in wells of the Los Alamos Canyon, Guaje Canyon, Pajarito Mesa, and Buckman well fields 28
12. Irrigation development plan as represented in the model 36
13. Projected water balances for the Pojoaque River and tributaries using the simulated flows from the digital model 50
14. Effect of represented saturated thickness on variations in vertical hydraulic gradients 53
15. Effect of variations in represented anisotropy ratio on vertical hydraulic gradients 58
16. Predicted maximum decline in hydraulic head (in feet) in 2030 after 50 years of withdrawals for irrigation development 71
17. Predicted source (in percent) of water withdrawals from wells in 2030 after 50 years of withdrawals for irrigation development 72

Mathematical Model of the Tesuque Aquifer System Near Pojoaque, New Mexico

By Glenn A. Hearne

Abstract

A three-dimensional digital model of ground-water flow was constructed to represent the dipping anisotropic beds of the Tesuque aquifer system underlying the Pojoaque River basin and vicinity, New Mexico. Simulations of steady-state conditions and historical ground-water withdrawals were consistent with observed data. The model was used to simulate the response of the aquifer system to an irrigation-development plan in the Pojoaque River basin. Storage is the main source of water; 34.05 cubic feet per second (86 percent of the withdrawal rate) was simulated to be withdrawn from storage after 50 years of withdrawals for irrigation development. The maximum simulated water-level decline was 334 feet, and the net simulated streamflow capture from the Rio Grande and the Santa Cruz, Pojoaque, and Santa Fe Rivers was 5.63 cubic feet per second (14 percent of the withdrawal rate). The sensitivity of the model was tested by varying aquifer characteristics to the limits of the plausible range. Change in hydraulic head in the Pojoaque River basin is most sensitive to hydraulic conductivity. In all simulations, after 50 years of withdrawals, the maximum simulated decline in hydraulic head ranged between 210 and 474 feet, storage in the aquifer system was the source of 80 to 90 percent of the water withdrawn from wells, and streamflow capture from the Rio Grande and its tributaries plus irrigation diversions from the tributaries of the Pojoaque River simulated a decrease in the flow of the Rio Grande of between 17.13 and 21.11 cubic feet per second.

INTRODUCTION

The U.S. Bureau of Indian Affairs has prepared a plan for an irrigation development within the Pojoaque River basin (fig. 1). The U.S. Geological Survey was requested to evaluate the effect of ground-water withdrawals on ground-water levels and streamflow.

The aquifer system from which water is to be withdrawn consists of interbedded layers of varied permeability, which dip from the horizontal. Flow through the aquifer system is such that the hydraulic heads are higher in the deeper units. The aquifer system exchanges water with streams whose average flows range from much less (0.54 cubic foot per second) to much more (1,300 cubic feet per second) than the projected withdrawals of about 40 cubic feet per second.

The effects of the proposed ground-water withdrawals were evaluated using a three-dimensional digital model of ground-water flow. The model met the following design criteria:

1. It must be in three dimensions to represent the increasing hydraulic head with depth.
2. To simplify mathematical description, its axes must be alined with the dip of the beds.
3. To represent the volume of interest in layers inclined to the horizontal, it must be able to simulate several layers economically.
4. In each layer both confined (artesian) and unconfined (water-table) conditions must be represented.
5. The model must be able to represent streams in which flow is small relative to applied stress.

The model was constructed using the computer program documented by Posson and others (1980). The total simulation period was divided into three stages: the first simulated a steady-state condition, the second simulated the response to historical withdrawals, and the third simulated the response to projected future withdrawals.

Most of the data contained in this report have been collected by others and reported elsewhere. Data contained herein that are not available in previously published reports are the data collected since 1975 at sites at the Pueblo Grants of San Ildefonso, Pojoaque, Nambe, and Tesuque. At each of these Pueblo Grants, a site was selected for evaluating the characteristics of the aquifer. Several wells were completed at each site. The wells were logged and

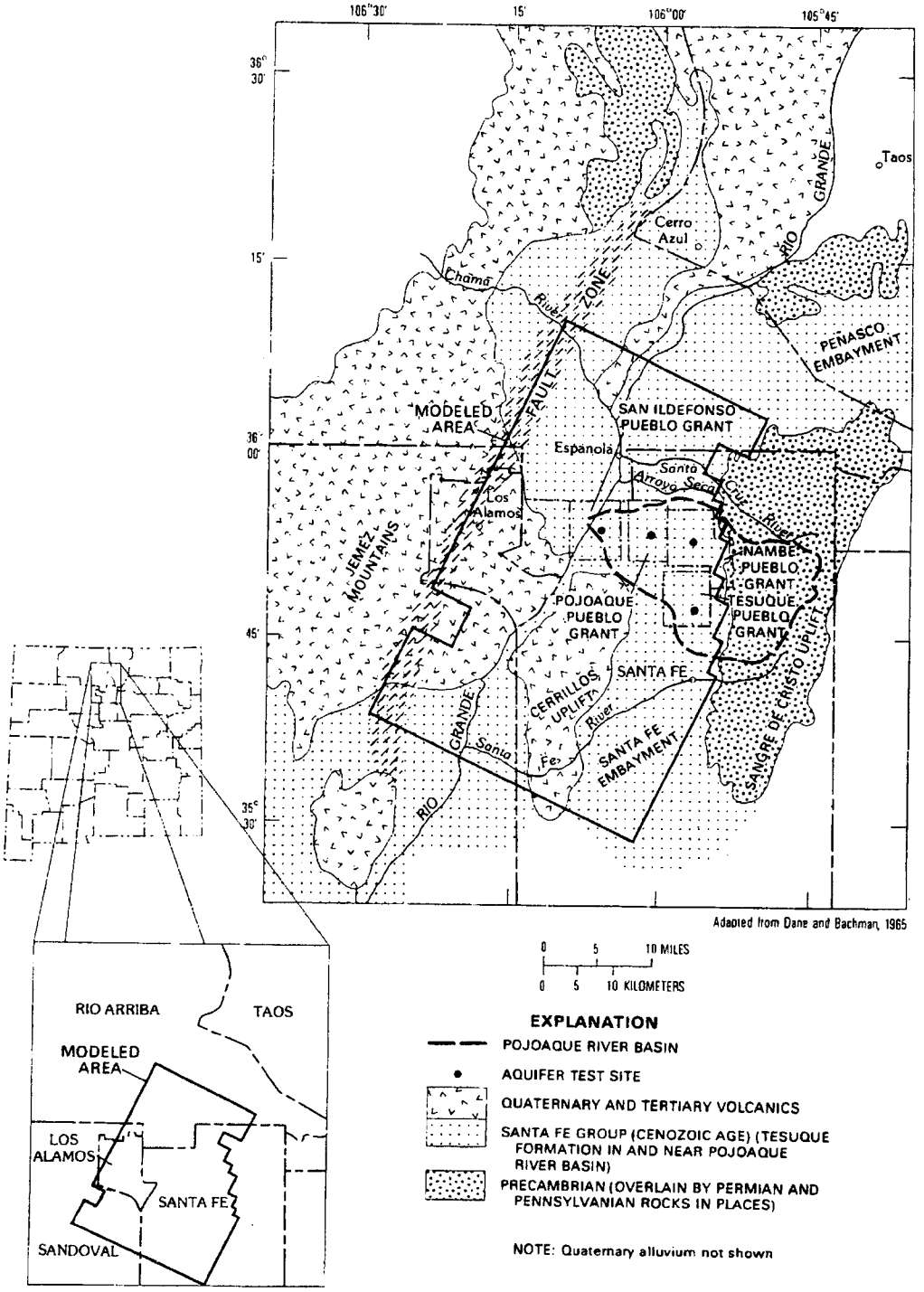

Figure 1. Location of the modeled area.

their water samples analyzed by the U.S. Geological Survey. The aquifer test at the Tesuque Pueblo Grant was conducted by the U.S. Geological Survey and was analyzed and reported by Hearne (1980). Core samples of the Tesuque Formation were collected at the Tesuque Pueblo Grant and analyzed by the U.S. Geological Survey. Tests at the San Ildefonso, Pojoaque, and Nambe Pueblo Grants were conducted by W. S. Gookin and Associates of Phoenix, Ariz. The tests then were analyzed (Gookin and Assoc., 1980, report in preparation for the U.S. Office of Water Research and Technology) and by Peter Balleau (U.S. Bureau of Indian Affairs, written commun., 1978).

The study of the irrigation development and its impact on the natural environment was guided by a technical committee composed of representatives of the U.S. Bureau of Indian Affairs, the U.S. Geological Survey, the U.S. Department of Justice, the Solicitor's Office of the U.S. Department of the Interior, the Northern Pueblo Tributary Water Rights Association, attorneys representing the association, consultants retained by the U.S. Bureau of Indian Affairs, and consultants retained by the association. The author is grateful to this group for providing guidelines for the direction of the study and a forum for discussing progress as the study evolved.

In addition, the author gratefully acknowledges the assistance of several individuals. George Pinder (School of Engineering/Applied Science, Princeton University), Edwin P. Weeks (U.S. Geological Survey), and Peter Balleau (U.S. Bureau of Indian Affairs) provided valuable technical advice. W. S. Gookin and Associates provided data from tests of aquifer characteristics. The author also thanks the Public Service Company of New Mexico for providing pumpage data and depth-to-water measurements for the Buckman well field.

MODEL DESCRIPTION

A model is a description or analogy that can be useful in visualizing something that cannot be directly observed. The system described by the model is called the prototype. A digital ground-water model is a mathematical description of a geohydrologic system. Although a digital model can assist in analyzing a system and can make predictions for use in management decisions, the user must realize that the model is only an approximate representation of the prototype system. The validity of the predictions made by the model depend on the closeness of this approximation. The state of the art of digital modeling does not permit a statement on the confidence limits bounding the projections made by the model. This still needs to be done subjectively. The model results are valid to the extent that the digital model resembles the Tesuque aquifer system in the Espanola Basin, the aquifer characteristics have the properties assumed, and the proposed stresses are of the same type and magnitude as the historical stresses. The confidence in the predicted response to these simulated withdrawals needs to be based on the subjective appraisal of the analogy between the Tesuque aquifer system and the model. Although the historical withdrawals used in this report are from outside the Pojoaque River basin, the model should not be used to simulate the response to stress outside of that basin, as the simulated response to such a stress would probably resemble the actual response only in very general terms.

The description of the prototype is simple enough to allow a mathematical simulation. The mathematical description, or digital model, is used to simulate both the steady-state condition and the responses to historical and projected future withdrawals. The steady-state simulation is compared with historical data to improve the understanding of the geohydrologic system and to motivate changes in the assumptions incorporated into the mathematical description. The comparison of the simulated response to historical withdrawals with the actual response provides a subjective measure of the model's ability to simulate the response of the geohydrologic system. The terms "calibration" and "verification" have been avoided because of their misleading connotations of control, accuracy, and certainty.

This section of the report describes the analogy between the prototype and the model. The description is divided into three subsections: structure, aquifer characteristics, and boundaries. In each instance a description of the prototype is followed by a description of the analogy used in the digital model.

Structure of the Prototype

The hydraulic unit of interest is the Tesuque aquifer system, which would be the source for ground water in the irrigation development plan presented by the U.S. Bureau of Indian Affairs. The Tesuque Formation (Santa Fe Group), of Miocene age, underlies the central part of Espanola Basin (Kelley, 1978), including most of the Pojoaque River basin (fig. 1). The Espanola Basin is one of several interconnected basins that form the Rio Grande depression. The eastern boundary of the basin is the Sangre de Cristo uplift. The western boundary is a complicated fault system, much of which has been covered by volcanic rocks of the Jemez Mountains. The basin is separated from the San Luis Basin to the north and from Albuquerque Basin to the south by constrictions in the bedrock.

Within these boundaries the Espanola Basin is a broad depression whose axis may coincide roughly with the Rio Grande (Kelley, 1978). The principal aquifer underlying the Pojoaque River basin and vicinity is the Tesuque Formation, which is composed of interbedded layers of gravel, sand, silt, and clay with some intercalated volcanic

ash beds. The degree of both sorting and cementation is variable, but the beds are typically poorly sorted and poorly cemented. Two important features of the Tesuque Formation are the dip of the beds and the lack of continuity of the individual beds.

West of the Rio Grande, the Tesuque Formation intertongues with other formations including the Puye Formation (Santa Fe Group) and the Tschicoma Formation, both of Pliocene age (Purtymun and Johansen, 1974). In this report these formations are included with the Tesuque Formation in the Tesuque aquifer system. Although these other formations may be quite important locally, their potential for affecting the geohydrology beneath the Pojoaque River basin is slight.

The beds of the Tesuque Formation in the eastern part of the Espanola Basin dip predominantly to the west and northwest. Dips for individual fault blocks vary and may be as much as 30° locally. However, the average dip of the beds is estimated to be between 5° and 10° (Kelley, 1952, p. 111), and toward the west or northwest. The strike and dip of the Tesuque Formation have been estimated from the geophysical logs made in wells constructed primarily for testing the aquifer characteristics. The dips at two of the four sites are in the range estimated by Kelley (1952). A group of wells was constructed on each of the San Ildefonso, Pojoaque, Nambe, and Tesuque Pueblo Grants (fig. 1). At the San Ildefonso site, the beds identified in the geophysical logs dip about 4° with a strike of N. 11° E. At the Pojoaque site, the beds dip about 1.5° and strike N. 0° E. At the Nambe site, the beds dip about 6.5° and strike N. 19° E. At the Tesuque site, the beds dip about 7° to the northwest and strike N. 35° E. Northwest of the Rio Grande the dips are less and the predominant direction is uncertain.

Except for the ash beds, the Tesuque Formation was deposited as coalescing alluvial fans. As a result, individual clastic beds are probably not continuous over the basin. Miller and others (1963, p. 50) report that "***few beds can be traced more than a mile or two." The predominantly north-trending faults further disrupt the continuity of individual beds of the Tesuque Formation (fig. 2). Most of the faults are less than 2 miles long (Manley, 1978, p. 12), have displacement of less than 300 feet (Galusha and Blick, 1971, p. 101), and are downthrown on the east (Galusha and Blick, 1971, p. 101). At each of the four sites where wells were constructed to test the aquifer characteristics (fig. 1), a sequence of interbedded gravel, sand, silt, and clay was penetrated. The composition of the beds shown by Hearne (1980, figs. 4 and 5) for the test site on the Tesuque Pueblo Grant is typical. Attempts to correlate individual beds from one site to another using geophysical logs were unsuccessful.

This complex group of faulted, dipping beds with variable cementation and sorting constitutes the Tesuque aquifer system. The ability of any one bed within this system to transmit water is likely to vary greatly within a relatively short distance. This variation may be due to bed thinning or thickening, variation in degree of cementation, variation in degree of sorting, or the bed's terminating against a bed of different permeability because of faulting.

Because of the interbedding of beds of different permeabilities, water flows parallel to the beds much more readily than perpendicular to the beds. Because these beds are not horizontal but dip 5°–10° to the west or northwest, the Tesuque aquifer system is anisotropic, with the principal axes of hydraulic conductivity skewed from the horizontal. The direction of greatest hydraulic conductivity is along the bedding plane, and the direction of least hydraulic conductivity is normal to the bedding plane. The Tesuque aquifer system appears consistent in that individual beds throughout are dipping, heterogeneous, anisotropic, of limited areal extent, and disrupted by faulting.

The thickness of the Tesuque Formation is unknown but has been estimated to exceed 3,700 feet in some places (Galusha and Blick, 1971, p. 44). Kelley (1978) estimated that the thickness of the Tesuque Formation may exceed 9,000 feet near the Rio Grande. Manley (1978) estimated the dip of the Precambrian crystalline-rock surface to be approximately 4°, which would indicate a depth of about 4,000 feet for the Tesuque Formation beneath Espanola.

The nature of the rocks underlying the Tesuque Formation is also unknown. Throughout most of the basin the Tesuque probably overlies Precambrian crystalline rock (fig. 2). In the southwestern part of the basin, rocks of Paleozoic, Mesozoic, and early Tertiary age overlie the Precambrian crystalline rock and underlie the Tesuque Formation. These units wedge out to the northeast, but their extent is unknown.

A complex pattern of streams and arroyos cuts the present surface of the Tesuque Formation to drain surface runoff to the Rio Grande. The alluvium associated with the Rio Grande and its tributaries has a larger average grain size and is better sorted than that of the Tesuque Formation. The alluvium ranges from about 2 miles wide along parts of the Rio Grande to less than a few hundred feet wide in the tributaries. The thickness of the alluvium varies but is probably less than 100 feet along most of the tributaries. Galusha and Blick (1971, p. 98) report a depth of the alluvium of at least 55 feet along the Rio Grande.

Structure Represented in the Model

To model the Tesuque aquifer system with all of the complexities indicated in the above section on prototype structure is beyond the present capabilities of modeling techniques. It is impractical to attempt to model each bed of the Tesuque aquifer system as a separate unit. This

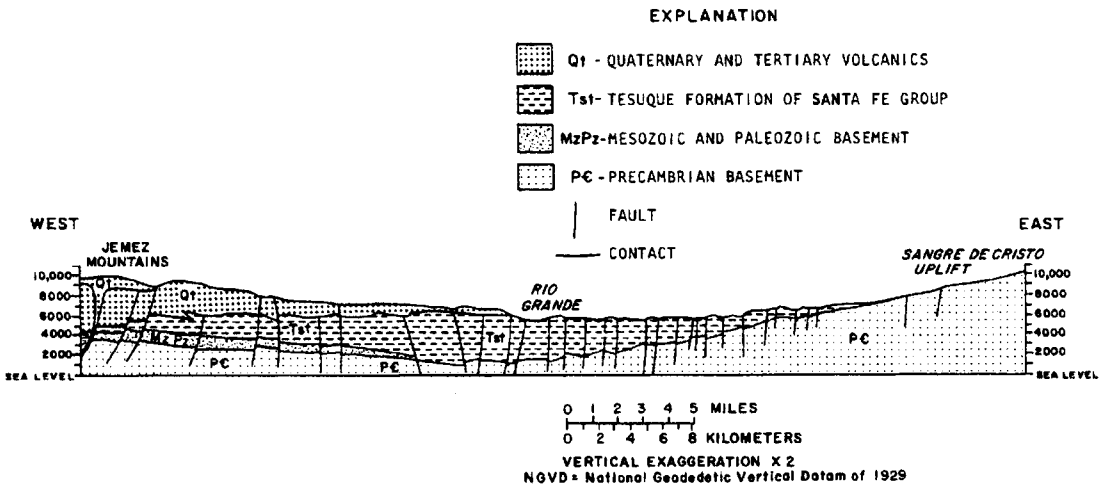

Figure 2. Generalized east-west geologic section near Pojoaque River basin.

would require data on the hydrologic characteristics, the areal extent, and hydraulic connection through semiconfining beds to beds both above and below as well as connection along any fault to other permeable beds. The model presented in this report relies on the consistent heterogeneity of the Tesuque aquifer system. As a unit, the salient structural features are the areal boundaries, the thickness, and the strike and dip of the beds. This section will discuss the assumptions made regarding these features in the digital model.

Flow of water in the Tesuque aquifer system is three-dimensional. That is, flow vectors can be resolved into three components: one parallel to each of three orthogonal axes. Conventionally, these axes are oriented so that the x- and y-axes are horizontal and the z-axis is vertical. For the Tesuque aquifer system it is convenient to orient the x- and y-axes along the plane of the beds and the z-axis orthogonal to the beds. With this orientation of axes, the equation for three-dimensional flow of ground water in a porous medium can be written similarly to Trescott's (1975) as

$$\frac{\partial}{\partial x}(K_x\frac{\partial h}{\partial x}) + \frac{\partial}{\partial y}(K_y\frac{\partial h}{\partial y}) + \frac{\partial}{\partial z}(K_z\frac{\partial h}{\partial z}) = S_s\frac{\partial h}{\partial t} + W(x,y,z,t) \qquad (1)$$

where

K_x, K_y,

and K_z = the hydraulic conductivities in the x, y, and z directions (L/T);

h = the hydraulic head (L);

S_s = the specific storage (L^{-1});

W = the volume of water released from or taken into storage per unit volume of the porous medium per unit time, and represents a source-sink term (T^{-1}); and

t = time (T).

To simulate a three-dimensional flow system, the description of the aquifer system provided by the conceptual model is divided into a large number of brick-shaped cells. The continuous physical properties of the porous medium (that is, the ability to store and transmit water) are assumed to be uniform within each cell and are represented as discrete functions of space. Heterogeneity is possible because the physical properties may be varied from cell to cell. The hydraulic head associated with each cell is that at the center of the cell. In each cell a finite-difference approximation for the derivatives in the three-dimensional flow equation yields an algebraic equation in seven unknowns (hydraulic head in the cell and hydraulic head in each of six adjacent cells). For a model with N cells, a set of N simultaneous equations in N unknowns is generated. The simulation program solves this set of simultaneous equations subject to prescribed initial and boundary conditions. Trescott (1975) and Trescott and Larson (1976) provide details of the solution algorithm. The computer program used for this study (Posson and others, 1980) evolved from that of Trescott.

The model describes the Tesuque aquifer system as a network of contiguous but discrete cells alined with the bedding planes in the Tesuque Formation. The bedding planes were assumed to strike N. 25° E., and dip to the northwest at about 8° on the east side of the Rio Grande

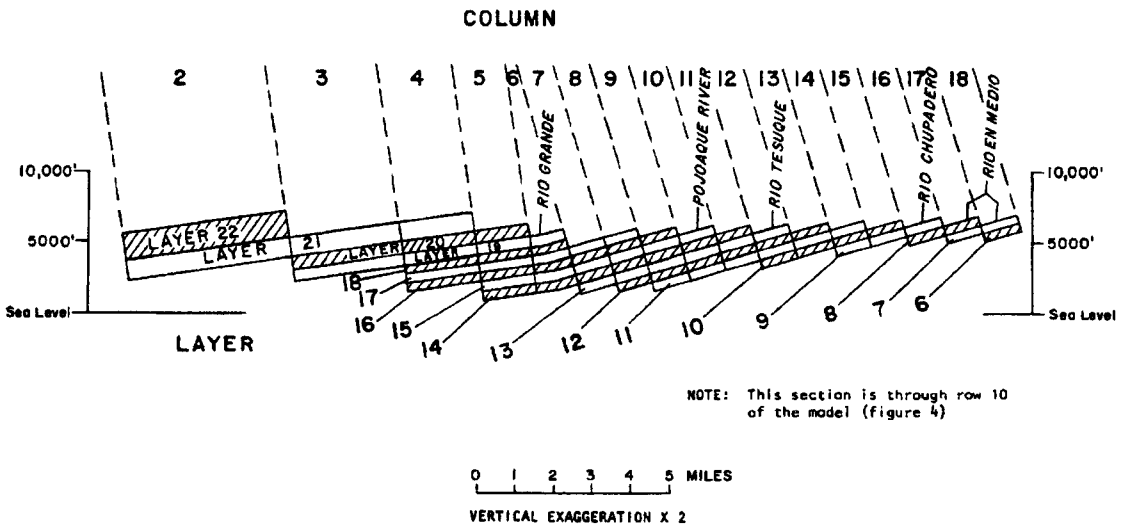

Figure 3. Dip represented along row 10 of the model.

and about 4° on the west side. The model grid was oriented with principal axes dipping to the northwest at 8° east of the Rio Grande and at 4° west of the Rio Grande (fig. 3) with a strike of N. 25° E. (fig. 4). Within the volume of interest the cells are 1 mile wide in each horizontal direction and 650 feet thick.

Outside the area of interest, the horizontal dimensions were increased to as much as 4.5 miles and the thickness was increased to as much as 1,950 feet, to decrease the number of variables to be stored and the number of equations to be solved by the computer.

The dimensions of 1 mile by 650 feet within the volume of interest were found to be convenient because with an average horizontal hydraulic gradient of about 100 feet per mile the saturated thickness of the unconfined cells is about the same throughout the volume of interest. For example, layer 14 represents the water table in column 11 of the digital model. The bottom altitude for layer 14 in column 11 is 5,500 feet. With the water level at about 5,800 feet, the saturated thickness of the water-table layer is about 300 feet. Layer 13, which is 650 feet thick, has a bottom altitude of 4,850 feet (5,500 minus 650) in column 11. With a dip of about 8°, the bottom altitude changes about 750 feet per mile along the dip. Therefore, at column 12 (one mile up-dip from column 11) the bottom altitude of layer 13 is about 5,600 feet (4,850 plus 750). With the water level at about 5,900 feet, the saturated thickness of the water table is about 300 feet. As a result of the increase in cell size, the saturated thickness of the water-table layer is more variable outside the area of interest.

The area included in the model is shown in figure 4. The irregular boundary to the east of the modeled area approximates the contact between the Tesuque Formation and the crystalline rocks of the Sangre deCristo Mountains. The boundary to the west of the modeled area approximates a fault zone beneath the Jemez Mountains (fig. 1). The southern boundary of the modeled area extends to include the confluence of the Rio Grande and the Santa Fe River. The northern boundary of the modeled area is located a few miles north of the Santa Cruz River. The north and south boundaries do not approximate geologic boundaries but are sufficiently distant from the Pojoaque River basin that the boundary effects are negligible.

The assumed thicknesses of the Tesuque Formation in the Pojoaque River basin used in the model (fig. 4) range from a few hundred feet along the mountain front to about 4,000 feet along the Rio Grande. These values are consistent with those estimated by many of the researchers (Galusha and Blick, 1971; Manley, 1978; Denny, 1940; and Spiegel and Baldwin, 1963). Because the depth of the Tesuque Formation is not known and because other researchers have postulated depths as much as 9,000 feet (Kelley, 1978), the sensitivity of the model to this aquifer characteristic was tested.

Aquifer Characteristics in the Prototype

The ability of the aquifer to transmit and store water is described by aquifer characteristics. This section discusses the ability of the Tesuque aquifer system to transmit

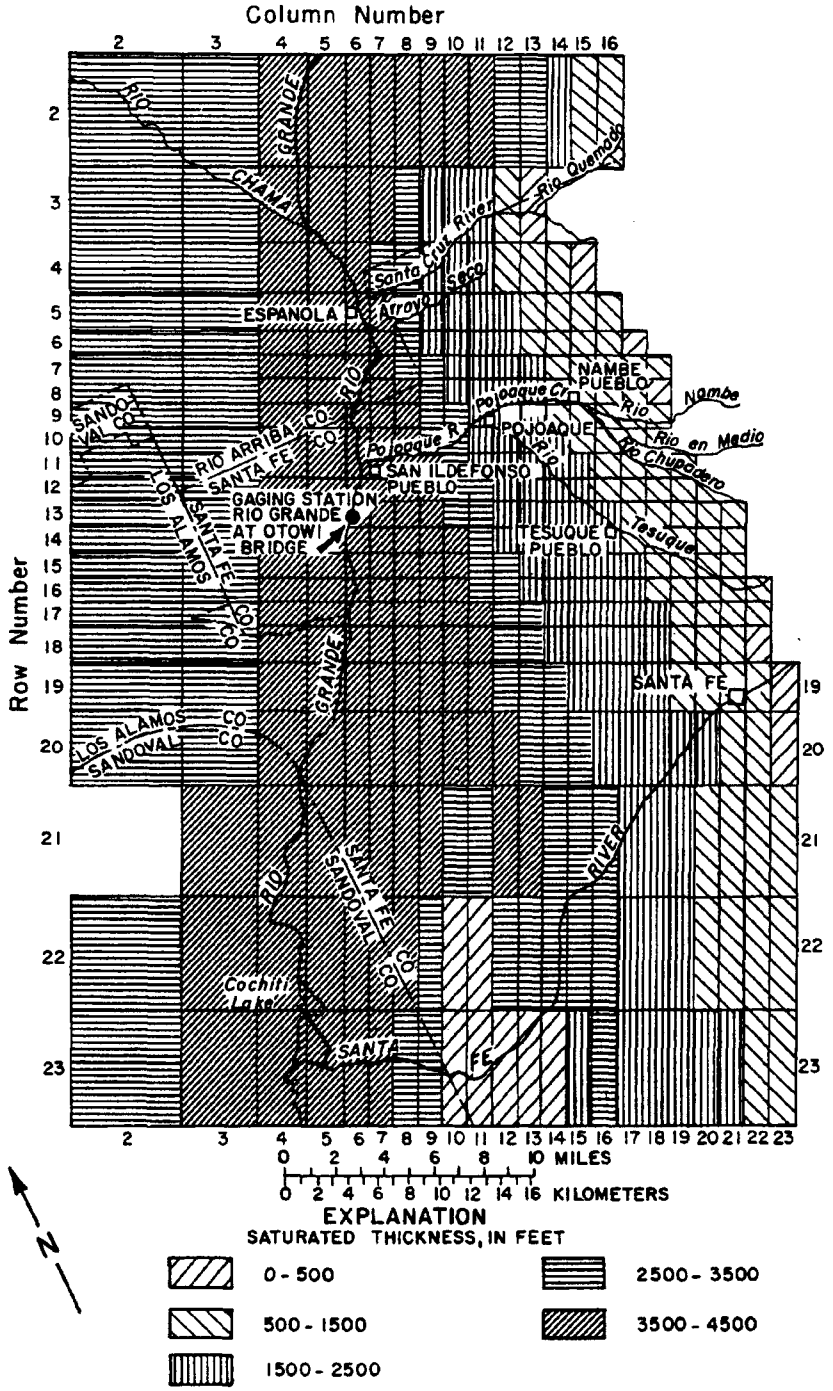

Figure 4. Saturated thickness of the Tesuque Formation represented in the model.

water both parallel and normal to the beds and to store water under both confined and unconfined conditions.

Hydraulic Conductivity

The ability of an aquifer to transmit water can be described by its hydraulic conductivity or by its transmissivity. Hydraulic conductivity is the volume of water that will flow in unit time through a unit area under a unit hydraulic gradient. Transmissivity is the product of the hydraulic conductivity and the saturated thickness. For an ideal aquifer, transmissivity may be determined by aquifer tests conducted using wells that are open to the total thickness of the aquifer. No wells are open to the full thickness of the Tesuque Formation; hence, no measurements of the total transmissivity of the aquifer are available. However, estimates of transmissivity can be obtained by aquifer tests using wells that partially penetrate the aquifer. Under these conditions, short-term aquifer tests provide an estimate of the transmissivity of the beds of the aquifer system to which the well is open. Several aquifer tests have been conducted using the Los Alamos municipal supply wells that partially penetrate the Tesuque aquifer system a short distance west of the Pojoaque River basin.

From an aquifer test on an 870-foot-deep well in Los Alamos Canyon, the transmissivity of the upper 1,000 feet of the Tesuque aquifer system was estimated (Theis and Conover, 1962, p. 16–19) at about 335 feet squared per day. A very short test conducted using a nearby 1,750-foot-deep well indicated a transmissivity of 870 feet squared per day. Because the deeper well did not affect the shallower wells in the field, Theis and Conover (1962, p. 19) suggest that the transmissivity calculated with this well applies to the 1,000–2,000-foot interval. Combining these estimates, they estimated the transmissivity for the upper 2,000 feet of the Tesuque at about 1,200 feet squared per day, or an average hydraulic conductivity of about 0.6 foot per day.

Cushman (1965, p. 39–41) conducted aquifer tests using four wells in Los Alamos Canyon penetrating about 2,000 feet of the Tesuque Formation. He obtained transmissivity values of 1,700 to 2,400 feet squared per day from these tests. Cushman's average transmissivity value of 2,100 feet squared per day is equivalent to a hydraulic conductivity of about 1 foot per day.

Griggs (1964, p. 96–99) conducted aquifer tests using five production wells in Guaje Canyon, about 2 miles northwest of the Los Alamos Canyon well field. These wells were all nearly 2,000 feet deep. Transmissivities determined by short-term tests on each of the five wells ranged from 1,000 to 2,100 feet squared per day, but a value of 1,300 to 1,600 feet squared per day was considered representative of the aquifer based on these tests. Later, the same investigator conducted a 13-day test by pumping two wells and observing drawdowns in them and in nearby idle production wells. He determined an average transmissivity of about 2,000 feet squared per day based on this test. The results of the tests by Griggs indicate a transmissivity of about 1,300 to 2,000 feet squared per day for about 2,000 feet of the Tesuque Formation, or equivalently an average hydraulic conductivity of about 0.6 to 1.0 foot per day.

Transmissivity also may be estimated from specific-capacity data. The specific capacity of a well is the ratio of the rate at which water is withdrawn to the drawdown of water level in the well. Koopman (1975, p. 23–24) estimated the transmissivity of the Tesuque aquifer system based on specific-capacity data from the Los Alamos municipal supply wells. The resultant transmissivity of 670 feet squared per day for a saturated thickness of 1,000 feet is equivalent to a hydraulic conductivity of about 0.67 foot per day, which is about the same as the estimates made from aquifer tests.

During 1975 an aquifer test was conducted using a well penetrating 500 feet of saturated Tesuque Formation underlying the Tesuque Pueblo Grant. Simulation of this aquifer test with a digital model (Hearne, 1980) provided an estimate of about 2 feet per day for the average hydraulic conductivity parallel to the beds.

During 1977 aquifer tests were conducted using wells penetrating from 200 to 1,000 feet of saturated Tesuque Formation. Three such tests were conducted: one each on the Pueblo Grants of San Ildefonso, Pojoaque, and Nambe (fig. 1). Analyses of these data along with data from the Tesuque test (Peter Balleau, U.S. Bureau of Indian Affairs, written commun., April 26, 1978) produced estimates of average hydraulic conductivity ranging from 0.3 to 2.8 feet per day.

According to all of the above data, the average hydraulic conductivity of several units that are likely to be penetrated at any particular site appears to range from about 0.5 to about 2 feet per day.

Anisotropy

A convenient way to express the anisotropy of a system is with the ratio of (1) the hydraulic conductivity normal to the bedding to (2) the hydraulic conductivity parallel to the bedding. In analyzing the aquifer test on the Tesuque Pueblo Grant, the anisotropy ratio was estimated to be about 0.004 in the vicinity of the Tesuque site. The equation used for this estimate (Hearne, 1980, p. 16) is

$$\frac{K_n}{K_p} = \frac{\sin A(\cos A \frac{\partial h}{\partial x} + \sin A \frac{\partial h}{\partial z})}{\cos A(\sin A \frac{\partial h}{\partial x} - \cos A \frac{\partial h}{\partial z})} \qquad (2)$$

where

K_n = the hydraulic conductivity normal to the bedding (L/T);

K_p = the hydraulic conductivity parallel to the bedding (L/T);

A = the angle of the dip of the bedding (negative for down-dip flow, positive for up-dip flow) (dimensionless);

$\frac{\partial h}{\partial x}$ = the horizontal hydraulic gradient in the direction of the dip (dimensionless); and

$\frac{\partial h}{\partial z}$ = the vertical hydraulic gradient (dimensionless).

The equation is invalid either if the basic assumptions are not true or if the data are inconsistent because of measurement errors. The equation assumes horizontal flow in the vertical plane containing the dip. This assumption is inadequate if there is a significant component of vertical flow or flow along the strike. The equation is sensitive to the ratio of vertical to horizontal gradients; that is, a small error in gradient may produce a large error in the estimated anisotropy ratio.

The dip of the beds and the horizontal gradients were determined at the test sites on the Pueblo Grants of San Ildefonso, Pojoaque, and Nambe. At the San Ildefonso and Nambe sites, the data were not adequate to estimate the anisotropy ratio.

At the Pojoaque site, the beds dip about 1.5° west. Because the flow is down-dip, angle A in eq. 2 is negative. Trauger (1967, fig. 1) shows a horizontal gradient of about 0.013. The vertical gradient between piezometers at the test site is about 0.12. The estimated ratio of hydraulic conductivities is about 0.002.

Based on data from the Pojoaque and Tesuque sites, the anisotropy of the Tesuque aquifer system as expressed by the ratio of hydraulic conductivities is estimated to be about 0.003. That half of the data (two sites) fell outside the constraint of the method reduces the confidence in the estimated value, and so anisotropy ratios beyond the range of 0.002 to 0.004 are not unlikely.

Specific Storage

Water is stored in the Tesuque aquifer system in both confined and unconfined conditions. Therefore, it was necessary to estimate both the specific storage and the specific yield. Under confined conditions, a decrease in hydraulic head is associated with expansion of the water and compression of the porous medium. Similarly, an increase in hydraulic head is associated with compression of the water and expansion of the porous medium. The specific storage is the volume of water released from or taken into storage per unit volume of the porous medium in response to a unit change in hydraulic head.

The compaction of the porous medium associated with declines in hydraulic head is a combination of elastic and inelastic (plastic) deformation. Elastic deformation is fully reversible if the hydraulic head returns to the initial condition. Plastic deformation is irreversible. Available data are adequate only to estimate the specific storage due to elastic compaction. Compaction of sandy beds is typically elastic. Clay or silty beds typically contain more water per unit volume, release water more slowly, and undergo more plastic deformation than sandy beds. The amount of plastic deformation to be expected from a clay or silty bed depends on the geologic history of the bed. Because of the permanence of the deformation, a bed will have very little plastic deformation until the stress exceeds the maximum stress to which the bed has been subjected. Because of this threshold effect and the slow release of water, the development of a ground-water reservoir (which generally produces a large change in hydraulic head after a long time) may produce plastic deformation that was not determined during aquifer tests (which generally produce a small change in hydraulic head after a short time).

Because of the general well construction practice of casing off the upper hundred feet or so of the aquifer, the response to pumping wells in the Tesuque Formation can be used to evaluate the specific storage due to elastic compaction of the sandy beds. The aquifer tests conducted by Theis and Conover (1962, p. 16–19) indicate a storage coefficient of about 0.0033. Assuming that the storage coefficient of the aquifer penetrated by this 870-foot-deep well is representative of the upper 1,000 feet of the aquifer would indicate a specific storage of about 3×10^{-6} per foot.

The 13-day aquifer test conducted by Griggs (1964, p. 99) indicates storage coefficients of 0.0002 and 0.0004. Assuming that the storage coefficients are representative of the upper 2,000 feet of the aquifer would indicate specific storage values of about 1×10^{-7} per foot to 2×10^{-7} per foot. Assuming that the storage coefficients are representative of the perforated or screened sections of about 400 feet would indicate specific storage values of about 5×10^{-7} per foot to 1×10^{-6} per foot.

The aquifer test at the Tesuque Pueblo Grant (Hearne, 1980) indicates a specific storage of about 2×10^{-6} per foot. The aquifer tests at the Pueblo Grants of San Ildefonso, Pojoaque, Nambe, and Tesuque indicate specific storage ranging from 1.5×10^{-7} per foot to 8.4×10^{-6} per foot (Peter Balleau, U.S. Bureau of Indian Affairs, written commun., April 26, 1978).

The specific storage associated with the development of the Tesuque aquifer system must include the compaction of the clay or silty beds in addition to that of the sandy beds. Therefore, the values in the range of 10^{-7} per foot are disregarded. The average specific storage is probably between 10^{-6} per foot and 10^{-5} per foot and is assumed to be about 2×10^{-6} per foot.

Specific Yield

For unconfined conditions, the change in the volume of water in storage per unit area as the result of a unit change in hydraulic head is produced primarily by the draining or filling of pore space. This change is dependent upon pore size, rate of change of the water surface, and time. Only an approximate measure of the relationship between hydraulic head and storage is obtainable for unconfined conditions. This measure is the specific yield. No aquifer tests of the Tesuque aquifer system have been conducted long enough to determine the specific yield. An estimate of the specific yield may be obtained from a knowledge of the materials comprising the formation. The materials are poorly sorted and generally contain considerable clay and silt. For these materials the fine-grain fraction will tend to determine the storage coefficient. Johnson (1967, p. D-1) has compiled storage coefficient values determined by various investigators and lists 12 values of storage coefficients for sandy clay and 16 for silt. The values range from 0.03 to 0.19. Johnson lists 17 values ranging from 0.10 to 0.28 for the specific yields of fine sands and 17 values for medium sand ranging from 0.15 to 0.32. An interbedded group of sands, silts, and clays, the Tesuque aquifer system is expected to have an average specific yield of about 0.10 to 0.20.

Driven samples were collected in 1976 from two augered holes on the Tesuque Pueblo Grant and analyzed by the hydrologic laboratory of the U.S. Geological Survey. The holes are located in the NE$\frac{1}{4}$SW$\frac{1}{4}$NE$\frac{1}{4}$ sec. 14, T. 18 N., R. 9 E. between U.S. Highway 285 and the site of the aquifer test on the Tesuque Pueblo Grant. In one hole, 8 samples were collected from between 5 and 60 feet below land surface. In the other hole, 9 samples were collected from between 11 and 81 feet below land surface. The samples taken were capped and wrapped in plastic to reduce moisture loss.

The hydrologic laboratory analyzed the 17 samples for moisture content and total porosity. If the same beds were sampled in saturated and unsaturated conditions, the difference in moisture content would indicate the specific yield, that is, the percentage of the total volume that is water which the unit, after being saturated, will yield by gravity. Because of the heterogeneity of the Tesuque aquifer system, the samples from above and below the water table are from different units. However, the average specific yield may be estimated to be the difference between the mean moisture contents above and below the water table. The moisture content of the 6 samples collected above the water table ranged from 2.4 to 14.4 percent by volume, with a median of 12.3 percent and a mean of 10.3 percent. Total porosity ranged from 31.3 to 44.5 percent, with a median of 41.3 percent and a mean of 39.9 percent. The moisture content of the 11 samples collected below the water table ranged from 21.5 to 35.6 percent, with a median of 24.5 percent and a mean of 25.7 percent. Total porosity ranged from 27.3 to 36.1 percent, with a median of 29.0 percent and a mean of 29.8 percent. The specific yield estimated from these data is 15.4 percent (25.7 minus 10.3).

Two of the samples were selected for a laboratory determination of specific yield using the mercury-injection method. One sample was from 40 feet below land surface and was about 61 percent silt and clay. The specific yield of this sample was about 4 percent. The other sample was from 71 feet below land surface and was about 94 percent sand. The specific yield of this sample was about 18 percent.

Based on the above data, the average specific yield of the Tesuque aquifer system is probably between 0.10 and 0.20 and is assumed to be about 0.15.

Aquifer Characteristics Represented in the Model

Aquifer characteristics must be estimated for each of the discrete cells in the model. The characteristics to be estimated are the hydraulic conductivity, the anisotropy, the specific storage, and the specific yield. The data available for estimating these characteristics indicate that the characteristics vary spatially within the aquifer system. However, the data are not adequate to describe this variation as a general pattern. At most places in the Pojoaque River basin, a well several hundred feet deep will intersect at least one sandy unit that transmits water readily. This sandy unit will be overlain and underlain by units less able to transmit water that serve to isolate this unit from other sandy units. However, it is doubtful if either the transmissive units or the confining units are very extensive. Within a few hundred feet, the unit may thin to extinction, be terminated by a fault that positions it adjacent to a unit of different character, or change in character from a sandy unit to a silty unit that does not transmit water as readily.

The approach adopted for this report was to estimate, from the available data, the most likely average value for each aquifer characteristic throughout the entire basin. The uncertainty in these estimates is indicated by a range of values called the plausible range. The model was constructed using the values estimated here as most likely values. If the simulation of steady-state conditions were contradicted by available data, the aquifer characteristics could be varied within the plausible range in an effort to resolve the contradiction. Although this was not necessary, the sensitivity of the model to each of the characteristics was tested for the plausible range of values. The results of the sensitivity tests appear in the section on "Model Sensitivity." The most likely average values for the various aquifer characteristics are given in table 1.

Table 1. Most likely value and plausible range of aquifer characteristics

Aquifer characteristic	Lower limit of plausible range	Most likely average value	Upper limit of plausible range
Hydraulic conductivity parallel to the beds (feet per day)	0.5	1.0	2.0
Anisotropy ratio	0.001	0.003	0.01
Specific storage (per foot)	1×10^{-6}	2×10^{-6}	1×10^{-5}
Specific yield	0.10	0.15	0.20

Boundaries in the Prototype

Boundaries define the limits of the system being modeled and specify the relationship with other systems. Exchanges of water may occur between the ground-water system and adjacent ground-water systems or surface-water systems. The major flows imposed on the Tesuque aquifer system are those in which water is exchanged with a surface-water system. These include not only recharge from and discharge to streams but also recharge from the percolation of storm flow in arroyos, recharge from percolation of precipitation or irrigation on the Tesuque Formation, and discharge through evapotranspiration. The description of the boundaries of the Tesuque aquifer system includes an evaluation of the anticipated change in the boundary condition in response to the projected withdrawals.

Adjacent Ground-Water Systems

Exchanges between the Tesuque aquifer system and adjacent ground-water systems are negligible. An impermeable boundary is one in which the Tesuque Formation is adjacent to rocks of sufficiently smaller hydraulic conductivity as to be considered impermeable relative to the Tesuque Formation. An impermeable boundary is located along the contact between the Tesuque Formation and the Sangre de Cristo Mountains to the east (fig. 1). The boundary between the Tesuque Formation and the underlying basement rocks also is impermeable.

The complicated fault zone to the west (fig. 1) may restrict the flow of ground water and control the flow into the modeled area. If so, changes in the ground-water flow across the fault zone will be small.

Rocks of the Tesuque Formation continue through the bedrock constrictions to the north and south. Because the relatively narrow channels have a small cross-sectional area, the ground-water flow through the channels is small. Because of the proximity to the Rio Grande, the existing gradients should be maintained by river flow. Therefore, changes in the ground-water flow through the channel will be small.

Rio Grande

The major stream in the modeled area is the Rio Grande. The mean flow of the Rio Grande at Otowi Bridge (fig. 4) near San Ildefonso is about 1,300 cubic feet per second (Reiland and Koopman, 1975, p. 24). Extremes range from 60 cubic feet per second on July 4 and 5, 1902, to 24,400 cubic feet per second on May 23, 1920 (U.S. Geological Survey, 1977). Flow during calendar year 1976 averaged 1,051 cubic feet per second. Ground-water flow to or from the Rio Grande may be altered by the withdrawal of water for irrigation in the Pojoaque River basin. However, the flow is so large relative to the projected withdrawals that the Rio Grande will continue to maintain the hydraulic head in the aquifer near the stream at or near the altitude of the streambed.

Santa Cruz River

The major tributaries to the Rio Grande in Espanola Basin are the Santa Cruz, Pojoaque, and Santa Fe Rivers. The mean flow of the Santa Cruz River near the boundary between the Tesuque aquifer system and the crystalline rocks is about 28.3 cubic feet per second (U.S. Geological Survey, 1977). Extremes range from 0.19 cubic foot per second on March 13, 1954, to 2,420 cubic feet per second on September 24, 1931. Flow during calendar year 1976 averaged 21.85 cubic feet per second. Ground-water flow to or from the Santa Cruz River may be altered by the withdrawal of water for irrigation in the Pojoaque River basin. Although the flow is not large relative to the projected withdrawals, the stream is far enough from the Pojoaque River basin that the Santa Cruz River will probably continue to maintain the hydraulic head in the aquifer along the stream at or near the altitude of the streambed.

Pojoaque River and Tributaries

Monthly streamflow at selected sites along the Pojoaque River was estimated from 1935 to 1972 by Reiland (1975) and Reiland and Koopman (1975) for undeveloped conditions. Flow available in the Pojoaque River basin for recharge to the ground-water system was estimated from the mean flow in the streams as they discharged from the mountain front. For the Rio Nambe, the mean flow near the boundary between the Tesuque aquifer system and the crystalline rocks is estimated to be about 10.59 cubic feet per second (Reiland and Koopman, 1975, table 1).

The Rio en Medio is estimated to have a mean flow of about 2.40 cubic feet per second at a site east of the boundary between the Tesuque aquifer system and the crystalline rocks (Reiland and Koopman, 1975, table 3).

The Rio Chupadero is estimated to have a mean flow of about 0.40 cubic foot per second (Reiland and Koopman, 1975, table 4) at a site about 1 mile west of the boundary between the crystalline rocks and the Tesuque aquifer system. Losses upstream from this site are estimated to be about 0.13 cubic foot per second (Reiland and Koopman, 1975, p. 14). The mean annual flow of the Rio Chupadero as it discharges from the Sangre de Cristo Mountains is therefore estimated to be about 0.54 cubic foot per second.

The headwaters of the Rio Tesuque are Tesuque Creek and Little Tesuque Creek. The mean flow for Tesuque Creek upstream from diversions is estimated to be about 2.82 cubic feet per second (Reiland and Koopman, 1955, table 4A). Flow in Little Tesuque Creek is estimated to be about 0.55 cubic foot per second (Reiland, 1975, p. 17).

An estimated total of 16.90 cubic feet per second flows in the headwaters of the streams in the Pojoaque River basin. Losses to the Tesuque aquifer system and evaporation from the river surface and river bed decrease the flow. Discharge from the Tesuque aquifer system and runoff of precipitation on the Tesuque Formation are added to the flow. Reiland and Koopman (1975, table 6) estimate the mean annual discharge from 1935 to 1972 at the mouth of the Pojoaque River to be about 14.35 cubic feet per second. Because this estimate is based on the assumption that the runoff of precipitation on the Tesuque Formation and the inflow from ground water very nearly balance the evapotranspiration loss, this estimate is considered less accurate than those for the flows at the boundary of the crystalline rocks.

At present (1980) some of the natural flow is diverted to irrigate about 3,700 acres (New Mexico State Engineer Office, 1978). Assuming a consumptive use of 1.5 acre-feet per acre (New Mexico State Engineer Office, 1966), about 7.67 cubic feet per second of water is consumed. The annual flow at the mouth of the Pojoaque River is estimated from the periodic measurements reported for the water years 1973–1977 (U.S. Geological Survey, 1973, 1974, 1975, 1976, 1977). The estimated annual flow ranges from about 1,500 acre-feet for the 1977 water year to about 19,200 acre-feet for the 1973 water year. The mean annual flow of about 6,000 acre-feet exceeds the estimated annual flow in each of the 5 years except 1973. The median annual flow of 2,630 acre-feet or about 3.63 cubic feet per second for the 5 years may be a better measure of central tendency.

Under natural conditions and at the present level of irrigation, the flow of the Pojoaque River is adequate to maintain the hydraulic head in the aquifer along the stream at or near the elevation of the streambed. However, the irrigation-development plan proposed by the U.S. Bureau of Indian Affairs calls for the diversion of water from the Rio Nambe, Rio en Medio, Rio Chupadero, and Rio Tesuque, as well as the withdrawal of ground water from the Tesuque aquifer system near the Pojoaque River and its tributaries. With this additional stress, the flow of the Pojoaque River will probably not be adequate to maintain the hydraulic head in the aquifer along the stream at or near the altitude of the streambed.

Santa Fe River

The mean flow of the Santa Fe River upstream from Cochiti Lake (fig. 4) was about 8.0 cubic feet per second for the 7 years of record. Extremes range from no flow on July 16-18, 1971, to 11,400 cubic feet per second on July 26, 1971. The flow is affected by diversions to and returns from the municipal supply of the city of Santa Fe. The flow of the Santa Fe River about 5 miles east of Santa Fe (U.S. Geological Survey, 1960) averaged about 12 cubic feet per second prior to the completion of McClure Reservoir in 1926 and about 8 cubic feet per second for the 64 years of record. Under pristine conditions, the flow of the Santa Fe River probably was adequate to maintain the hydraulic head in the aquifer along the stream at or near the altitude of the streambed. With present (1980) diversions, the upstream reach of the river is dry much of the year, but occasional flows still may be adequate to maintain the hydraulic head in the aquifer along the stream at or near the altitude of the streambed. However, declines in the hydraulic head in the aquifer are not likely to induce additional recharge. Due to gains from ground-water seepage, the downstream reach of the river is perennial. The withdrawal of ground water in Pojoaque River basin may affect the rate of flow to the downstream reach of the Santa Fe River.

Storm Runoff

In addition to the major tributaries, there are many arroyos that flow only in response to storms or spring snowmelt. Some of this storm or snowmelt runoff recharges the ground-water system. Some recharge also may occur from infiltration of precipitation on the surface of the Tesuque Formation. However, these recharge rates are not likely to change due to the withdrawal of water for irrigation in the Pojoaque River basin.

Native Vegetation

Native vegetation that may consume water from the aquifer system is found along most streams where the flow is adequate to maintain the hydraulic head in the aquifer along the stream at or near the land surface. For the Rio Grande, the Santa Cruz River, and the downstream reach

of the Santa Fe River, the flow probably will continue to maintain the hydraulic head in the aquifer and supply water for the native vegetation. For these streams the water consumed by the native vegetation can be considered part of the surface-water system rather than a separate discharge from the ground-water system. However, the streams in the Pojoaque River basin will be more heavily affected by the projected withdrawals. If flow in the river were to be completely terminated and the water table lowered abruptly, the native vegetation might be unable to obtain adequate ground water. A more likely scenario would be for the streamflow to be reduced and the ground-water levels to decline gradually. The native vegetation may continue consuming ground water at the present rate regardless of the flow or lack of flow in the stream.

The National Resources Committee (1938, table B, p. 418–19) reported 315 acres of trees in the Pojoaque River basin. This figure is consistent with the U.S. Bureau of Reclamation's (1965, p. B–27) estimate of 144 acres of trees for the part of the basin upstream from Pojoaque Bridge. If the trees consumed 2.5 acre-feet per acre annually (U.S. Bureau of Reclamation, 1965), the total discharge would be about 800 acre-feet per year or 1.10 cubic feet per second.

Channel Losses

Evaporation from river and canal surfaces and exposed channel beds also may be discharging water. The present rate of discharge will probably be maintained by the flow in the streams except for the streams in the Pojoaque River basin. The National Resources Committee (1938, table B, p. 418–19) reported 963 acres of river and canal surfaces and exposed channel beds. If evaporation from these surfaces were about 2.5 feet per year (U.S. Bureau of Reclamation, 1965), total evaporation would be about 3.32 cubic feet per second.

Boundaries Represented in the Model

The computer program allows for a boundary to be represented as one of three types: specified-flow, specified-hydraulic-head, or hydraulic-head-dependent. At specified-flow boundaries, water is recharged to or discharged from the aquifer system at a rate that is independent of the hydraulic head in the aquifer system. An impermeable or no-flow boundary is a specified-flow boundary. At specified-hydraulic-head boundaries the hydraulic head is maintained at the specified value. As hydraulic heads in the aquifer system change adjacent to the specified-hydraulic-head boundary, the rate of flow at the specified-hydraulic-head boundary will change. A hydraulic-head-dependent boundary (Posson and others, 1980) is designed to represent streams in which the flow is small relative to the stress to be imposed on the aquifer system. At a hydraulic-head-dependent boundary, the hydraulic head is allowed to change as the aquifer is stressed. The rate at which water is recharged to or discharged from the aquifer is calculated as a function of the hydraulic head in the aquifer, the streambed altitude, and the flow in the river. Each of the boundaries described for the prototype is represented in the model as one of these boundaries. Boundary conditions represented in the model are shown in figure 5.

Adjacent Ground-Water Systems

The boundaries between the Tesuque aquifer system in the modeled area and other ground-water systems are represented in the model as impermeable or no-flow boundaries (fig. 5). The irregular boundary to the east represents the contact between the Tesuque Formation and the Sangre deCristo Mountains. The boundary to the west represents the complicated fault zone beneath the Jemez Mountains. Any flow across the fault zone, which is treated as a constant-flow boundary, is not distinguished from recharge from storm runoff. Although the boundaries to the north and the south do not represent geologic boundaries, reasonable steady-state conditions were produced with no flow across them. The boundaries are sufficiently distant from the Pojoaque River basin that the effect on the response to the proposed withdrawals is negligible.

Rio Grande and Santa Cruz River

The Rio Grande and the Santa Cruz River were represented in the model as a specified hydraulic-head boundary. The hydraulic head specified at each cell is at or near the altitude of the streambed as estimated from topographic maps. Hydraulic heads along specified-hydraulic-head boundaries are shown in table 2.

Pojoaque River and Tributaries

The Pojoaque River and its major tributaries are represented as a hydraulic-head dependent boundary. This requires not only defining the stream network and estimating the inflow at the upstream end of each stream, but also estimating the hydraulic head in the stream, the constant of proportionality (leakance coefficient) between the hydraulic head difference and the rate of flow between the river and the aquifer, and a maximum infiltration rate.

Stream network.—The Pojoaque River and its tributaries were represented by eight reaches as shown in figure5. The first reach represented the Rio Nambe. Flow into the upstream end of the reach is estimated to be about 10.59 cubic feet per second (Reiland and Koopman, 1975). Flow from the downstream end of the reach is routed to reach 4 (Pojoaque Creek).

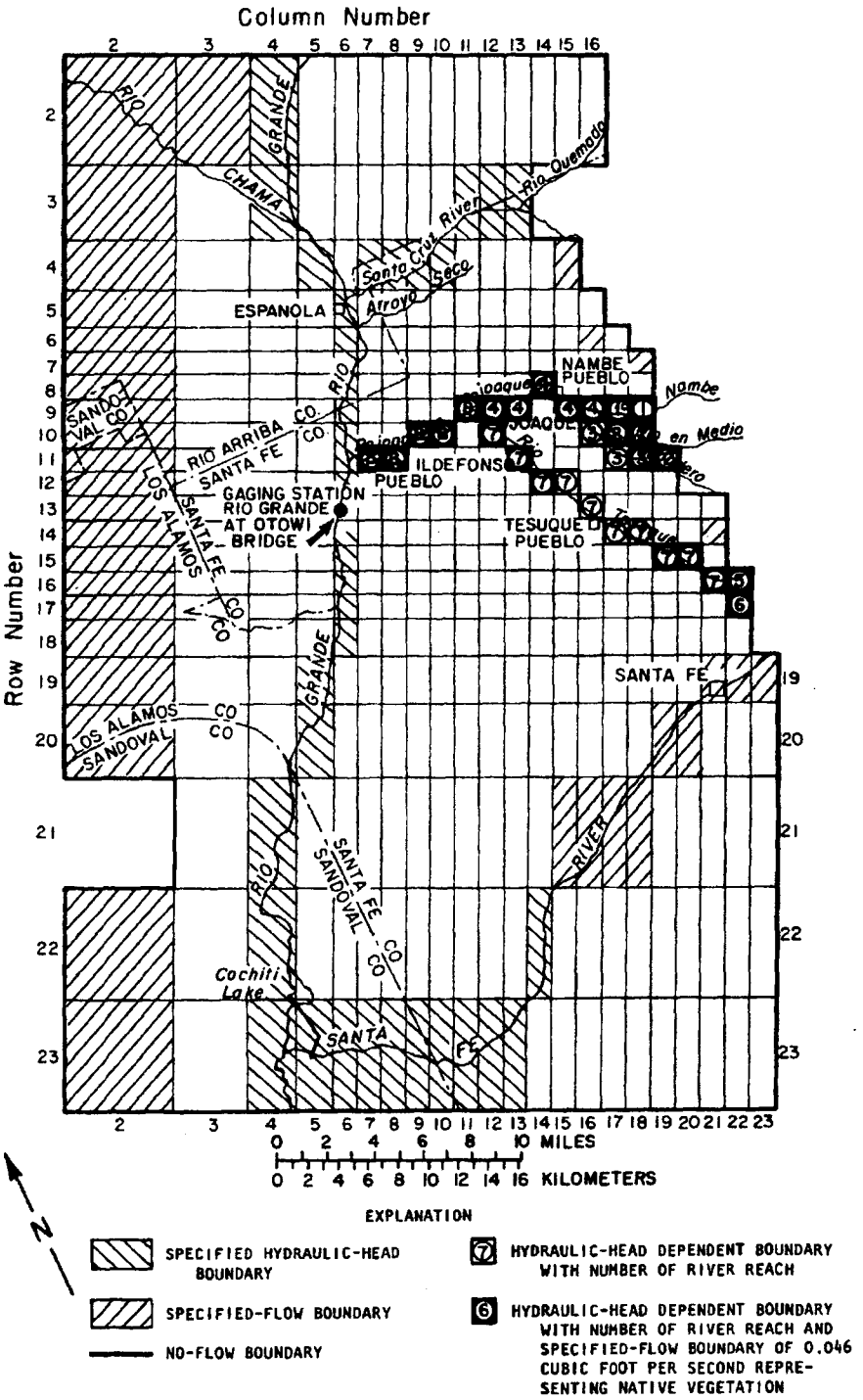

Figure 5. Boundary conditions represented in the model.

Table 2. Specified hydraulic-head boundaries represented in the model

Location			Specified hydraulic head
Row	Column	Layer	(feet)
2	4	21	5,672
3	4	21	5,622
4	5	20	5,591
5	6	19	5,572
6	6	19	5,558
7	6	19	5,549
8	6	19	5,540
9	6	19	5,529
10	6	19	5,519
11	6	19	5,512
12	6	19	5,505
13	6	19	5,496
14	6	19	5,475
15	6	19	5,462
16	6	19	5,448
17	6	19	5,434
18	6	19	5,417
19	5	20	5,397
20	5	20	5,369
21	4	20	5,319
22	4	20	5,267
23	4	20	5,213
3	13	12	6,095
3	12	13	6,014
3	11	14	5,928
4	10	15	5,838
4	9	16	5,742
4	8	17	5,693
4	7	18	5,617
22	14	11	6,040
23	13	12	5,710
23	12	13	5,610
23	11	14	5,515
23	10	15	5,470
23	9	16	5,425
23	8	17	5,385
23	7	18	5,350
23	6	19	5,300
23	5	20	5,260

The second reach represents the Rio enMedio. Flow into the upstream end of the reach is estimated to be about 2.40 cubic feet per second (Reiland and Koopman, 1975). Flow from the downstream end of the reach is routed to reach 4 (Pojoaque Creek).

The third reach represents the Rio Chupadero. Flow into the upstream end of the reach is estimated to be about 0.54 cubic foot per second (Reiland and Koopman, 1975). Flow from the downstream end of the reach is routed to reach 4 (Pojoaque Creek).

The fourth reach represents Pojoaque Creek. Flow into the upstream end of the reach is the sum of the flows routed to this reach from reaches 1 (Rio Nambe), 2 (Rio enMedio), and 3 (Rio Chupadero). Flow from the downstream end of the reach is routed to reach 8 (Pojoaque River).

The fifth reach represents Tesuque Creek. Flow into the upstream end of the reach is estimated to be about 2.82 cubic feet per second (Reiland and Koopman, 1975). Flow from the downstream end of the reach is routed to reach 7 (Rio Tesuque).

The sixth reach represents Little Tesuque Creek. Flow into the upstream end of the reach is estimated to be about 0.55 cubic foot per second (Reiland, 1975). Flow from the downstream end of the reach is routed to reach 7 (Rio Tesuque).

The seventh reach represents the Rio Tesuque. Flow into the upstream end of the reach is the sum of the flows routed to this reach from reach 5 (Tesuque Creek) and reach 6 (Little Tesuque Creek). Flow from the downstream end of the reach is routed to reach 8 (Pojoaque River).

The eighth reach represents the Pojoaque River. Flow into the upstream end of the reach is the sum of the flows routed to this reach from reach 4 (Pojoaque Creek) and reach 7 (Rio Tesuque). Flow from the downstream end of the reach is to the Rio Grande.

Estimation of stream leakage characteristics.—The rate of flow between the river and the aquifer is calculated (Posson and others, 1980) as the minimum of the simulated flow available in the stream, the specified maximum infiltration rate, and the flow calculated from

$$q = K_R(H - h)A \tag{3}$$

where

q = the flow from the river to the cell (L^3/T);
K_R = the leakance coefficient (T^{-1});
H = the hydraulic head in the stream (L);
h = the calculated hydraulic head in the cell at the last time step (L); and
A = the surface area of the cell (L^2).

To complete the definition of the boundary, the hydraulic head in the stream, H, the leakance coefficient, K_R, and the maximum infiltration rate must be specified. The hydraulic head, H, at each node of the stream was assumed to be at or near the altitude of the streambed. Altitudes shown in table 3 were estimated from topographic maps. The leakance coefficient, K_R, was assumed to be 5×10^{-10} per second. The maximum infiltration rate is assumed to be 1.0 cubic foot per second.

Table 3. Hydraulic-head dependent boundaries represented in the model

Location			River reach	Estimated hydraulic head in stream (feet)
Row	Column	Layer		
9	18	7	1	6,450
9	17	8	1	6,325
11	19	6	2	6,810
10	18	7	2	6,650
10	17	8	2	6,370
11	18	7	3	6,670
11	17	8	3	6,460
10	16	9	3	6,230
9	16	9	4	6,188
9	15	10	4	6,100
8	14	11	4	6,015
9	13	12	4	5,930
9	12	11	4	5,860
16	22	3	5	7,175
17	22	3	6	7,220
16	21	4	7	6,950
15	20	5	7	6,810
15	19	6	7	6,640
14	18	7	7	6,490
14	17	8	7	6,410
13	16	9	7	6,290
12	15	10	7	6,190
12	14	11	7	6,090
11	13	12	7	5,950
10	12	13	7	5,870
9	11	14	8	5,790
10	10	15	8	5,718
10	9	16	8	5,670
11	8	17	8	5,617
11	7	18	8	5,565

The value of 5×10^{-10} per second is plausible if the leakance coefficient, K_R, is associated with aquifer characteristics by simplifying the flow system within an individual river cell and making an approximate comparison with an expression of Darcy's law. Flow can be calculated from Darcy's law as

$$q = KIA_f \tag{4}$$

where

q = the flow (L^3/T);
K = the hydraulic conductivity in the direction of flow (L/T);
I = the hydraulic gradient in the direction of flow (dimensionless); and
A_f = the cross-sectional area normal to the flow (L^2).

To compare the two expressions for flow from the river to the aquifer requires that the gradient, I, be expressed as the ratio of (1) the difference, Δh, between the hydraulic head specified for the stream and the hydraulic head simulated in the cell and (2) an appropriate distance, d, so that $I = \Delta h/d$. Making this substitution, setting the two expressions for flow from the river to the cell equal to each other, and solving for the constant of proportionality, K_R, yields

$$K_R = \frac{-KA_f}{dA} \tag{5}$$

Therefore, K_R must incorporate the hydraulic conductivity, K; the part, A_f, of the area of the cell, A, through which flow occurs; and an appropriate distance, d; so that $\Delta h/d$ approximates the hydraulic gradient, I.

In general, K_R is assigned based on the geometry of the presumed flow system and the directional hydraulic conductivity of the corresponding beds. As described above, the model represents the dipping anisotropic beds of the Tesuque aquifer system as a network of homogeneous, anisotropic cells oriented parallel to the beds. Each cell in this model represents several interbedded more permeable and less permeable beds. To illustrate the presumed flow system, an individual river cell is shown (fig. 6) with alternating more permeable and less permeable beds. If the river is assumed to flow in the direction of dip, the river alluvium intersects the upturned ends of these beds (fig. 6). In this case, flow from the river to the aquifer will be predominantly through the more permeable beds. Therefore, the hydraulic conductivity in the direction of flow is the mean hydraulic conductivity parallel to the beds, K_x, or about 1.0 foot per day.

The cross-sectional area normal to the flow is the area of the upturned ends of the beds normal to the flow. Because the river is assumed to flow in the direction of the dip and the angle between the river alluvium and the beds is assumed to be 7° (fig. 6), the aggregate thickness

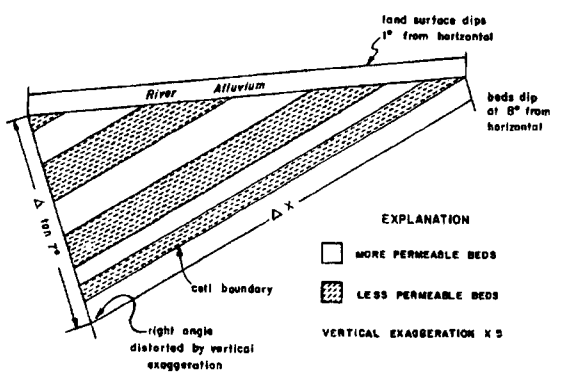

Figure 6. Simplified geometry for an individual cell used to estimate the constant of proportionality (K_R) for hydraulic-head dependent boundaries.

of the upturned ends of the beds in the cell is the product of the horizontal grid dimensions, Δx, and the tangent of 7°.

The width of the flow path is assumed to be the width of the cell, Δy. Therefore, the area of flow is estimated to be (Δx tan 7°) (Δy), about 12 percent of the surface area of the cell.

The appropriate distance, d, so that $\Delta\ h/d$ approximates the gradient, I, is assumed to be half the horizontal grid spacing, $\Delta\ y/2$.

Combining these assumptions and estimates, the constant of proportionality for this model is

$$K_R = \frac{K_x}{\Delta y/2} \cdot \frac{(\Delta x \tan 7°)(\Delta y)}{\Delta x \Delta y} \qquad (6)$$

where

K_x = the hydraulic conductivity parallel to the beds of the Tesuque aquifer system (LT^{-1}); and

$\Delta x, \Delta y$ = the dimensions of the cell (L).

For all cells specified as hydraulic-head-dependent boundaries, $\Delta x = \Delta y = 5{,}280$ feet. Therefore, for K_x = 1.0 foot per day, K_R is specified as 5×10^{-10} per second.

Santa Fe River

The boundary representing the Santa Fe River is divided into a downstream reach and an upstream reach. The criterion for this division is whether the model indicates a steady-state flow to or from the ground water. In the downstream reach the model simulates flow of ground water to the river. The downstream reach of the Santa Fe River is represented as a specified-hydraulic-head boundary (table 2). As hydraulic heads in the model decline due to simulated ground-water withdrawals, the simulated flow to the river decreases. In the upstream reach of the Santa Fe River, the model simulates a steady-state flow to ground water from the river. The upstream reach is represented as a specified-flow boundary. The recharge from the river is assumed to be adequate to maintain the hydraulic head in the aquifer along the stream at about the altitude of the streambed. However, as hydraulic heads in the model decline in response to simulated ground-water withdrawals, the simulated ground-water recharge will not be allowed to increase. The flow rate specified for each cell was estimated by a preliminary steady-state simulation in which the cells were treated as specified- hydraulic-head boundaries. The specified hydraulic heads were assumed to be at or near the altitude of the streambed and were estimated from topographic maps. The flow rate at each specified-flow boundary is shown in table 4.

Table 4. Specified-flow boundaries represented in the model
[ft³/s = cubic foot per second]

Location			Specified flow to aquifer (ft³/s)
Row	Column	Layer	
9	18	7	−0.046
9	17	8	− .046
10	18	7	− .046
10	17	8	− .046
11	19	6	− .046
11	18	7	− .046
9	16	9	− .046
9	15	10	− .046
8	14	11	− .046
9	13	12	− .046
9	12	13	− .046
16	22	3	− .046
17	22	3	− .046
16	21	4	− .046
15	20	5	− .046
15	19	6	− .046
12	14	11	− .046
11	13	12	− .046
10	12	13	− .046
9	11	14	− .046
10	10	15	− .046
10	9	16	− .046
11	8	17	− .046
11	7	18	− .046
2	3	21	1.3605
2	2	22	− .3365
3	2	22	.0371
4	2	22	.1667
5	2	22	.2370
6	2	22	.2427
7	2	22	.3366
8	2	22	.4361
9	2	22	.5436
10	2	22	.5311
11	2	22	.5247
12	2	22	.3974
13	2	22	.3974
14	2	22	.2764
15	2	22	.2732
16	2	22	.5130
17	2	22	.7732
18	2	22	1.1698
19	2	22	1.0982
20	2	22	1.0660
22	2	22	1.7389
23	2	22	.9800
4	15	10	.7139
6	16	9	.5239
7	18	7	1.2749
14	21	4	1.2716
19	23	2	.7978
19	22	3	.1640
19	21	4	.4651
20	20	5	1.3025
20	19	6	.8045
21	18	7	1.8127
21	17	8	.4371
21	16	9	.9099
21	15	10	.5159

Storm Runoff

Recharge from storm runoff in arroyos and infiltration of precipitation on the surface of the Tesuque Formation is represented as a specified-flow boundary. The rate of flow was estimated by a preliminary steady-state simulation in which the cells were treated as specified-hydraulic-head boundaries. This recharge may occur throughout the entire basin. However, to represent the entire surface of the modeled area as a specified-hydraulic-head boundary would probably generate spurious flows to and from the ground-water reservoir in response to heterogeneity of the aquifer system, which is not represented in the model, and errors in estimated hydraulic head. To avoid these errors, recharge from storm runoff was concentrated on the perimeter of the model. Specified-flow boundaries were designated along the western edge of the model. East of the Rio Grande, specified-flow boundaries were designated for some of the larger arroyos along the eastern limit of the Tesuque aquifer system. At these locations, the rate of recharge was assumed to be adequate to maintain the water level at its present estimated position. For the preliminary simulation the specified hydraulic heads were estimated from water-level contour maps (Borton, 1968; Purtymun and Johansen, 1974). The flow rates at specified-flow boundaries are shown in table 4.

Native Vegetation

Water consumption by native vegetation along the Pojoaque River and its major tributaries is represented as a specified-flow boundary. Few trees are evident in the channel of the Rio Chupadero at its mouth or in the channel of the Rio Tesuque on either side of Tesuque Pueblo. No discharge was represented for these reaches. The estimated 1.10 cubic feet per second of consumption was divided evenly among the remaining 24 cells representing the Pojoaque River system. Each of the cells at which the flow from the aquifer is specified as 0.046 cubic foot per second is shown in table 4.

Channel Losses

Evaporation from the river and canal surfaces and exposed channel beds in the Pojoaque River basin, as well as any current irrigation diversions, was assumed to be a loss from the surface-water system and was not represented separately in the ground-water model. The calculated value described as the flow remaining in the river at each cell represents the sum of flow in the river, evaporation from water surfaces and exposed channel beds, and any current diversion from the river.

STEADY-STATE CONDITION

This section of the report presents the steady-state condition as established in the prototype and as simulated with the model as described in the preceding sections on structure, characteristics, and boundaries. Two facets are considered: the hydraulic-head distribution and the flow between ground water and surface water. For each, a consideration of the prototype is followed by a description of the simulated results.

Preliminary models with different structures and boundaries were discarded because the steady-state condition that they simulated was too dissimilar to that established in the prototype. Structures that were found unsatisfactory included grid blocks oriented with a north-south strike or with no dip west of the Rio Grande. Models that did not extend south far enough to include the Santa Fe River as a boundary also were rejected, as were models that did not include recharge along the contact with the Sangre deCristo Mountains. In each of these preliminary models, adjustment of aquifer characteristics failed to significantly improve the comparison between simulated and measured hydraulic heads. And with the model described in the preceding sections on structure and boundaries, the steady-state condition was acceptable without adjusting the aquifer characteristics.

Hydraulic-Head Distribution in the Prototype

A steady-state condition is assumed to have existed in the prototype in 1946. Irrigation with surface water diverted to lands near the principal streams consumes water which would otherwise contribute to the flow in the streams. However, the effect on the ground-water system is assumed to be negligible. Significant withdrawals from ground water began outside of Pojoaque River basin in 1947 as described more completely in the section on "History in the Prototype." Because of these withdrawals, the present water levels near the points of withdrawal may be a few tens of feet lower than in 1946. However, within the Pojoaque River basin, the water levels are assumed to have remained in the 1946 steady-state condition.

Contours of the water surface east of the Rio Grande (figs. 7 and 8) have been published by Trauger (1967) and Borton (1968). The contours of Trauger (fig.7) were modified from those of Spiegel and Baldwin (1963, plates 6 and 7) who described them as contours on extrapolated prepumping water levels." The contours of Borton (fig.8) approximate the ground-water elevation as measured or reported for 71 wells and springs in and near the Pojoaque River basin (Borton, 1968, table2). Because most of the water levels were measured during late 1967 and early 1968, they are taken to indicate the 1968 water surface. Because the water levels within the Pojoaque

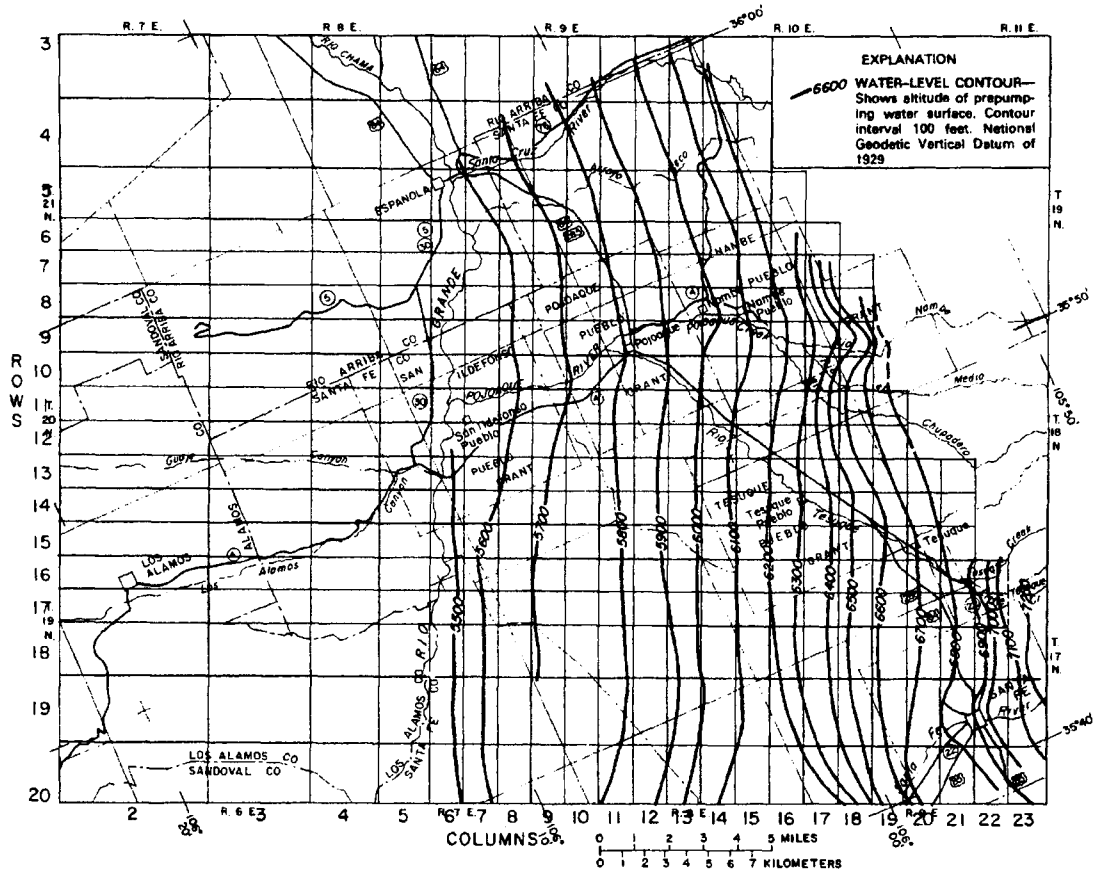

Figure 7. Contours of prepumping water surface east of the Rio Grande.

River basin are assumed to have remained in the 1946 steady-state condition, these contours are considered representative of the steady-state condition within that basin. Both sets of contours indicate ground-water flow from the mountain front toward the Rio Grande.

Purtymun and Johansen (1974, fig.3) contoured the water levels west of the Rio Grande in the Espanola Basin. Because the water levels were reported when the wells were drilled, these are described (fig.9) as prepumping water levels. As on the east side, the contours imply ground-water flow toward the Rio Grande.

The hydraulic head in more permeable units below the water surface has been observed at each of the four test sites on the Pueblo Grants of San Ildefonso, Pojoaque, Nambe, and Tesuque. The vertical hydraulic gradients are about 0.12 at the San Ildefonso, Pojoaque, and Tesuque sites, and about 0.20 at the Nambe site.

Hydraulic-Head Distribution Simulated by the Model

Hydraulic heads in the model were obtained by simulating a steady-state condition. The hydraulic heads described in this section were simulated with the model described in the previous sections on structure, aquifer characteristics, and boundaries. The grid blocks are oriented with a strike of N. 25° E., a dip to the northwest of 8° east of the Rio Grande and 4° west of the Rio Grande. The aquifer characteristics are those shown in table 1 as the most likely value. The hydraulic conductivity parallel to the beds is 1 foot per day. The vertical-to-horizontal anisotropy ratio is 0.003. The boundaries include the Rio Grande and the Santa Cruz, Pojoaque, and Santa Fe Rivers and recharge on the perimeter of the basin, as shown in figure 5 and tables 2, 3, and 4.

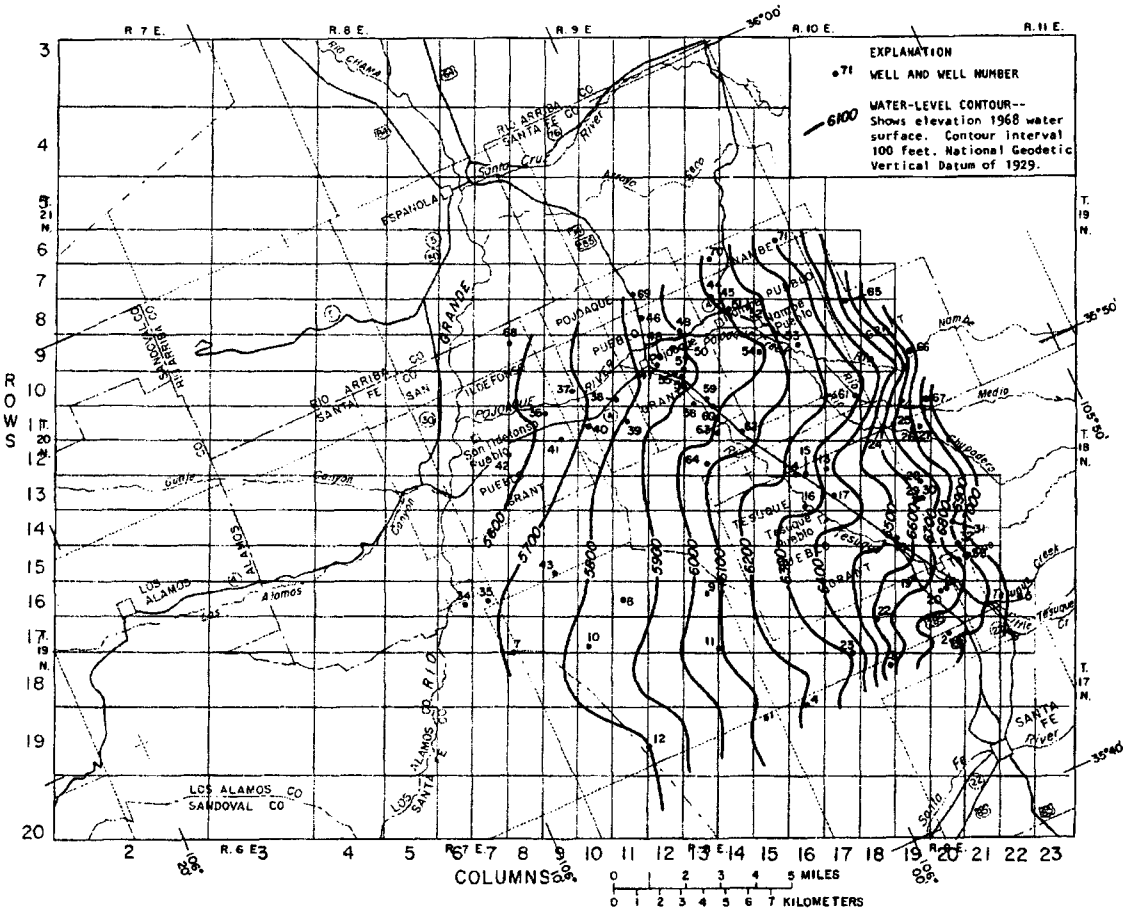

Figure 8. Contours of 1968 water surface east of the Rio Grande.

A comparison of simulated water levels with historical levels shows the extent to which the model represents the historical initial conditions. The water levels reported by Borton (1968) for 71 wells and springs (fig. 8) are compared (fig. 10) with the simulated water surface for the cell representing the square mile in which the well or spring is located. Some of the variability in this relationship (fig. 10) may be due to the representation of the continuous system with discrete cells. For example, wells 13, 14, and 15 are so close together that they are represented by the same cell even though the measured hydraulic heads range from 6,235 feet to 6,391 feet. A slight change in the locations of wells 33 and 54 would have placed them in cells in which the simulated hydraulic heads of 6,805 feet and 6,020 feet, respectively, compare more favorably with the measured hydraulic heads of 6,808 feet and 5,989 feet, respectively. Wells 66 and 67 are located so near the mountain front that the corresponding cells have been defined as being outside the Tesuque aquifer system. These wells are compared with the nearest cells representing the Tesuque aquifer system. Some of the variability in this relationship (fig. 10) may be due to a measured or reported water level unrepresentative of the Tesuque aquifer system. For example, water levels for wells 21, 29, 30, and 42 and springs 9 and 32 are qualified by Borton as representing perched water. Finally, some of the variability in this relationship (fig. 10) is undoubtedly due to the model's not representing the detailed heterogeneity of the Tesuque aquifer system. The author considered the comparison between simulated and historical water levels (fig. 10) to be acceptable.

By comparing the simulated results with contours of water levels rather than historical water-level data, the interpretation of the data also is considered. Contours of the water surface simulated by the model are shown in figure 11. These can be compared to the contours of Trauger (fig. 7) and Borton (fig. 8) that involve interpretation of measured and reported data. The differences between the

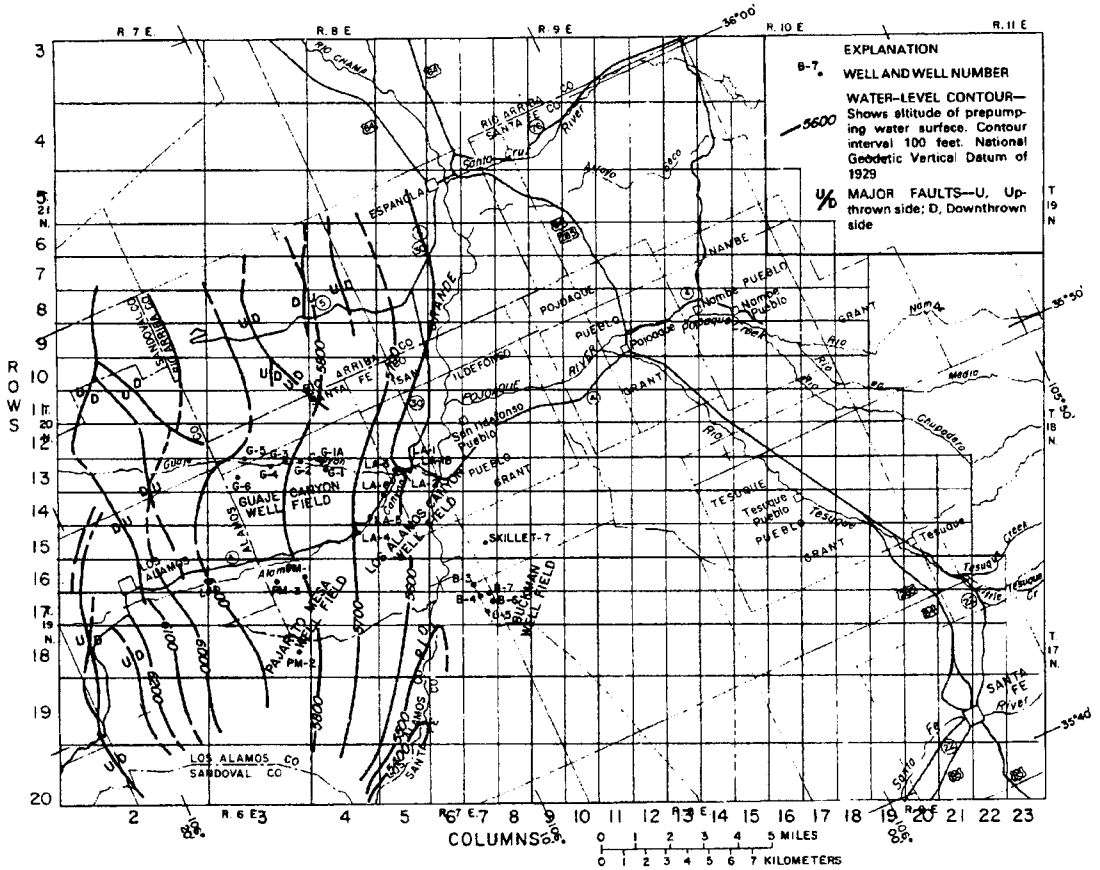

Figure 9. Contours of prepumping water surface west of the Rio Grande.

contours of simulated water levels and those of Trauger are typically less than the differences between the contours of Trauger and those of Borton. For example, Tesuque Pueblo overlies the 6,300-foot contour for the simulated surface (fig. 11) and that of Trauger (fig. 7), and is about one-third of the way between the 6,300- and 6,400-foot contours of Borton (fig. 8). The water surface simulated by the model appears to approximate that of the prototype as closely as the two interpretations of historical data presented by the contours of Trauger and Borton.

Outside of the Pojoaque River basin, the simulated and historical water levels show greater disagreement. This may be due to the arbitrary nature in which boundaries to the north, south, and west are represented. For example, compare the simulated contours (fig. 11) west of the Rio Grande with those of Purtymun and Johansen (fig. 9). However, the effect of these differences is reduced because they are several miles from the area of interest in Pojoaque River basin.

The vertical hydraulic gradients simulated by the steady-state model may be compared (table 5) with those observed at the aquifer test sites on the San Ildefonso, Pojoaque, Nambe, and Tesuque Pueblo Grants. At the individual sites the comparison is variable. The simulated vertical gradients vary from 0.09 for the San Ildefonso and Pojoaque sites to 0.21 for the Tesuque site, although the observed vertical gradient was 0.12 at each of the 3 sites. At the Nambe site the simulated vertical gradient of 0.15 is 25 percent less than the observed value of 0.20. However, the mean of the four simulated values, 0.14, is the same as the mean of the four observed values.

Flow Between Ground Water and Surface Water in the Prototype

Flow between ground water and surface water is typically diffuse and difficult to estimate. The estimate of

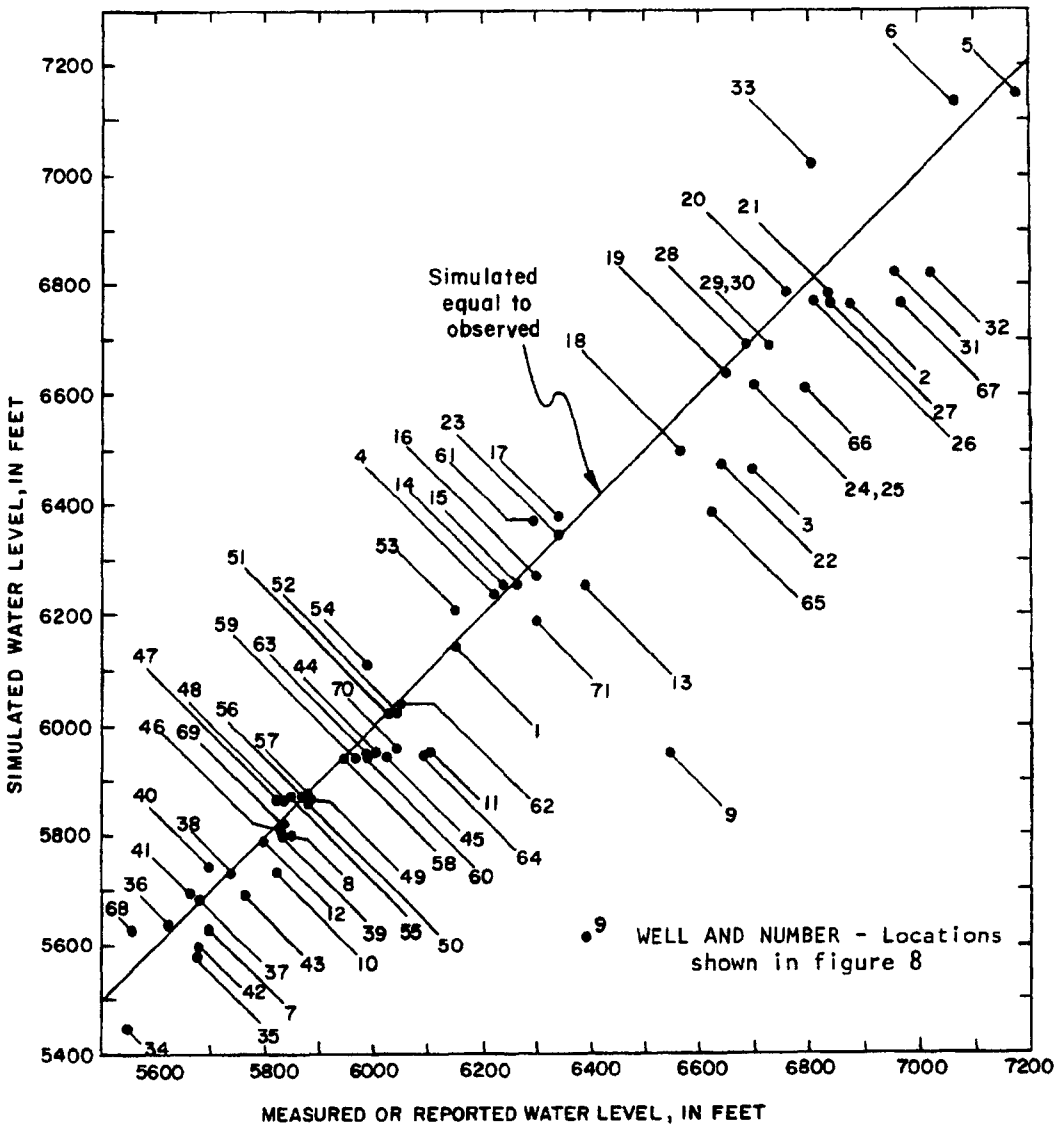

Figure 10. Comparison between measured or reported water levels for selected wells and springs and water levels simulated by the model.

the total gain or loss along a reach of the stream is typically not accurate because the flow to or from the ground-water reservoir is small relative to the flow in the stream.

Rio Grande

The major stream in the modeled area is the Rio Grande. The volume of discharge that reaches the Rio Grande directly from the ground-water system may be estimated. Spiegel and Baldwin (1963, p. 200) estimated that the average discharge of ground water to the Rio Grande is about 25 cubic feet per second in the 20-mile (direct distance) reach downstream from Otowi Bridge (fig. 4) or about 1.2 cubic feet per second per mile. However, days that showed an apparent loss of flow were excluded from this average (Spiegel and Baldwin, 1963, p. 201). If the apparent losses of flow result from errors in measurement, they are probably random and their exclusion may introduce a statistical bias resulting in too

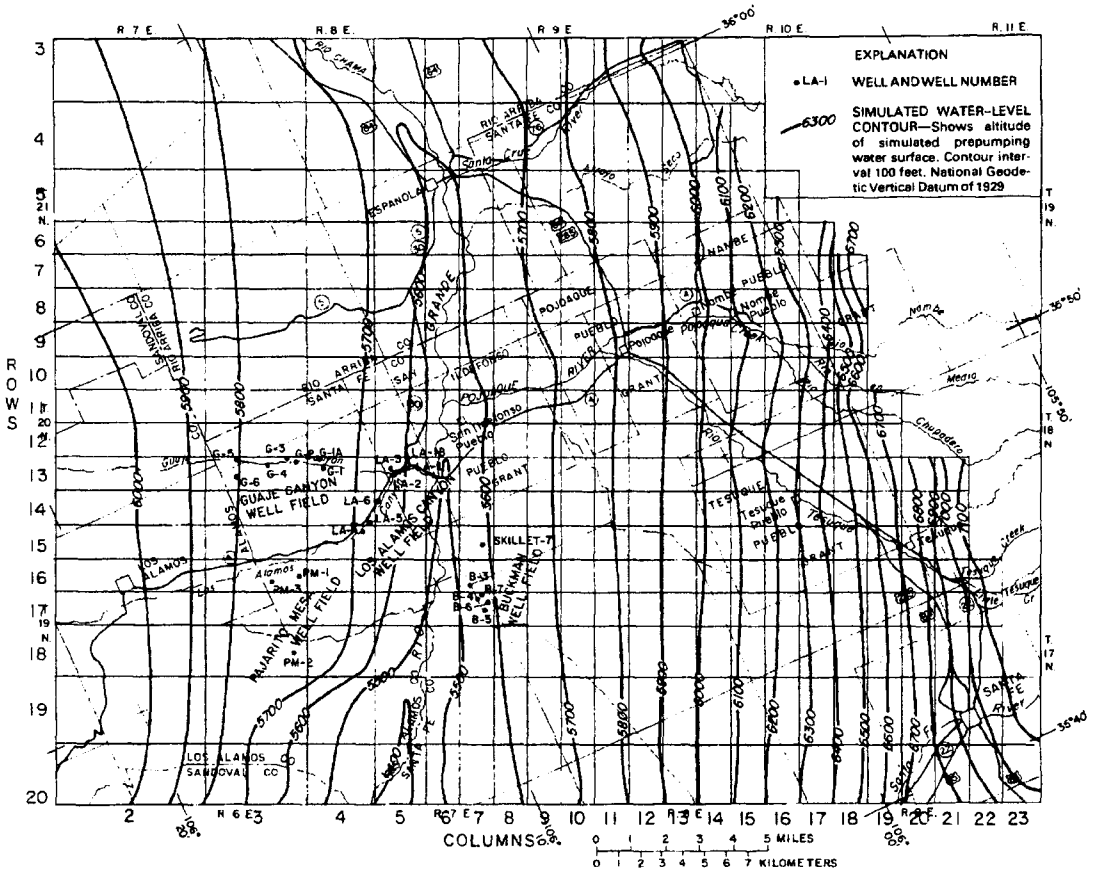

Figure 11. Contours of steady-state water surface simulated by the model.

large an estimated average discharge from the ground-water reservoir. Therefore, the value given by Spiegel and Baldwin probably overestimates the discharge to the Rio Grande.

Another estimate of the average discharge from the Tesuque aquifer system to the Rio Grande can be obtained from the 1961-70 record at the gaging stations at Otowi and Cochiti for periods of low flow. The period of record is prior to the construction of Cochiti Dam. The only gaged inflow between the station at Otowi and the station at Cochiti is from Rito de los Frijoles in Bandelier National Monument, N. Mex. For this 10 years of record, the January flow of the Rio Grande at Otowi was increased by the flow of the Rito de los Frijoles and compared with the flow in the Rio Grande at Cochiti. The mean gain in the flow of the Rio Grande was 4.4 cubic feet per second. The straight-line distance between the two gages of approximately 20 miles indicates an incremental increase of about 0.2 cubic foot per second per mile. The individual monthly records range from losses of 87 cubic feet per second to gains of 47 cubic feet per second. If years showing an apparent loss are eliminated (as done by Spiegel and Baldwin), the biased sample indicates a gain of 21 cubic feet per second or about 1.0 cubic foot per second per mile.

Table 5. Vertical hydraulic gradients

Site at pueblo grant (location shown in fig. 1)	Vertical hydraulic gradient	
	Observed	Simulated
San Ildefonso	0.12	0.09
Pojoaque	.12	.09
Nambe	.20	.15
Tesuque	.12	.21
Mean	.14	.14

Table 6. Water balance for the Pojoaque River and tributaries

Description of flow	Flow, in cubic feet per second	
Tributary inflow		16.90
Consumption by native vegetation		-1.10
Evaporation from river and riverbed		-3.32
Pojoaque River discharge and consumption by irrigation	[1] -14.35	[2] -11.30
Net flow from (+) or to (−) ground-water reservoir, calculated as a residual	[1] +1.87	[2] -1.18

[1] Pojoaque River discharge estimated by Reiland and Koopman (1975) with no diversions for irrigation

[2] Sum of Pojoaque River discharge and diversion for irrigation estimated in previous section on boundaries of the prototype.

Seepage investigations were conducted along the 17.2-mile reach of the Rio Grande upstream from Otowi Bridge on October 18, 1967, March 19, 1968, and September 12, 1968 (U.S. Geological Survey, 1968). The results of these seepage investigations indicate a net loss of 8 cubic feet per second out of 336 cubic feet per second on October 18, 1967, and a net loss of 7 cubic feet per second out of 440 cubic feet per second on September 12, 1968. A net gain of 33 cubic feet per second out of 856 cubic feet per second was indicated by the seepage investigation on March 19, 1968. If the differences between these measurements are the additive effect of many factors acting at random, then the mean provides a more accurate estimate. The mean net gain for these three observations is about 0.3 cubic foot per second per mile.

From the above data it is reasonable to presume that the discharge to the Rio Grande throughout the Espanola Basin averages about 0.5 cubic foot per second per mile or less and is certainly no more than about 1 cubic foot per second per mile.

Santa Cruz and Santa Fe Rivers

The relationship between the Tesuque aquifer system and the Santa Cruz and Santa Fe Rivers is less important to this study because of their distance from the area of interest. No attempt was made to quantify these flows.

Pojoaque River and Tributaries

The flow between surface water and ground water in the Pojoaque River basin is estimated by developing a water balance for the surface-water system. By estimating all other items in the budget, the net recharge to or discharge from ground water can be calculated as a residual. The quantities to be estimated for the water balance are the flow of the tributaries as they discharge onto the Tesuque Formation, losses due to consumption by vegetation, channel losses, and discharge from the Pojoaque River into the Rio Grande.

Reiland (1975) and Reiland and Koopman (1975) estimate the flow of the tributaries as they discharge from the Sangre deCristo Mountains onto the Tesuque Formation. The flows summarized in the previous section on boundaries total about 16.90 cubic feet per second.

Losses due to consumption by vegetation include native vegetation. In the previous section on boundaries, the estimated 315 acres of trees were estimated to consume about 1.10 cubic feet per second.

Losses due to evaporation from 963 acres of river and canal surfaces and exposed channnel beds are estimated in the previous section on boundaries to be about 3.32 cubic feet per second.

Two estimates are available for the sum of the discharge from the Pojoaque River to the Rio Grande and the consumption by irrigation. Reiland and Koopman (1975) estimate the flow, with no diversions for irrigation, to be 14.35 cubic feet per second. In the previous section on boundaries of the prototype, the discharge under the present (1980) irrigation conditions is estimated to be about 3.63 cubic feet per second.

Under present (1980) conditions, water is diverted for about 3,700 acres of irrilgated land. The previous section on boundaries assumed a consumption use of 1.5 acre-feet per acre per year to estimate irrigation consumption at about 7.67 cubic feet per second.

The net flow calculated as a residual (table 6) ranges from 1.87 cubic feet per second from the ground- water reservoir (using the Reiland-Koopman estimate) to 1.18 cubic feet per second to the ground- water reservoir (using the second estimate). The two residuals appear quite different because they are each less than the error of estimating the other items in the water balance. A 20-percent error in the estimate of the sum of the Pojoaque River discharge and consumption by irrigation would result in a difference of about 2.87 cubic feet per second using the Reiland-Koopman estimate and 0.73 cubic foot per second for present (1980) irrigation conditions. Assuming a 20 percent error in each item results in residuals ranging from −7.70 cubic feet per second to +9.00 cubic feet per second. Because of this uncertainty, any change in the relationship between ground water and surface water from pristine conditions to the present (1980) irrigation condition is not detected in the water balance.

From the above water balances, it seems reasonable to conclude that the net flow between the Pojoaque River and its tributaries and the Tesuque aquifer system is probably less than 5 cubic feet per second and could be either to or from the aquifer system.

Table 7. Simulated steady-state flow rates at specified hydraulic-head boundaries.

[ft^3/s = cubic foot per second]

Location			Flow rate to aquifer (ft^3/s)
Row	Column	Layer	
2	4	21	−0.8170
3	4	21	− .6055
4	5	20	−1.1390
5	6	19	− .8328
6	6	19	− .3961
7	6	19	− .4041
8	6	19	.4114
9	6	19	− .4280
10	6	19	− .4364
11	6	19	− .4268
12	6	19	− .4250
13	6	19	− .4286
14	6	19	− .4914
15	6	19	− .5052
16	6	19	− .5241
17	6	19	− .5456
18	6	19	− 1.1329
19	5	20	−1.0344
20	5	20	− .8202
21	4	20	−4.0078
22	4	20	−3.0804
23	4	20	−3.1699
3	13	12	1.3444
3	12	13	1.2669
3	11	14	.9599
4	10	15	.5394
4	9	16	− .1299
4	8	17	− .4804
4	7	18	− .8998
22	14	11	−1.2114
23	13	12	− .0168
23	12	13	− .0203
23	11	14	− .0149
23	10	15	− .2130
23	9	16	.5167
23	8	17	− .6400
23	7	18	− .6475
23	6	19	− .9872
23	5	20	− .0793

Flow Between Ground Water and Surface Water Simulated by the Model

The model, as defined above, was used to simulate a steady-state condition. The simulated steady-state flow rates between ground water and surface water are shown in table 4 for specified-flow boundaries, table 7 for specified-hydraulic-head boundaries, and table 8 for hydraulic-head dependent boundaries. All boundaries are shown in figure 5. The simulated flow rates are given to a precision that exceeds the predictive accuracy of the model. This is done to be consistent with the flow rates given in table 4, where the values are given in the precision with which they were entered into the model.

Rio Grande

Discharge of ground water to the Rio Grande is simulated as 22.06 cubic feet per second or about 0.5 cubic foot per second per mile. Because there is no change in storage in a steady-state condition, recharge must equal discharge. An estimate was made of the contribution from each side of the Rio Grande in the model by considering the recharge to that side as a percentage of the total discharge. Recharge on the west of the Rio Grande is about 12.76 cubic feet per second or 58 percent, and recharge on the east is about 9.29 cubic feet per second or 42 percent of the total discharge to the Rio Grande. On the east of the Rio Grande, estimates were made of the contributions from the Pojoaque River basin, north of the basin, and south of the basin.

Santa Cruz and Santa Fe Rivers

The Santa Cruz River, as represented in the model, recharges 4.11 cubic feet per second to the ground- water reservoir and discharges 1.50 cubic feet per second for a net recharge of 2.61 cubic feet per second.

Table 8. Simulated steady-state flow rates at hydraulic-head dependent boundaries

[ft^3/s = cubic foot per second]

Location			River reach	Flow rate to aquifer (ft^3/s)
Row	Column	Layer		
9	18	7	1	1.005
9	17	8	1	.301
11	19	6	2	.639
10	18	7	2	.551
10	17	8	2	.039
11	18	7	3	.536
11	17	8	3	0
10	16	9	3	0
9	16	9	4	− .287
9	15	10	4	− .101
8	14	11	4	− .031
9	13	12	4	.016
9	12	13	4	− .027
16	22	3	5	.419
17	22	3	6	.553
16	21	4	7	− .262
15	20	5	7	.066
15	19	6	7	.064
14	18	7	7	− .078
14	17	8	7	.272
13	16	9	7	.276
12	15	10	7	.341
12	14	11	7	.363
11	13	12	7	.083
10	12	13	7	.044
9	11	14	8	.090
10	10	15	8	− .181
10	9	16	8	.198
11	8	17	8	− .237
11	7	18	8	− .294

Table 9. Water balance for the Pojoaque River and tributaries using simulated flows from the digital model.

Description of flow	Flow, in cubic feet per second
Tributary inflow[1]	16.90
Consumption by native vegetation[2]	−1.10
Net flow to ground water[3]	−0.04
Evaporation from the river and riverbed[4]	−3.32
Pojoaque River discharge[4] and consumption by irrigation calculated as a residual	−12.44

[1] This value was represented as flow available for recharge to the ground-water reservoir as leakage from streams.
[2] Consumption by native vegetation is represented as specified flows from the ground-water reservoir.
[3] Simulated by the digital model.
[4] The sum of these values is calculated by the model as flow remaining in the Pojoaque River.

Recharge concentrated at the headwaters of Arroyo Seco is simulated as 0.71 cubic foot per second. The net recharge east of the Rio Grande and north of Pojoaque River basin is 3.32 cubic feet per second or about 36 percent of the total recharge east of the Rio Grande.

The Santa Fe River, as represented in the model, recharges 7.21 cubic feet per second to the ground- water reservoir and discharges 4.35 cubic feet per second for a net recharge of 2.86 cubic feet per second or about 31 percent of the total recharge east of the Rio Grande. This is the only recharge south of Pojoaque River basin.

Pojoaque River and Tributaries

The remaining one-third of the recharge east of the Rio Grande is simulated in the Pojoaque River basin. The Pojoaque River and its major tributaries, as represented in the model, recharge 4.25 cubic feet per second to the ground-water reservoir. Discharge simulated by the model includes 3.11 cubic feet per second to the Pojoaque River and 1.10 cubic feet per second to native vegetation and is nearly equal to the recharge. Recharge concentrated along the mountain front in the Pojoaque River basin is simulated as 3.07 cubic feet per second. The net recharge simulated for the Pojoaque River basin is 3.11 cubic feet per second or about 33 percent of the total recharge east of the Rio Grande.

With the flows between the Tesuque aquifer system and the Pojoaque River simulated by the model, the water balance shown in table 6 can be restructured with the flow from the Pojoaque River to the Rio Grande and consumption by irrigation calculated as the residual (table 9). The sum calculated from the steady-state simulation is 12.44 cubic feet per second, 13 percent less than the Pojoaque River discharge of 14.35 cubic feet per second estimated by Reiland and Koopman (1975) and 10 percent more than the sum of 11.30 cubic feet per second estimated in the previous section on boundaries of the prototype (table 6). The flow remaining in the Pojoaque River is simulated as 15.76 cubic feet per second. Allowing 7.67 cubic feet per second for irrigation and 3.32 cubic feet per second for river and riverbed evaporation, the Pojoaque River discharge to the Rio Grande is calculated to be 4.77 cubic feet per second, 30 percent more than the 5-year median estimated from periodic measurements (table 6).

The simulated flow between ground water and surface water is compatible with observed data. A more precise adjustment of the model is not justified by available data.

CHANGES SUPERIMPOSED ON STEADY-STATE CONDITION

The second stage of the simulation represents the history of ground-water withdrawals. The historical withdrawals and the resultant changes in hydraulic head and in flow between ground water and surface water are presented first for the prototype and then as represented in and simulated by the model. The projected withdrawals for irrigation development are presented first as they may occur in the prototype and then as they are represented in the model. The simulated response to the withdrawals for irrigation development is discussed in a separate section.

History in the Prototype

Two stresses have been applied to the Tesuque aquifer system for a sufficiently long time to affect the ground-water levels and streamflows in the modeled area. These are irrigation and the municipal withdrawals at the Los Alamos Canyon, Guaje Canyon, Pajarito Mesa, and Buckman well fields.

Withdrawals

Historical irrigation has primarily diverted surface water to irrigate lands near the principal streams: the Pojoaque River, the Santa Cruz River, and the Rio Grande. The effect of this irrigation on the ground-water system is assumed to be negligible. The irrigation consumes water which would otherwise be contributing to the flow in the streams. The net ground-water contribution has probably not changed significantly.

Ground-water withdrawals for the municipal supply of Los Alamos have been made from the Los Alamos Canyon well field since 1947, the Guaje Canyon well field since 1950, and the Pajarito Mesa well field (fig. 11) since

Table 10. History of withdrawals from the Los Alamos Canyon, Guaje Canyon, Pajarito Mesa, and Buckman well fields

[From Purtymun, 1978, appendix B for LA, G, and PM wells. From oral communication with Public Service Company of New Mexico for B wells. Well locations shown on fig. 11]

	Well																				
Year	LA-1	LA-1B	LA-2	LA-3	LA-4	LA-5	LA-6	G-1	G-1A	G-2	G-3	G-4	G-5	G-6	PM-1	PM-2	PM-3	B-3	B-4	B-5	B-6
1947	54.0		27.6	64.9																	
1948	34.7		59.3	82.5	42.7	40.4	4.9														
1949	26.7		41.8	41.7	37.5	58.5	95.8														
1950	10.5		15.6	57.8	164.9	130.1	167.9	2.8													
1951	14.6		57.7	66.9	173.6	187.4	201.6	37.7		3.9	7.3	12.5	6.7								
1952	3.4		46.3	58.6	119.6	109.6	110.3	75.5		78.3	65.4	56.9	73.8								
1953	0.0		47.2	69.7	109.1	103.9	113.8	97.3		105.6	76.4	55.2	37.8								
1954	0.0		56.8	57.3	78.2	80.1	107.1	77.8	4.6	86.3	66.1	58.8	80.9								
1955	9.7		49.4	48.7	94.5	97.3	108.0	70.5	53.0	78.8	69.4	22.7	80.4								
1956	0.0		44.2	42.1	120.2	104.5	125.8	83.2	107.7	95.8	87.9	33.9	97.0								
1957	0.0		29.6	26.1	105.4	86.0	102.4	55.9	87.0	76.1	70.2	24.2	64.1								
1958	0.0		31.1	33.6	110.3	89.9	106.9	68.1	92.5	80.1	69.5	35.9	49.1								
1959	0.0		40.7	35.0	113.5	93.5	108.3	82.4	102.7	84.6	74.6	31.6	101.7								
1960	0.0	36.3	51.6	38.4	145.6	119.1	138.6	96.0	122.8	96.6	82.5	37.0	98.0								
1961	0.0	124.7	44.4	34.7	129.7	100.3	112.5	112.4	147.3	105.3	79.9	45.0	134.0								
1962	0.0	129.1	35.7	45.4	129.3	107.7	129.4	93.6	136.1	99.8	83.7	41.7	142.0								
1963	0.0	117.4	40.7	42.5	130.5	105.0	102.9	114.9	149.7	105.7	86.7	46.4	151.0								
1964	0.0	130.3	34.2	50.4	155.0	118.8	138.3	113.8	129.3	105.3	78.6	42.9	150.4	45.0							
1965	0.0	97.9	39.8	43.4	111.4	50.5	103.8	90.7	116.5	82.6	65.6	23.8	117.1	74.9	99.2						
1966	0.0	83.9	21.4	46.1	115.6	79.3	104.0	102.6	133.4	94.7	73.7	33.6	83.2	92.2	108.0	18.9					
1967	0.0	84.9	4.9	47.4	77.1	73.7	85.4	69.9	91.3	67.6	52.9	44.8	80.0	57.8	110.0	370.0					
1968	0.0	74.0	11.3	42.7	81.7	63.3	71.6	78.9	103.2	66.5	56.5	31.4	81.2	56.2	68.1	328.2	187.4				
1969	0.0	75.7	3.8	40.1	61.8	68.5	81.6	68.3	90.7	68.6	50.8	17.4	83.3	55.6	34.4	279.9	254.7				
1970	0.0	79.7	7.2	44.0	83.5	66.1	79.1	64.7	92.5	72.8	55.4	7.7	88.9	51.0	66.2	300.6	227.8				
1971	0.0	89.1	31.8	45.4	89.0	74.4	82.5	67.9	111.8	87.4	64.2	21.0	88.3	42.8	101.0	339.5	216.3				
1972	0.0	75.3	39.3	39.7	82.6	64.4	79.2	66.1	94.0	73.4	50.9	33.3	92.4	57.0	84.9	385.3	192.1	([1])	([1])	([1])	([1])
1973	0.0	87.2	46.7	20.3	92.4	68.3	90.6	67.5	87.9	72.4	47.3	37.2	97.5	65.3	46.5	380.6	257.8	254.7	238.2	0.0	244.7
1974	0.0	73.9	36.8	43.5	82.2	52.5	79.8	62.3	92.7	82.0	49.3	34.3	69.0	63.8	96.3	450.9	255.3	337.0	305.6	60.1	368.7
1975	0.0	74.4	40.2	43.3	82.3	63.9	51.9	55.7	85.3	74.5	43.1	41.0	74.7	56.7	94.8	385.3	269.3	215.6	238.0	24.7	294.9
1976	0.0	79.6	39.9	42.3	98.2	77.6	5.1	65.1	91.6	81.1	82.6	57.8	95.0	57.8	106.8	442.0	268.3	290.3	312.7	0.3	277.1
1977	0.0	84.2	42.5	47.3	96.4	74.8		57.9	88.7	80.4	78.9	62.4	92.1	54.4	105.4	272.8	235.5	325.9	342.1	0.0	292.2

[1] Total production of field is 270 million gallons, but no data for individual wells.

1965 (table 10). Total withdrawals from the three well fields have ranged from 147 million gallons in 1947 to 1,691 million gallons in 1976.

Withdrawals from the Tesuque aquifer system in the Buckman well field (fig. 11) provide some of the municipal supply of Santa Fe. Estimates of these withdrawals have been provided by the Public Service Company of New Mexico (table 10). Withdrawals from the Buckman well field have ranged from 270 million gallons in 1972 to 1,071 million gallons in 1974.

Change in Hydraulic Head

The response of the Tesuque aquifer system to withdrawals in the well fields supplying Los Alamos has been monitored in the production wells. The changes in water levels have been recorded as changes in the average annual nonpumping water level in production wells (Purtymun, 1978, appendix B). Depths of the water levels below land surface are shown in table 11.

The response of the Tesuque aquifer system to withdrawals made at the Buckman well field has been reported as changes in depth to water in wells of the Buckman well field. Depth to water measurements in Buckman Well No. 7 (B-7) provided by the Public Service Company of New Mexico are shown in table 11.

Change in Flow between Ground Water and Surface Water

Effects of historical withdrawals on the flows between ground water and the surface water or on water levels in Pojoaque River basin have not been quantified.

Table 11. Measured depths to water in wells of the Los Alamos Canyon, Guaje Canyon, Pajarito Mesa, and Buckman well fields

[From Purtymun, 1978, Appendix B for LA.G. and PM wells. From oral communication with Public Service Company of New Mexico for well B-7. Well location shown in figure 11; first measurement in each column indicates year well was drilled.]

	Well																	
Year	LA-1	LA 1B	LA-2	LA-3	LA-4	LA-5	LA-6	G-1	G-1A	G-2	G-3	G-4	G-5	G-6	PM-1	PM-2	PM-3	B-7
1947																		
1948																		
1949																		
1950	19.0		59.0	97.0	278.0	131.0	83.0	195.0										
1951	59.0		111.0	116.0	285.0	162.0	115.0	202.0		259.0	281.0	357.0	414.0					
1952	40.0		101.0	94.0	267.0	147.0	108.0	213.0		279.0	310.0	374.0	422.0					
1953	36.0		100.0	103.0	264.0	141.0	95.0	221.0		290.0	322.0	380.0	425.0					
1954	44.0		116.0	101.0	255.0	137.0	92.0	221.0		291.0	322.0	383.0	429.0					
1955	51.0		110.0	91.0	268.0	145.0	97.0	226.0	265.0	299.0	316.0	378.0	427.0					
1956	33.0		84.0	74.0	273.0	150.0	106.0	235.0	273.0	310.0	324.0	377.0	431.0					
1957	33.0		53.0	56.0	270.0	150.0	107.0	236.0	274.0	311.0	324.0	373.0	424.0					
1958	10.0		60.0	49.0	270.0	151.0	108.0	238.0	279.0	315.0	323.0	370.0	428.0					
1959	13.0		71.0	54.0	275.0	155.0	115.0	245.0	284.0	320.0	326.0	378.0	435.0					
1960	13.0	7.0	76.0	68.0	296.0	168.0	130.0	254.0	291.0	328.0	335.0	385.0	437.0					
1961	59.0	54.0	101.0	85.0	296.0	165.0	129.0	260.0	298.0	336.0	343.0	389.0	438.0					
1962	84.0	72.0	111.0	93.0	286.0	172.0	135.0	258.0	295.0	338.0	348.0	386.0	440.0					
1963	90.0	74.0	127.0	81.0	280.0	171.0	125.0	265.0	301.0	344.0	352.0	388.0	441.0					
1964	95.0	81.0	137.0	104.0	291.0	184.0	132.0	269.0	302.0	346.0	355.0	396.0	446.0	581.0				
1965	76.0	63.0	121.0	79.0	279.0	180.0	120.0	268.0	302.0	346.0	350.0	394.0	443.0	582.0	746.0			
1966	70.0	50.0	108.0	81.0	285.0	180.0	129.0	269.0	306.0	349.0	353.0	391.0	445.0	585.0	740.0	826.0		
1967	52.0	39.0	78.0	86.0	278.0	168.0	118.0	266.0	302.0	344.0	344.0	388.0	444.0	580.0	737.0	834.0		
1968	42.0	32.0	64.0	82.0	280.0	161.0	109.0	264.0	302.0	344.0	341.0	386.0	443.0	574.0	735.0	838.0	743.0	
1969	38.0	22.0	50.0	58.0	282.0	161.0	109.0	266.0	303.0	344.0	338.0	387.0	450.0	568.0	733.0	838.0	746.0	
1970	37.0	22.0	59.0	55.0	286.0	157.0	106.0	264.0	300.0	343.0	336.0	384.0	453.0	569.0	733.0	839.0	750.0	
1971	51.0	31.0	88.0	77.0	287.0	155.0	119.0	258.0	303.0	345.0	342.0	389.0	450.0	573.0	733.0	841.0	751.0	
1972	49.0	31.0	96.0	73.0	282.0	153.0	117.0	264.0	302.0	348.0	341.0	391.0	441.0	578.0	735.0	845.0	752.0	
1973	55.0	37.0	106.0	65.0	294.0	156.0	118.0	271.0	302.0	344.0	341.0	392.0	444.0	579.0	736.0	849.0	755.0	124.2
1974	53.0	35.0	109.0	73.0	286.0	154.0	120.0	283.0	307.0	347.0	342.0	392.0	440.0	579.0	740.0	853.0	756.0	160.1
1975	58.0	42.0	103.0	80.0	272.0	149.0	113.0	293.0	304.0	341.0	341.0	403.0	433.0	577.0	741.0	854.0	757.0	200.0
1976	69.0	50.0	113.0	88.0	277.0	150.0	96.0		302.0	344.0	374.0	406.0	442.0	584.0	744.0	866.0	758.0	239.6
1977	74.0	47.0	118.0	89.0	278.0	147.0	82.0	275.0	302.0	346.0	368.0	406.0	444.0	586.0	745.0	868.0	758.0	203.5

History Represented in the Model

The second stage of the simulation begins in 1947 with the first withdrawals from the Los Alamos Canyon wells and continues through 1980. The simulation of historical withdrawals was superimposed on the steady-state condition described previously. The historical withdrawals are represented in the model as an additional specified-flow boundary condition. The response simulated by the mathematical model is presented with a precision that exceeds the accuracy of the model in order to show the magnitude of small simulated changes.

Withdrawals

To extend the historical phase of the simulation through 1980, the withdrawals through 1980 are estimated. For the Buckman wells, the withdrawals from 1977 through 1980 are assumed to continue at the 1977 rate (table 10). Total production in 1977 from the well fields supplying Los Alamos was the smallest since 1970. This reduction is believed to be temporary; the withdrawals from 1978 through 1980 are assumed to continue at the 1976 rate (table 10).

Change in Hydraulic Head

Two characteristics of the data need to be considered in evaluating the comparison between simulated and historical changes in water level. First, the model simulates the change in water level relative to the steady-state water level for the entire cell in response to the average annual withdrawals. Because the points of withdrawal are distant from the Pojoaque River basin, the simulated withdrawals are from very large cells; some of the cells are approximately 3 miles across. As a result, the simulated water level should approximate only the general downward trend of the historical water-level changes; seasonal responses are not simulated. Second, in the wells supplying Los Alamos, the water level is the annual average of nonpumping water levels measured in the production wells. These water levels represent the average of several measurements in a production well after it has stopped withdrawing water for some time. Because the wells are used in production, the nonpumping water level fluctuates in response to a variety of factors including the length of time during which withdrawals were made, the rate of withdrawal before the pumping was stopped, and the length of time the well has been allowed to recover before the measurement was made. In spite of these variations,

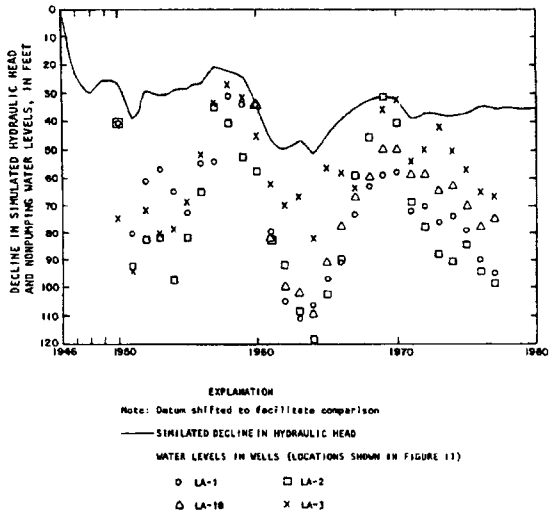

Figure 12. Comparison between decline in hydraulic head simulated at row 13, column 5, layer 19 of the mathematical model and declines in nonpumping water levels measured in wells LA–1, LA–1B, LA–2, and LA–3.

long-term trends can be observed in the nonpumping water levels (table 11). Because of these factors, measurements during years in which withdrawals are small may be more representative than other years of the aquifer system in the vicinity of the well.

The graphical comparison of simulated and historical declines in water level is facilitated by shifting the datum for the vertical scale. In figures 12-20, the datum for the historical declines in water level is shifted vertically to where the simulated response forms an upper envelope for all values. For example, in figure 12 the datum for nonpumping water levels for well LA-1 was shifted vertically to where the water level for 1960 coincides with the curve showing simulated water-level declines; all other water levels for well LA-1 are below the curve. Similarly, the datum for nonpumping water levels for well LA-2 was shifted vertically to the position where the water level for 1969 coincides with the curve showing simulated water-level declines; all other water levels for LA-2 are below the curve.

The declines in nonpumping water levels measured in wells LA-1, LA-1B, LA-2, and LA-3 (table 11) in the Los Alamos Canyon well field were compared with the water-level declines simulated in row 13, column 5, layer 19 of the model (fig. 12). This cell measures 1 mile by 1.5 miles by 650 feet thick. Some of the difference between observed and simulated declines appear to be due to the measurements being made in a production well. The sags in measured water levels (fig. 12) correspond approximately to periods of large withdrawals (table 10); from 1950 through 1954 the withdrawals from LA-3 were large; during 1960 withdrawals from well LA-1B were started; and during 1971 withdrawals from well LA-2 were increased after 4 years of relative nonuse.

The declines in nonpumping water levels in well LA-4 (table 11) in the Los Alamos Canyon well field were compared with the water-level declines simulated in row 15, column 4, layer 20 of the model (fig. 13). This cell measures 1 mile by 2 miles by 975 feet thick. The peak withdrawal years (table 10) of 1950, 1951, 1960, and 1964 correspond to sags in the measured water levels (fig. 13).

The declines in nonpumping water levels in well LA-5 (table 11) in the Los Alamos Canyon well field were compared with the water-level declines simulated in row 14, column 4, layer 20 of the model (fig. 14). This cell measures 1 mile by 2 miles by 975 feet thick. As the annual discharge ranged from 80.1 to 187.4 million gallons from 1950 through 1964 (table 10), the sag in measured water levels gradually increased (fig. 14). As the annual discharge decreased to a range of 50.5 to 79.3 million gallons from 1965 through 1977 (table 10), the sag in measured water levels gradually decreased (fig. 14).

The declines in nonpumping water levels in well LA-6 (table 11) in the Los Alamos Canyon well field were compared with the water-level declines simulated in row 14, column 5, layer 19 of the model (fig. 15). This cell measures 1 mile by 1.5 miles by 650 feet thick. The rapid rise in measured water levels during 1976 and 1977 (fig. 15) corresponds to the period in which the well was placed on standby (Purtymun, 1978, p. 11) and withdrawals ceased (table 10).

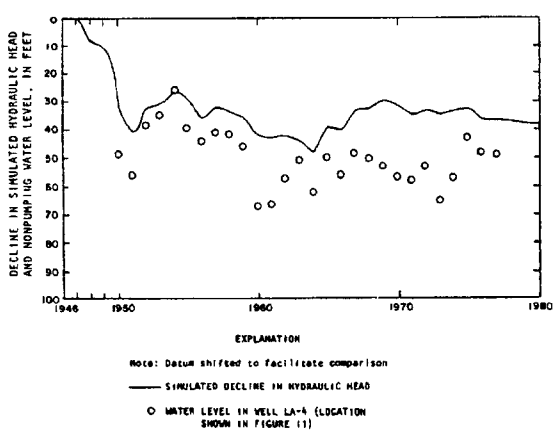

Figure 13. Comparison between decline in hydraulic head simulated at row 15, column 4, layer 20 of the mathematical model and decline in nonpumping water level measured in well LA–4.

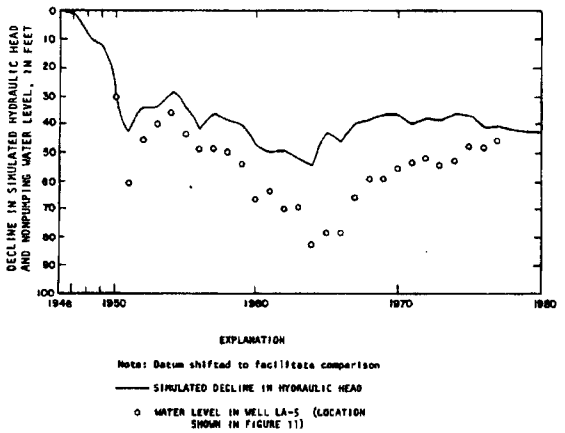

Figure 14. Comparison between decline in hydraulic head simulated at row 14, column 4, layer 20 of the mathematical model and decline in nonpumping water level measured in well LA–5.

The declines in nonpumping water levels in wells G-1 and G-1A (table 11) in the Guaje Canyon well field were compared with the water-level declines simulated in row 13, column 4, layer 20 of the model (fig. 16). This cell measures 1 mile by 2 miles by 975 feet thick. The rate of decline in water level from about 1954 through about 1964 is about the same for measured and simulated data (fig. 16). However, the simulated water levels show an increase of about 15 feet by 1980 that is not apparent in the measured water-level data (fig. 16). There is no obvious correlation between the annual withdrawals (table 10) and the difference between measured and simulated water levels (fig. 16).

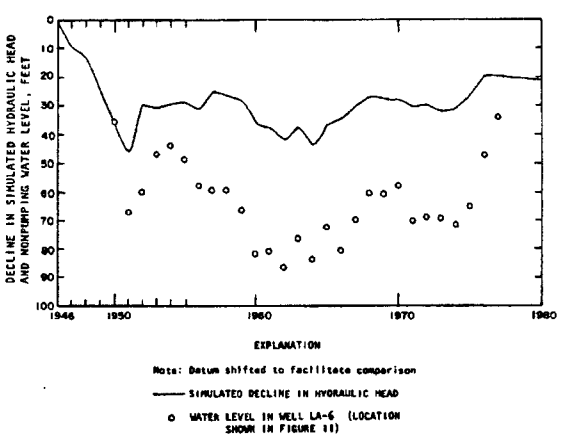

Figure 15. Comparison between decline in hydraulic head simulated at row 14, column 5, layer 19 of the mathematical model and decline in nonpumping water level measured in well LA–6.

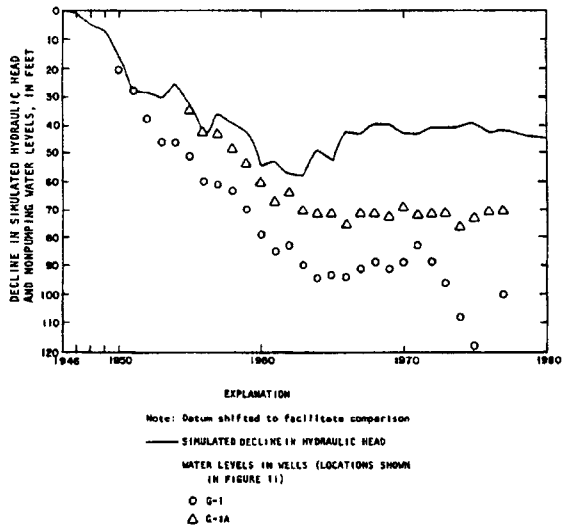

Figure 16. Comparison between decline in hydraulic head simulated at row 13, column 4, layer 20 of the mathematical model and declines in nonpumping water levels measured in wells G–1 and G–1A.

The declines in nonpumping water levels in wells G-2, G-3, G-4, G-5, and G-6 (table 11) in the Guaje Canyon well field were compared with the water-level declines simulated in row 13, column 3, layer 21 of the model (fig. 17). This cell, which measures 1 mile by 3 miles by 1,300 feet thick, is a water-table cell with a saturated thickness of about 1,170 feet under steady-state conditions. The measured water levels of wells G-4, G-5, and G-6 follow the trend of the simulated water-level declines more closely than do the measured water levels for wells G-2 and G-3 (fig. 17).

The declines in nonpumping water levels in wells PM-1 and PM-3 (table 11) in the Pajarito Mesa well field were compared with the water-level declines simulated in row 16, column 3, layer 21 of the model (fig. 18). This cell, which measures 1 mile by 3 miles by 1,300 feet thick, is a water-table cell with a saturated thickness of about 1,150 feet under steady-state conditions. After 1969 the simulated declines in water level closely approximate the measured declines (fig. 18).

The declines in nonpumping water levels in well PM-2 (table 11) in the Pajarito Mesa well field were compared with the water-level declines simulated in row 18, column 3, layer 21 of the model (fig. 19). This cell, which measures 1.5 miles by 3 miles by 1,300 feet thick, is a water-table cell with a saturated thickness of about 1,140 feet under steady-state conditions.

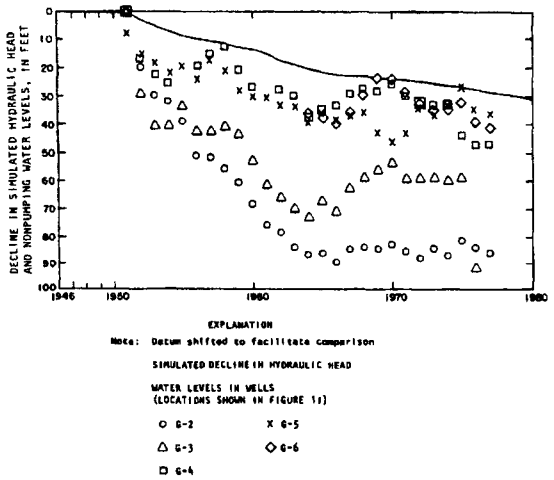

Figure 17. Comparison between decline in hydraulic head simulated at row 13, column 3, layer 21 of the mathematical model and declines in nonpumping water levels measured in wells G–2, G–3, G–4, G–5, and G–6.

The declines in water levels in well B-7 (table 11) in the Buckman well field were compared with the water-level declines simulated in row 17, column 7, layer 17 of the model (fig. 20). This cell measures 1 mile square by 650 feet thick.

As anticipated, the simulated water-level declines reflect the general trend of changes in measured water levels, but the short-term responses are severely damped. The agreement is best during periods of small withdrawal rates.

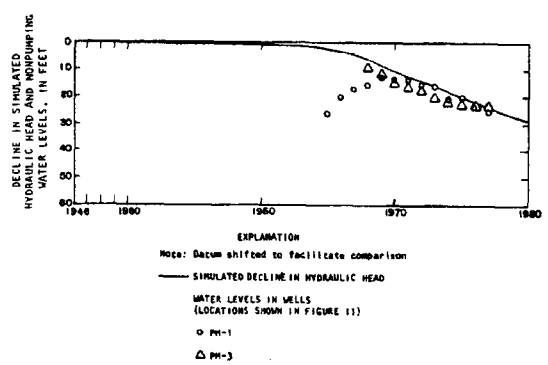

Figure 18. Comparison between decline in hydraulic head simulated at row 16, column 3, layer 21 of the mathematical model and declines in nonpumping water levels measured in wells PM–1 and PM–3.

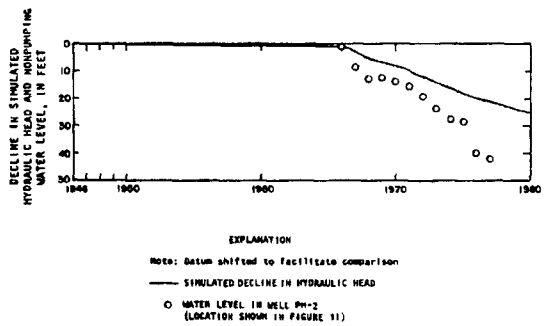

Figure 19. Comparison between decline in hydraulic head simulated at row 18, column 3, layer 21 of the mathematical model and decline in nonpumping water level measured in well PM–2.

Simulated changes in hydraulic head in the Pojoaque River basin vary from negligible along the mountain front to a few feet just east of the Rio Grande. Near San Ildefonso Pueblo, the hydraulic head simulated at the water-table cell declined about 2 feet and the hydraulic head simulated at the underlying artesian cell declined about 4 feet from 1946 through 1980.

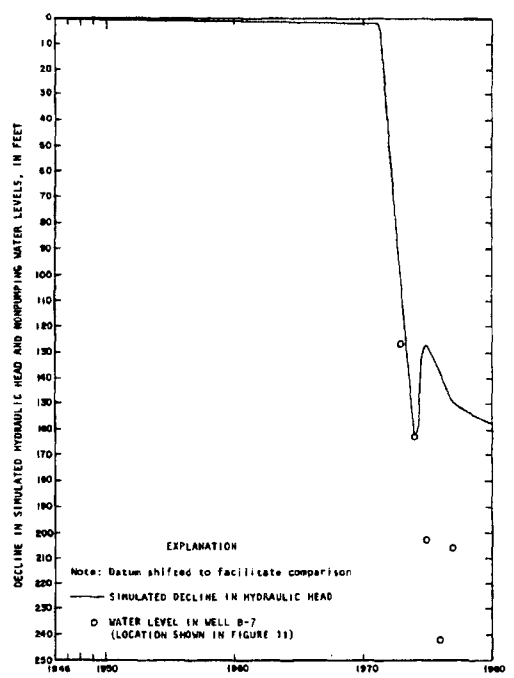

Figure 20. Comparison between decline in hydraulic head simulated at row 17, column 7, layer 17 of the mathematical model and decline in water level measured in well B-7.

Change in Flow between Ground Water and Surface Water

The simulated change in flow between ground water and surface water is concentrated in the simulated discharge to the Rio Grande, which decreases from 22.06 cubic feet per second in steady-state condition to 21.04 cubic feet per second in 1980. This decrease of 1.02 cubic feet per second is only about 2 percent of the minimum streamflow of 60 cubic feet per second and less than 0.1 percent of the average streamflow recorded for the Rio Grande at Otowi Bridge.

The net flow from the Santa Cruz River to ground water is simulated to increase from 2.61 cubic feet per second in steady-state condition to 2.65 cubic feet per second in 1980.

Ground-water discharge to the Pojoaque River is simulated to decrease from 3.11 cubic feet per second in steady-state condition to 3.06 cubic feet per second in 1980. Recharge from the Pojoaque River is simulated to remain the same as in steady-state condition, 4.25 cubic feet per second.

Simulated flow from the Tesuque aquifer system to the Santa Fe River declined from 4.35 cubic feet per second at steady-state condition to 4.34 cubic feet per second in 1980. Changes of these magnitudes would be difficult to observe by direct measurement.

Projected Withdrawals and Diversions in the Prototype

The U.S. Bureau of Indian Affairs has proposed that the water resources of Pojoaque River basin be used for the development of irrigation. To evaluate the impact of such a development, the Bureau has projected the ground-water withdrawals and surface-water diversions during the next 100 years for two alternative conditions. The null future condition is one of no development; historical withdrawals are continued, but no additional withdrawals or diversions are projected. The alternative future condition includes withdrawals and diversions for a tribal irrigation development, irrigation of nontribal land, and supply for additional municipal, industrial, and domestic demand in addition to continued historical withdrawals.

The projection of historical stresses assumes no change in stress. Withdrawals from the Los Alamos Canyon, Guaje Canyon, and Pajarito Mesa well fields were assumed to continue at the 1976 rate (table 10). Withdrawals from the Buckman well field were assumed to continue at the 1977 rate (table 10). Total projected withdrawals are 11.24 cubic feet per second.

The alternative future condition projects a net withdrawal of 28.39 cubic feet per second in addition to the 11.24 cubic feet per second for continued historical withdrawals, for a total withdrawal of 39.63 cubic feet per second. The additional withdrawals of 28.39 cubic feet per second include 25.06 cubic feet per second (88 percent) for irrigation of tribal land, 2.99 cubic feet per second (11 percent) for irrigation of nontribal land, and 0.33 cubic foot per second (1 percent) for increased municipal and domestic demands.

The plan for the tribal irrigation development includes surface-water diversions to canals from the major tributaries of the Pojoaque River. During periods of low surface-water flow, the flow of the canals would be augmented by ground water. Farms along the canals would draw water from the canals for irrigation. Farms distant from the canals would draw water from the Tesuque aquifer system. A total of 11,337 acres is proposed to be irrigated with 37.45 cubic feet per second withdrawn from ground water and 10.68 cubic feet per second diverted from the tributaries of Pojoaque River: 8.59 cubic feet per second from Rio Nambe, 0.84 cubic foot per second from Rio enMedio, 0.17 cubic foot per second from Rio Chupadero, and 1.08 cubic feet per second from Rio Tesuque.

Some fraction of water delivered to the irrigated land will infiltrate below the root zone. This water may seep into a unit of the Tesuque Formation that is underlain by a unit that has little permeability. Flow along this unit may carry the water to a surface-discharge point or to the regional ground-water system. If the underlying less permeable unit is not continuous, the water may descend to a deeper less permeable unit. Water that is returned to the regional ground-water system is called return flow. The irrigation development plan estimates that 12.39 cubic feet per second, about 26 percent of the water used for irrigation, will be return flow; therefore, the net withdrawals from ground water for irrigation of tribal lands will be 25.06 cubic feet per second.

In addition to the irrigation development plan, the projected stress includes the irrigation of nontribal lands. The plan calls for a total of 2,628 acres of nontribal lands to be irrigated with 8.43 cubic feet per second withdrawn from ground water and 2.46 cubic feet per second diverted from the tributaries of the Pojoaque River; 1.86 cubic feet per second from Rio Nambe, 0.11 cubic foot per second from Rio enMedio, 0.13 cubic foot per second from Rio Chupadero, and 0.36 cubic foot per second from Rio Tesuque. Return flow from these lands is estimated to be 5.44 cubic feet per second, about 50 percent of the water used for irrigation; therefore, the net withdrawals from ground water for irrigation of nontribal lands will be 2.99 cubic feet per second.

Withdrawals for municipal, industrial, and domestic water supply also are projected to increase. The plan calls for a total of 0.46 cubic foot per second to be withdrawn from ground water to meet these increased demands. Return flow is estimated to be 0.13 cubic foot per second, about 28 percent of the withdrawals; therefore, the net

withdrawals from ground water for increased municipal, industrial, and domestic water supply will be 0.33 cubic foot per second.

Projected Withdrawals and Diversions Represented in the Model

The representation of the projected withdrawals and diversions in the digital model makes several simplifications to the plan as it might be implemented in the prototype. The effect of these simplifications on the general response during several years probably is negligible.

Some simplifications result from the network of discrete cells used to represent the Tesuque aquifer system. Withdrawals are represented as a specified-flow boundary condition at the center of the cell. In the area of interest the cells are 1 mile square by 650 feet thick. The upper cell contains the water surface and has a saturated thickness of about 300 feet. The representation of withdrawals and return flow is shown in figure 21 for a typical cluster of cells representing the Tesuque aquifer system. Withdrawals are represented in the model at the cell representing the Tesuque aquifer system from about 300 to 950 feet below the water surface. Return flow is represented at the node in the cell representing the water surface. If the irrigated area is represented by two or more cells, the return flow is apportioned among the cells containing the water surface (fig. 21).

Additional simplifications result from holding the withdrawals constant through time. The withdrawals are represented as beginning in 1981 and continuing uninterrupted for 100 years. There is no period of gradual development as individual wells or diversions are constructed. There are no periods of relatively small withdrawals because of timely precipitation or abundant streamflow. There are no periods of relatively large withdrawals because of low streamflow. There are no cycles of drawdown and recovery because of the withdrawals being concentrated during an irrigation season.

The withdrawals as represented in the digital model (table 12; fig. 22) include not only those directly associated with the tribal irrigation plan but also withdrawals for irrigating nontribal lands and withdrawals required to meet projected municipal, industrial, and domestic demands. Some of the sites of nontribal withdrawals (wells B-19A, D-11A, D-12A, D-13A, E-10A, E-11A, and E-13A) are located outside the boundaries of the model. These withdrawals were represented in the model by withdrawals at the nearest cell to the mountain front.

Withdrawals for the irrigation development represented in the model total 28.41 cubic feet per second, which is 0.02 cubic foot per second more than the total

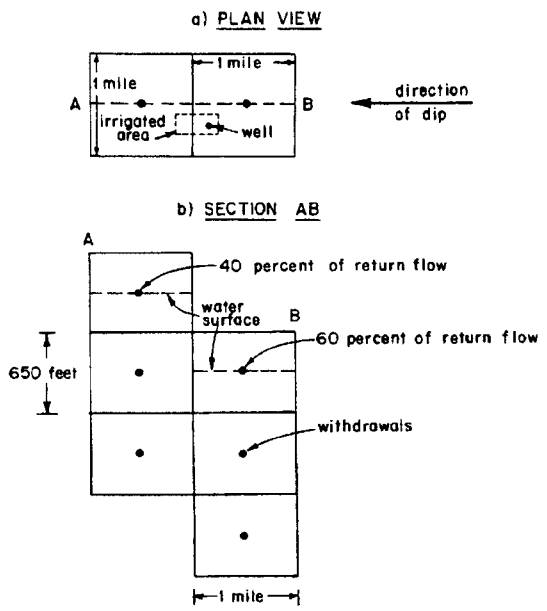

Figure 21. Representation of withdrawals and return flow in a typical cluster of cells representing the Tesuque aquifer system.

previously estimated for the prototype. The 0.07 percent difference due to round-off error is negligible.

In addition to the withdrawals and return flows, the model is stressed by decreasing the flow of the tributaries to the Pojoaque River by the amount to be diverted in the plan proposed by the U.S. Bureau of Indian Affairs. For Rio Nambe, the flow was decreased from 10.59 cubic feet per second to 0.14 cubic foot per second, for Rio enMedio from 2.40 cubic feet per second to 1.45 cubic feet per second, for Rio Chupadero from 0.54 cubic foot per second to 0.24 cubic foot per second, and for Tesuque Creek from 2.82 cubic feet per second to 1.38 cubic feet per second.

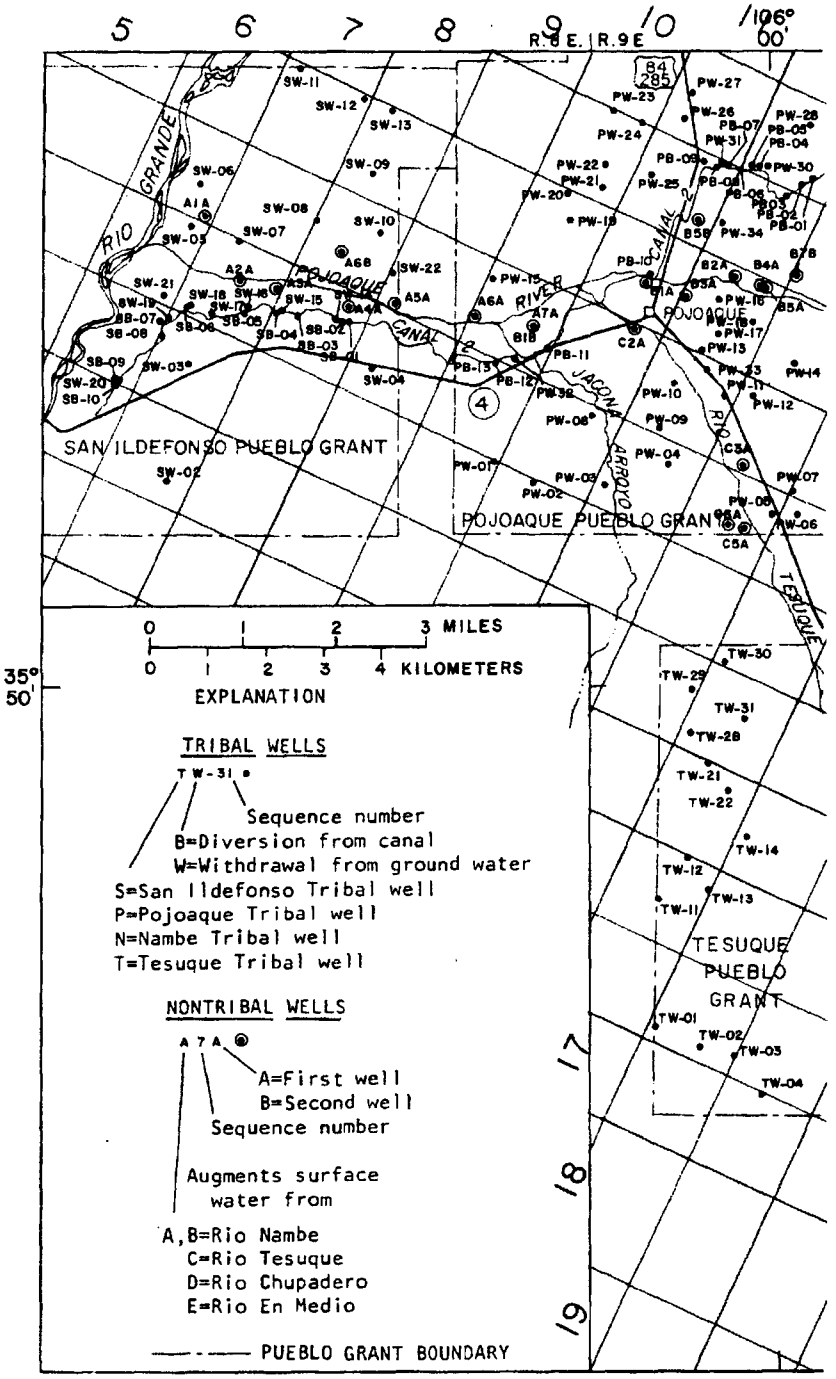

Figure 22. Location of wells and canals of the irrigation development plan.

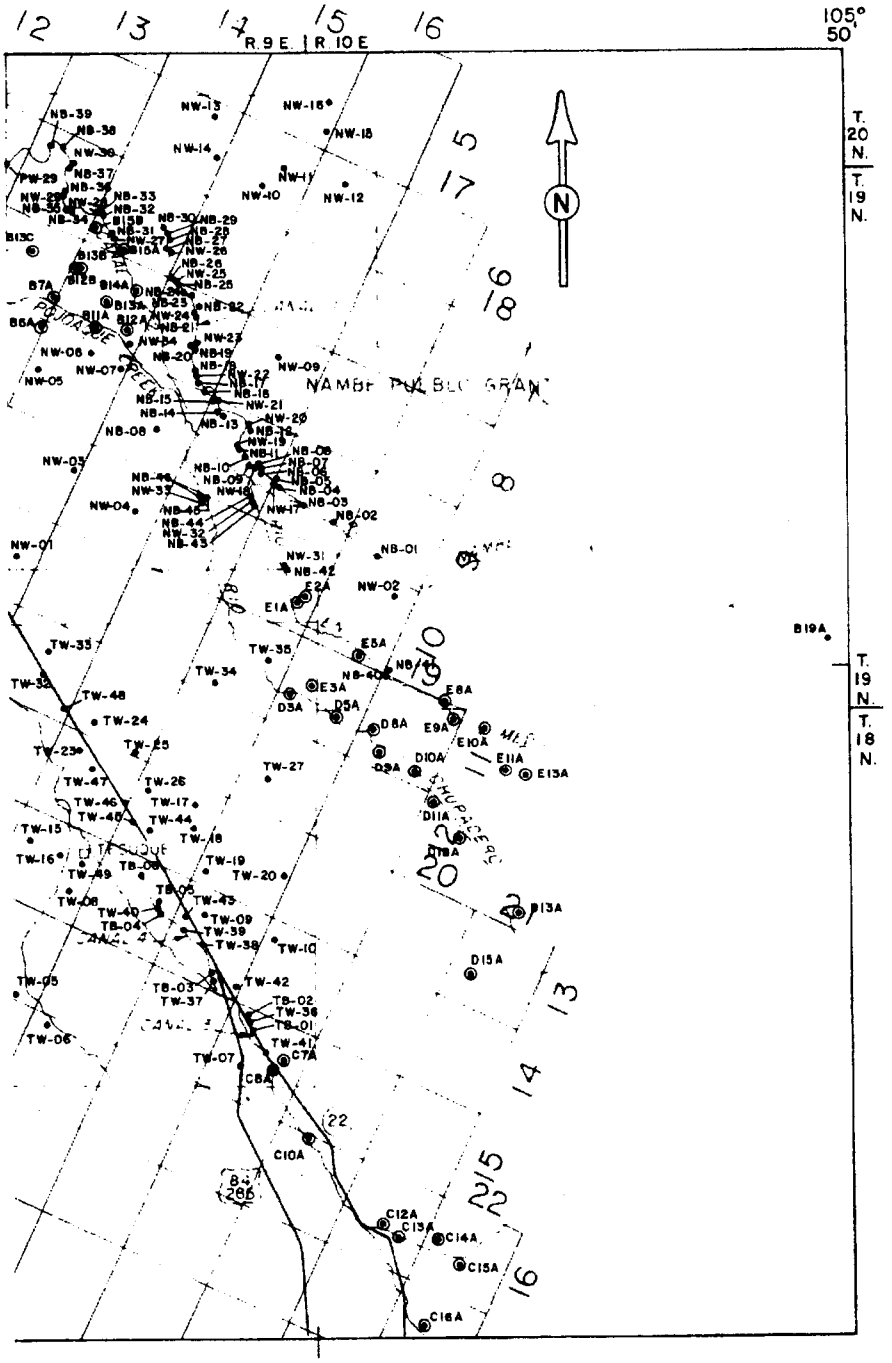
R.9E. | R.10E
105° 50'
T. 20 N.
T. 19 N.
T. 19 N.
T. 18 N.
N
NAMBE PUEBLO GRANT
NB-39
NB-38
NW-13
NW-16
NW-15
NW-14
NW-11
NW-10
NW-12
NW-06
NW-07
NW-05
NW-09
NW-03
NW-04
NW-01
NW-02
NB-01
NB-02
NB-08
NB-13
NB-14
NB-15
NB-18
NB-19
NB-20
NB-21
NB-22
NB-23
NB-24
NB-25
NB-26
NB-27
NB-28
NB-29
NB-30
NB-31
NB-32
NB-33
NB-34
NB-35
NB-36
NB-37
NB-40
NB-41
NB-42
NB-43
NB-44
NB-45
NB-46
NB-47
NB-48
NB-49
NW-21
NW-20
NW-19
NW-17
NW-31
NW-32
NW-33
NW-34
NW-35
NW-36
NW-37
NW-38
NW-39
NW-40
NW-41
NW-42
NW-43
NW-44
NW-45
NW-46
NW-47
NW-48
NW-49
NW-50
NW-51
NW-52
NW-53
NW-54
NW-55
NW-56
NW-57
NW-58
NW-59
NW-60
NW-61
NW-62
NW-63
NW-64
NW-65
NW-66
NW-67
NW-68
NW-69
NW-70

Table 12. Irrigation development plan as represented in the model

EXPLANATION

Well number: Well location and well-numbering key are shown in fig. 22. Blank spaces in last column indicate water not used for irrigation.

Type of stress:

3–return flow of 0.002072 cubic foot per second per acre of nontribal irrigation;
4–withdrawal of 0.004204 cubic foot per second per acre of tribal irrigation;
5–return flow of 0.001093 cubic foot per second per acre of tribal irrigation;
6–same as 4;
7–same as 5;
8–withdrawal of 0.06906 cubic foot per second to supplement surface water diverted from Rio en Medio for tribal irrigation;
9–withdrawal of 0.1174 cubic foot per second to supplement surface water diverted from Rio Chupadero for tribal irrigation;
10–withdrawal of 0.2521 cubic foot per second on Nambe Pueblo Grant to supplement surface water diverted from Rio Nambe for tribal irrigation along canal 1;
11–withdrawal of 0.2486 cubic foot per second to supplement surface water diverted from Rio Nambe for tribal irrigation along canal 2;
12–withdrawal of 0.1844 cubic foot per second on Pojoaque Pueblo Grant to supplement surface water diverted from Rio Nambe for tribal irrigation along canal 1;
13–withdrawal of 0.1747 cubic foot per second on San Ildefonso Pueblo Grant to supplement surface water diverted from Rio Nambe for tribal irrigation along canal 1;
14–withdrawal of 0.2659 cubic foot per second to supplement surface water diverted from Rio Tesuque for tribal irrigation along canal 3;
15–withdrawal of 0.2659 cubic foot per second to supplement surface water diverted from Rio Tesuque for tribal irrigation along canal 4;
17–withdrawal for projected increase in municipal/domestic demand–(acre- feet of withdrawals);
18–return flow of 28 percent of projected increase in municipal/domestic demand–(return flow is 28 percent of this number of acre-feet);
21–withdrawal of 0.003228 cubic foot per second per acre of nontribal irrigation to supplement surface water diverted from Rio Nambe;
22–withdrawal of 0.001945 cubic foot per second per acre of nontribal irrigation to supplement surface water diverted from Rio en Medio;
23–withdrawal of 0.003239 cubic foot per second per acre of nontribal irrigation to supplement surface water diverted from Rio Chupadero;
24–withdrawal of 0.003259 cubic foot per second per acre of nontribal irrigation to supplement surface water diverted from Rio Tesuque.

Well number	Location in model			Type of stress	Irrigated acres
	Row	Column	Layer		
NW-01	11	14	10	4	63
NW-01	11	14	11	5	33
NW-01	11	15	10	5	30
NW-02	10	18	6	4	46
NW-02	10	18	7	5	45
NW-02	9	18	7	5	1
NW-03	10	14	10	6	27
NW-03	10	14	11	7	20
NW-03	10	15	10	7	7
NW-04	10	15	9	4	54
NW-04	10	15	10	5	30
NW-04	11	15	10	5	9
NW-04	10	16	9	5	15
NW-05	9	14	10	4	64
NW-05	9	14	11	5	32
NW-05	9	13	12	5	32
NW-06	9	14	10	4	68
NW-06	9	14	11	5	60
NW-06	8	14	11	5	8
NW-07	9	14	10	4	54

Table 12. Irrigation development plan as represented in the model—Continued

Well number	Location in model			Type of stress	Irrigated acres
	Row	Column	Layer		
NW-07	9	14	11	5	30
NW-07	9	15	10	5	24
NW-08	9	15	9	4	76
NW-08	9	15	10	5	70
NW-08	10	15	10	5	6
NW-09	8	16	8	4	79
NW-09	8	16	9	5	63
NW-09	8	15	10	5	7
NW-09	7	16	9	5	9
NW-10	6	15	9	4	54
NW-10	6	15	10	5	51
NW-10	6	16	9	5	3
NW-11	6	15	9	4	85
NW-11	6	15	10	5	70
NW-11	6	14	11	5	10
NW-11	6	16	9	5	5
NW-12	6	16	8	4	64
NW-12	6	16	9	5	64
NW-13	6	14	10	4	88
NW-13	6	14	11	5	88
NW-14	6	14	10	4	96
NW-14	6	14	11	5	86
NW-14	6	15	10	5	10
NW-15	5	15	9	4	80
NW-15	5	15	10	5	40
NW-15	6	15	10	5	30
NW-15	5	16	9	5	10
NW-16	5	15	9	4	30
NW-16	5	15	10	5	10
NW-16	5	16	9	5	20
NB-01	9	18	7	5	12
NB-02	9	17	8	5	70
NB-03	9	17	8	5	26
NW-17	9	17	7	10	
NW-18	9	16	8	10	
NW-19	9	16	8	10	
NW-20	9	16	8	10	
NW-21	9	16	8	10	
NW-22	8	15	9	10	
NW-23	8	15	9	10	
NW-24	8	15	9	10	
NW-25	8	15	9	10	
NW-26	7	14	10	10	
NB-04	9	17	8	5	12
NB-04	9	16	9	5	4
NB-05	9	17	8	5	15
NB-05	9	16	9	5	5
NB-06	9	16	9	5	6
NB-07	9	16	9	5	2
NB-08	9	16	9	5	21
NB-08	9	17	8	5	5
NB-08	8	16	9	5	2
NB-08	8	17	8	5	1
NB-09	9	16	9	5	6
NB-10	9	16	9	5	9

Table 12. Irrigation development plan as represented in the model—Continued

Well number	Location in model			Type of stress	Irrigated acres
	Row	Column	Layer		
NB-11	9	16	9	5	22
NB-12	9	16	9	5	13
NB-13	9	16	9	5	30
NB-14	9	16	9	5	23
NB-14	9	15	10	5	12
NB-15	9	16	9	5	3
NB-15	9	15	10	5	5
NB-16	9	15	10	5	12
NB-17	9	15	10	5	6
NB-17	8	15	10	5	4
NB-18	8	15	10	5	9
NB-18	9	15	10	5	10
NB-19	8	15	10	5	35
NB-19	8	16	9	5	44
NB-20	8	15	10	5	107
NB-21	8	15	10	5	53
NB-21	8	14	11	5	14
NB-22	8	15	10	5	75
NB-22	8	16	9	5	20
NB-22	7	16	9	5	8
NB-22	7	15	10	5	7
NB-23	8	15	10	5	8
NB-24	7	15	10	5	15
NB-24	7	16	9	5	6
NB-25	8	15	10	5	17
NB-25	7	15	10	5	18
NB-26	8	15	10	5	30
NB-26	8	14	11	5	123
NB-26	7	14	11	5	10
NB-27	7	14	11	5	47
NB-27	8	14	11	5	39
NB-28	7	14	11	5	15
NB-28	7	15	10	5	10
NB-29	7	14	11	5	20
NB-29	7	15	10	5	31
NB-30	7	14	11	5	67
NW-27	7	14	10	11	
NW-28	7	13	11	11	
NW-29	7	13	11	11	
NW-30	7	13	11	11	
NB-31	7	14	11	5	27
NB-31	7	13	12	5	10
NB-31	8	14	11	5	6
NB-32	7	14	11	5	18
NB-33	7	14	11	5	70
NB-33	7	13	12	5	10
NB-33	6	14	11	5	3
NB-34	7	13	12	5	7
NB-35	7	13	12	5	3
NB-36	7	13	12	5	19
NB-37	7	13	12	5	50
NB-37	7	14	11	5	4
NB-38	7	13	12	5	57
NB-38	6	14	11	5	6
NB-38	6	13	12	5	65

Table 12. Irrigation development plan as represented in the model—Continued

Well number	Location in model			Type of stress	Irrigated acres
	Row	Column	Layer		
NB-39	7	13	12	5	13
NB-39	6	13	12	5	90
NW-31	10	17	7	8	
NW-32	9	16	8	8	
NB-40	11	18	7	5	28
NB-40	11	19	6	5	8
NB-41	10	18	7	7	23
NB-41	11	18	7	7	2
NB-42	10	17	8	5	50
NB-42	9	17	8	5	38
NB-42	9	16	9	5	2
NB-42	10	18	7	5	10
NB-42	9	18	7	5	1
NB-43	9	16	9	5	44
NB-43	9	17	8	5	3
NB-43	10	17	8	5	3
NB-44	9	16	9	5	18
NW-33	10	16	8	9	
NB-45	10	16	9	7	28
NB-46	10	16	9	5	12
NB-46	9	16	9	5	8
NB-46	9	15	10	5	20
NW-34	8	14	10	17	[1]50
NW-34	8	14	11	18	[2]50
PW-01	12	10	14	4	46
PW-01	12	11	14	5	15
PW-01	12	10	15	5	16
PW-01	11	10	15	5	15
PW-02	12	11	13	4	63
PW-02	12	11	14	5	20
PW-02	11	11	14	5	43
PW-03	11	12	12	4	88
PW-03	11	12	13	5	45
PW-03	12	12	13	5	5
PW-03	11	11	14	5	38
PW-04	11	12	12	4	90
PW-04	11	12	13	5	60
PW-04	11	13	12	5	25
PW-04	10	12	13	5	5
PW-05	11	13	11	4	53
PW-05	11	13	12	5	41
PW-05	11	14	11	5	12
PW-06	11	14	10	4	72
PW-06	11	14	11	5	55
PW-06	10	14	11	5	17
PW-07	10	14	10	4	89
PW-07	10	14	11	5	17
PW-07	11	13	12	5	19
PW-07	11	14	11	5	15
PW-07	10	13	12	5	38
PW-08	11	11	13	4	74
PW-08	11	11	14	5	30
PW-08	11	12	13	5	25
PW-08	10	11	14	5	19
PW-09	10	12	12	4	33

Table 12. Irrigation development plan as represented in the model—Continued

Well number	Location in model			Type of stress	Irrigated acres
	Row	Column	Layer		
PW-09	10	12	13	5	22
PW-09	11	12	13	5	11
PW-10	10	12	12	4	60
PW-10	10	12	13	5	50
PW-10	10	11	14	5	10
PW-11	10	12	12	4	31
PW-11	10	12	13	5	17
PW-11	10	13	12	5	14
PW-12	10	13	11	4	85
PW-12	10	13	12	5	70
PW-12	9	13	12	5	15
PW-13	9	12	12	6	73
PW-13	9	12	13	7	25
PW-13	10	12	13	7	38
PW-13	10	13	12	7	10
PW-14	9	13	11	4	110
PW-14	9	13	12	5	105
PW-14	9	12	13	5	5
PW-15	10	10	14	4	55
PW-15	10	10	15	5	20
PW-15	10	9	16	5	30
PW-15	9	9	16	5	5
PW-16	9	12	12	6	72
PW-16	9	12	13	7	60
PW-16	9	11	14	7	12
PW-17	9	12	12	4	72
PW-17	9	12	13	5	72
PW-18	9	12	12	4	76
PW-18	9	12	13	5	40
PW-18	9	13	12	5	36
PW-19	9	10	14	4	106
PW-19	9	10	15	5	106
PW-20	9	10	14	4	118
PW-20	9	10	15	5	78
PW-20	8	10	15	5	25
PW-20	9	11	14	5	15
PW-21	8	10	14	4	81
PW-21	8	10	15	5	29
PW-21	9	10	15	5	15
PW-21	9	11	14	5	32
PW-21	8	11	14	5	5
PW-22	8	10	14	4	119
PW-22	8	10	15	5	75
PW-22	8	11	14	5	39
PW-22	9	11	14	5	5
PW-23	8	10	14	4	98
PW-23	8	10	15	5	80
PW-23	7	10	15	5	18
PW-24	8	10	14	4	76
PW-24	8	10	15	5	39
PW-24	8	11	14	5	7
PW-24	7	10	15	5	30
PW-25	8	11	13	4	105
PW-25	8	11	14	5	105
PW-26	7	11	13	4	85

Table 12. Irrigation development plan as represented in the model—Continued

Well number	Location in model			Type of stress	Irrigated acres
	Row	Column	Layer		
PW-26	7	11	14	5	40
PW-26	8	11	14	5	40
PW-26	7	10	15	5	5
PW-27	7	11	13	4	50
PW-27	7	11	14	5	50
PW-28	7	12	12	4	37
PW-28	7	12	13	5	30
PW-28	6	12	13	5	7
PW-29	7	12	12	12	
PW-30	7	12	12	12	
PW-31	8	11	13	12	
PW-32	10	10	14	12	
PB-01	7	12	13	5	33
PB-01	8	12	13	5	50
PB-01	8	13	12	5	10
PB-02	7	12	13	5	29
PB-02	8	12	13	5	10
PB-03	8	12	13	5	52
PB-03	7	12	13	5	5
PB-04	7	12	13	5	10
PB-04	8	12	13	5	50
PB-05	7	12	13	5	32
PB-05	7	11	14	5	4
PB-06	8	12	13	5	3
PB-06	7	12	13	5	5
PB-06	7	11	14	5	5
PB-07	8	11	14	5	16
PB-07	8	12	13	5	50
PB-08	8	11	14	5	53
PB-08	8	12	13	5	5
PB-08	7	11	14	5	22
PB-09	8	11	14	5	45
PB-09	7	11	14	5	21
PB-10	9	11	14	5	12
PB-11	10	10	15	5	10
PB-11	10	11	14	5	39
PB-11	11	11	14	5	5
PB-12	10	10	15	5	7
PB-12	11	10	15	5	27
PB-12	11	11	14	5	33
PB-13	11	10	15	5	89
PW-33	10	12	12	17	[1]66
PW-33	10	12	13	18	[2]66
PW-34	8	12	12	17	[1]15
PW-34	8	12	13	18	[2]15
SW-02	13	7	17	4	81
SW-02	13	7	18	5	40
SW-02	14	7	18	5	31
SW-02	13	8	17	5	10
SW-03	12	7	17	4	80
SW-03	12	7	18	5	80
SW-04	11	9	15	4	71
SW-04	11	9	16	5	40
SW-04	12	9	16	5	28
SW-04	11	8	17	5	3

Table 12. Irrigation development plan as represented in the model—Continued

Well number	Location in model			Type of stress	Irrigated acres
	Row	Column	Layer		
SW-05	11	6	18	4	81
SW-05	11	6	19	5	60
SW-05	10	6	19	5	11
SW-05	11	7	18	5	10
SW-06	10	6	18	4	94
SW-06	10	6	19	5	71
SW-06	9	6	19	5	3
SW-06	10	7	18	5	20
SW-07	11	7	17	4	81
SW-07	11	7	18	5	36
SW-07	10	7	18	5	30
SW-07	11	6	19	5	10
SW-07	10	6	19	5	5
SW-08	10	8	16	4	128
SW-08	10	8	17	5	60
SW-08	11	8	17	5	20
SW-08	10	7	18	5	33
SW-08	11	7	18	5	15
SW-09	9	8	16	4	99
SW-09	9	8	17	5	60
SW-09	10	8	17	5	39
SW-10	10	8	16	4	100
SW-10	10	8	17	5	100
SW-11	9	7	17	4	101
SW-11	9	7	18	5	51
SW-11	8	7	18	5	15
SW-11	9	6	19	5	35
SW-12	9	7	17	4	87
SW-12	9	7	18	5	37
SW-12	8	7	18	5	30
SW-12	9	8	17	5	20
SW-13	9	8	16	4	89
SW-13	9	8	17	5	30
SW-13	8	8	17	5	34
SW-13	8	7	18	5	25
SW-14	11	8	16	13	
SW-15	11	8	16	13	
SW-16	11	7	17	13	
SW-17	11	7	17	13	
SW-18	11	7	17	13	
SW-19	12	7	17	13	
SW-20	12	6	18	13	
SB-01	11	8	17	5	5
SB-01	11	9	16	5	4
SB-02	11	8	17	5	53
SB-02	12	8	17	5	1
SB-02	11	9	16	5	15
SB-03	11	8	17	5	6
SB-04	11	8	17	5	13
SB-04	12	8	17	5	5
SB-05	11	7	18	5	38
SB-05	12	7	18	5	12
SB-05	11	8	17	5	7
SB-06	11	7	18	5	106
SB-06	12	7	18	5	5

Table 12. Irrigation development plan as represented in the model—Continued

Well number	Location in model			Type of stress	Irrigated acres
	Row	Column	Layer		
SB-06	11	6	19	5	103
SB-07	12	6	19	5	138
SB-07	11	6	19	5	50
SB-08	12	7	18	7	5
SB-08	12	6	19	7	23
SB-09	12	6	19	5	98
SB-09	13	6	19	5	110
SB-10	12	6	19	5	15
SB-10	13	6	19	5	35
SB-10	12	7	18	5	5
SB-10	13	7	18	5	42
SW-21	11	6	18	17	[1]96
SW-21	11	6	19	18	[2]96
SW-22	10	9	15	4	25
SW-22	10	9	16	5	25
TW-01	16	15	9	4	111
TW-01	16	15	10	5	50
TW-01	17	15	10	5	40
TW-01	16	14	11	5	21
TW-02	16	15	9	4	113
TW-02	16	15	10	5	83
TW-02	17	15	10	5	30
TW-03	16	15	9	4	101
TW-03	16	15	10	5	25
TW-03	17	15	10	5	23
TW-03	17	16	9	5	23
TW-03	16	16	9	5	30
TW-04	17	16	8	4	52
TW-04	17	16	9	5	25
TW-04	16	16	9	5	27
TW-05	15	16	8	4	62
TW-05	15	16	9	5	27
TW-05	16	16	9	5	28
TW-05	16	17	8	5	7
TW-06	16	17	7	4	122
TW-06	16	17	8	5	52
TW-06	15	17	8	5	35
TW-06	15	16	9	5	20
TW-06	16	18	7	5	15
TW-07	15	19	5	6	36
TW-07	15	19	6	7	36
TW-08	14	16	8	4	123
TW-08	14	16	9	5	68
TW-08	15	16	9	5	35
TW-08	14	17	8	5	20
TW-09	14	18	6	4	98
TW-09	14	18	7	5	68
TW-09	13	18	7	5	15
TW-09	14	17	8	5	15
TW-10	14	19	5	4	97
TW-10	14	19	6	5	35
TW-10	13	19	6	5	20
TW-10	14	18	7	5	35
TW-10	13	18	7	5	7
TW-11	15	14	10	4	39

Table 12. Irrigation development plan as represented in the model—Continued

Well number	Location in model			Type of stress	Irrigated acres
	Row	Column	Layer		
TW-11	15	14	11	5	39
TW-12	15	14	10	4	82
TW-12	15	14	11	5	27
TW-12	14	14	11	5	55
TW-13	15	14	10	4	94
TW-13	15	14	11	5	25
TW-13	15	15	10	5	28
TW-13	14	14	11	5	31
TW-13	14	15	10	5	10
TW-14	14	15	9	4	70
TW-14	14	15	10	5	49
TW-14	15	15	10	5	1
TW-14	14	14	11	5	20
TW-15	14	16	8	4	106
TW-15	14	16	9	5	65
TW-15	13	16	9	5	35
TW-15	13	15	10	5	6
TW-16	14	16	8	4	86
TW-16	14	16	9	5	71
TW-16	13	16	9	5	5
TW-16	15	16	9	5	10
TW-17	13	17	7	4	83
TW-17	13	17	8	5	81
TW-17	12	17	8	5	2
TW-18	13	17	7	4	75
TW-18	13	17	8	5	37
TW-18	13	18	7	5	38
TW-19	13	18	6	4	72
TW-19	13	18	7	5	30
TW-19	13	17	8	5	38
TW-19	14	17	8	5	4
TW-20	13	18	6	4	55
TW-20	13	18	7	5	30
TW-20	13	19	6	5	25
TW-21	14	14	10	4	89
TW-21	14	14	11	5	74
TW-21	13	14	11	5	15
TW-22	14	14	10	4	87
TW-22	14	14	11	5	37
TW-22	13	14	11	5	38
TW-22	14	15	10	5	12
TW-23	13	16	8	4	88
TW-23	13	16	9	5	65
TW-23	12	16	9	5	3
TW-23	13	15	10	5	20
TW-24	12	16	8	4	92
TW-24	12	16	9	5	77
TW-24	13	16	9	5	15
TW-25	12	16	8	4	72
TW-25	12	16	9	5	27
TW-25	13	16	9	5	20
TW-25	12	17	8	5	20
TW-25	13	17	8	5	5
TW-26	13	17	7	4	75
TW-26	13	17	8	5	40

Table 12. Irrigation development plan as represented in the model—Continued

Well number	Location in model			Type of stress	Irrigated acres
	Row	Column	Layer		
TW-26	13	16	9	5	35
TW-27	12	18	6	4	90
TW-27	12	18	7	5	50
TW-27	12	17	8	5	35
TW-27	11	17	8	5	5
TW-28	13	14	10	4	72
TW-28	13	14	11	5	59
TW-28	14	14	11	5	10
TW-28	13	13	12	5	3
TW-29	13	13	11	4	92
TW-29	13	13	12	5	55
TW-29	12	13	12	5	2
TW-29	14	13	12	5	30
TW-29	13	14	11	5	2
TW-29	14	14	11	5	3
TW-30	12	14	10	4	106
TW-30	12	14	11	5	30
TW-30	12	14	11	5	51
TW-30	13	13	12	5	5
TW-30	12	13	12	5	20
TW-31	13	14	10	4	72
TW-31	13	14	11	5	72
TW-32	12	15	9	4	102
TW-32	12	15	10	5	97
TW-32	12	14	11	5	5
TW-33	12	15	9	4	92
TW-33	12	15	10	5	62
TW-33	12	16	9	5	30
TW-34	11	17	7	4	89
TW-34	11	17	8	5	45
TW-34	12	17	8	5	9
TW-34	11	16	9	5	35
TW-35	11	17	7	6	16
TW-35	11	17	8	7	16
TW-36	15	19	5	14	
TW-41	15	19	5	14	
TB-01	15	19	6	5	34
TB-01	14	19	6	5	40
TB-02	15	19	6	5	5
TB-02	14	19	6	5	50
TB-02	14	18	7	5	40
TW-37	14	18	6	15	
TW-38	14	18	6	15	
TW-39	14	18	6	15	
TW-40	14	17	7	15	
TB-03	14	18	7	5	56
TB-03	14	17	8	5	15
TB-04	14	17	8	5	71
TB-05	14	17	8	5	30
TB-06	14	17	8	5	87
TB-06	13	17	8	5	50
TB-06	14	16	9	5	50
TB-06	13	16	9	5	90
TW-42	14	18	6	17	[1]6
TW-42	14	18	7	18	[2]6

Table 12. Irrigation development plan as represented in the model—Continued

Well number	Location in model			Type of stress	Irrigated acres
	Row	Column	Layer		
TW-43	14	18	6	17	[1]5
TW-43	14	18	7	18	[2]5
TW-44	13	17	7	17	[1]6
TW-44	13	17	8	18	[2]6
TW-45	13	17	7	17	[1]6
TW-45	13	17	8	18	[2]6
TW-46	13	16	8	17	[1]5
TW-46	13	16	9	18	[2]5
TW-47	13	16	8	17	[1]26
TW-47	13	16	9	18	[2]26
TW-48	12	15	9	17	[1]25
TW-48	12	15	10	18	[2]25
TW-49	14	16	8	17	[1]31
TW-49	14	16	9	18	[2]31
A1A	10	6	18	21	24
A1A	10	6	19	3	24
A2A	11	7	17	21	13
A2A	11	6	19	3	7
A2A	12	6	19	3	6
A3A	11	7	17	21	7
A3A	11	7	18	3	4
A3A	11	8	17	3	3
A4A	11	8	16	21	89
A4A	10	8	17	3	18
A4A	11	8	17	3	18
A4A	11	7	18	3	53
A5A	10	9	15	21	68
A5A	11	9	16	3	35
A5A	11	8	17	3	33
A6A	10	10	14	21	101
A6A	10	8	17	3	44
A6A	10	9	16	3	19
A6A	10	7	18	3	19
A6A	11	7	18	3	19
A6B	10	8	16	21	101
A6B	10	8	17	3	44
A6B	10	9	16	3	19
A6B	10	7	18	3	19
A6B	11	7	18	3	19
A7A	10	10	14	21	103
A7A	10	10	15	3	45
A7A	10	9	16	3	29
A7A	11	9	16	3	29
B1A	9	11	13	21	69.5
B1A	10	10	15	3	25
B1A	10	11	14	3	11
B1A	10	9	16	3	11
B1A	9	10	15	3	11
B1A	9	11	14	3	11
B1B	10	10	14	21	69.5
B1B	10	10	15	3	25
B1B	10	11	14	3	11
B1B	10	9	16	3	11
B1B	9	10	15	3	11
B1B	9	11	14	3	11

Table 12. Irrigation development plan as represented in the model—Continued

Well number	Location in model			Type of stress	Irrigated acres
	Row	Column	Layer		
B2A	9	12	12	21	76
B2A	9	11	14	3	40
B2A	9	12	13	3	18
B2A	8	12	13	3	18
B3A	9	12	12	21	90
B3A	9	11	14	3	90
B4A	9	12	12	21	14
B4A	9	12	13	3	14
B5A	9	12	12	21	93
B5A	8	11	14	3	19
B5A	9	11	14	3	19
B5A	8	12	13	3	36
B5A	9	12	13	3	19
B5B	8	11	13	21	93
B5B	8	11	14	3	19
B5B	9	11	14	3	19
B5B	8	12	13	3	36
B5B	9	12	13	3	19
B6A	9	13	11	21	107
B6A	9	13	12	3	26
B6A	9	12	13	3	39
B6A	9	11	14	3	21
B6A	8	13	12	3	21
B7A	8	14	10	21	95
B7A	8	13	12	3	38
B7A	8	12	13	3	38
B7A	9	12	13	3	19
B7B	8	13	11	21	95
B7B	8	13	12	3	38
B7B	8	12	13	3	38
B7B	9	12	13	3	19
B11A	8	14	10	21	43
B11A	8	14	11	3	14
B11A	9	13	12	3	29
B12A	8	14	10	21	72
B12A	8	14	11	3	36
B12A	8	13	12	3	18
B12A	8	12	13	3	18
B12B	8	14	10	21	71
B12B	8	14	11	3	35
B12B	8	13	12	3	18
B12B	8	12	13	3	18
B13A	8	14	10	21	73
B13A	8	14	11	3	36
B13A	8	13	12	3	37
B13B	8	14	10	21	74
B13B	8	14	11	3	37
B13B	8	13	12	3	37
B13C	8	13	11	21	74
B13C	8	14	11	3	37
B13C	8	13	12	3	37
B14A	8	14	10	21	91
B14A	8	14	11	3	91
B15A	7	14	10	21	92
B15A	8	13	12	3	26

Table 12. Irrigation development plan as represented in the model—Continued

Well number	Location in model			Type of stress	Irrigated acres
	Row	Column	Layer		
B15A	7	14	11	3	22
B15A	7	13	12	3	44
B15B	7	14	10	21	91
B15B	8	13	12	3	25
B15B	7	14	11	3	22
B15B	7	13	12	3	44
B19A	9	18	7	21	39
B19A	9	18	7	3	39
C2A	10	11	13	24	67
C2A	10	11	14	3	67
C3A	10	13	11	24	30
C3A	10	13	12	3	15
C3A	10	12	13	3	15
C5A	11	13	11	24	61
C5A	10	13	12	3	61
C6A	11	13	11	24	35
C6A	10	12	13	3	9
C6A	11	13	12	3	17
C6A	10	13	12	3	9
C7A	15	19	5	24	18
C7A	15	19	6	3	18
C8A	15	19	5	24	5
C8A	15	19	6	3	3
C8A	15	20	5	3	2
C10A	16	20	4	24	62
C10A	16	20	5	3	21
C10A	15	20	5	3	21
C10A	15	19	6	3	20
C12A	16	21	3	24	95
C12A	16	21	4	3	29
C12A	16	20	5	3	26
C12A	15	20	5	3	40
C13A	16	21	3	24	11
C13A	16	21	4	3	11
C14A	16	22	3	24	14
C14A	16	22	3	3	8
C14A	16	21	4	3	6
C15A	16	22	3	24	5
C15A	16	22	3	3	5
C16A	17	22	3	24	9
C16A	17	22	3	3	9
D3A	11	18	6	23	4
D3A	11	18	7	3	4
D5A	11	18	6	23	12
D5A	11	18	7	3	12
D8A	11	19	5	23	2
D8A	11	18	7	3	2
D9A	11	19	5	23	19
D9A	11	18	7	3	10
D9A	11	19	6	3	9
D10A	11	19	5	23	3
D10A	11	19	6	3	3
D11A	12	19	5	23	14
D11A	12	19	6	3	7
D11A	11	19	6	3	7

Table 12. Irrigation development plan as represented in the model—Continued

Well number	Location in model			Type of stress	Irrigated acres
	Row	Column	Layer		
D12A	12	19	5	23	66
D12A	12	19	6	3	19
D12A	11	18	7	3	28
D12A	11	19	6	3	19
D13A	13	21	4	23	2
D13A	13	21	4	3	2
D15A	13	21	4	23	17
D15A	13	21	4	3	17
E1A	10	17	7	22	1
E1A	10	17	8	3	1
E2A	10	17	7	22	1
E2A	10	17	7	3	1
E3A	11	18	6	22	6
E3A	11	18	7	3	3
E3A	10	17	8	3	3
E5A	10	18	6	22	5
E5A	10	18	7	3	5
E8A	11	19	5	22	9
E8A	11	19	6	3	9
E9A	11	19	5	22	11
E9A	11	19	6	3	6
E9A	11	19	6	3	5
E10A	11	19	5	22	5
E10A	11	19	6	3	5
E11A	11	19	5	22	5
E11A	11	19	6	3	10
E13A	11	19	5	22	1
E13A	11	19	6	3	1

[1] Acre-feet of withdrawals.

[2] Return flow is 28 percent of this number of acre-feet.

SIMULATED RESPONSE TO PROJECTED WITHDRAWALS AND DIVERSIONS

The projection stage of the simulation estimates the response of the Tesuque aquifer system to 100 years of withdrawals as projected by the U.S. Bureau of Indian Affairs. For the null-future condition, the projected withdrawals are 11.24 cubic feet per second at the Los Alamos Canyon, Guaje Canyon, Pajarito Mesa, and Buckman well fields. For the alternative-future condition, the projected withdrawals are 39.65 cubic feet per second, an increase of 28.41 cubic feet per second. The response simulated by the mathematical model is presented with a precision that exceeds the predictive accuracy of the model. Although water levels should probably be rounded to the nearest 10 feet, they are reported to the nearest 0.1 foot to show the

magnitude of small simulated changes. Similarly, although flow rates should probably be rounded to the nearest cubic foot per second, they are reported to the nearest 0.01 cubic foot per second. Thus, quantities reported as negligible are in fact negligible and not merely small values that have been rounded off.

Under steady-state conditions, the discharge from the aquifer system is equal to the recharge; the water surface and the hydraulic head in confined beds do not change with time. The withdrawals by wells are an additional discharge superimposed on this stable condition. As water is withdrawn from the aquifer system, the hydraulic head is lowered. Eventually, the hydraulic head will change in areas of natural recharge or discharge, and the rate of recharge or discharge may change. Given sufficient time, all withdrawals will be balanced by decreases in natural discharge or increases in recharge. (A more complete discussion of this phenomenon is offered by Theis, 1938, and 1940.) The simulation with the digital model describes this process quantitatively. This section describes changes in hydraulic head and changes in recharge and discharge simulated by the digital model in response to the withdrawals by wells. Two alternative conditions have been simulated: in one the withdrawals are continued historical withdrawals only; in the other the withdrawals include those for the tribal irrigation development, nontribal irrigation, and municipal, industrial, and domestic water supply as well as continued historical withdrawals. Comparing the response of these two conditions provides estimates of the impact of the additional withdrawals. Although the additional withdrawals include nontribal irrigation and municipal, industrial, and domestic supply, the comparisons are phrased as being between simulations "with irrigation development" and "without irrigation development."

As described in the previous section on boundaries represented in the model, the boundaries to the north and south are arbitrarily located. The boundary to the west is represented as a constant-flow boundary even though the flow may change if water is drawn from storage west of the fault zone. The common assumption is that the boundaries are sufficiently distant that the type and location of the boundaries has a negligible effect on the response within the Pojoaque River basin. This assumption can now be verified by noting the simulated change in hydraulic head at the boundary and estimating the effect on the simulated hydraulic heads in the Pojoaque River basin.

The effect of these arbitrary boundaries on the simulated heads in the Pojoaque River basin is estimated analytically using image wells (Lohman, 1972, p.57-61). The effect of a no-flow boundary on the drawdown caused by a discharging well is estimated by locating an image the same distance outside the boundary as the real well is inside the boundary. The calculated drawdown at any point inside the boundary is computed by adding the drawdown calculated for the discharging image well to that for the real well. Therefore, the effect of the boundary is approximated by the additional drawdown calculated for an image well located twice as far from the real well as is the boundary. Drawdown at any radius from the image well is assumed to be proportional to $W(u)$ (Lohman, 1972, p. 15) where

$$u = \frac{r^2 S_s}{4Kt} \qquad (7)$$

where

r = the radius from the well (in feet);

S_s = the specific storage (2×10^{-6} per foot);

K = the hydraulic conductivity (1 foot per day); and

t = time (50 years).

The northern no-flow boundary of the modeled area is located a few miles north of the Santa Cruz River (fig. 1) and does not approximate a geologic boundary. This boundary is 10 miles or more from the Pojoaque River basin. After 50 years of withdrawals for irrigation development, the maximum drawdown simulated along this arbitrary boundary would be about 8 feet. Using image wells, this drawdown represents the sum of 4 feet due to the real well and 4 feet due to the image well located more than 20 miles from the Pojoaque River basin. An image well that produces a drawdown of 4 feet at 10 miles is estimated to produce a drawdown of less than 2 feet at 20 miles. Therefore, the arbitrary northern boundary is estimated to affect drawdowns in the Pojoaque River basin by less than 2 feet.

The southern no-flow boundary of the modeled area extends to the confluence of the Rio Grande and the Santa Fe River, and does not approximate a geologic boundary. This boundary is 20 miles or more from he Pojoaque River basin. After 50 years of withdrawals for irrigation development, the maximum drawdown simulated along this arbitrary boundary would be about 4 feet. This drawdown represents the sum of 2 feet due to the real well and 2 feet due to the image well more than 40 miles from the Pojoaque River basin. An image well that produces a drawdown of 2 feet at 20 miles is estimated to produce a drawdown of less than 0.4 foot at 40 miles. Therefore, the arbitrary southern boundary is estimated to affect drawdowns in Pojoaque River basin by less than 0.4 foot.

The western boundary of the modeled area approximates a fault zone beneath the Jemez Mountains (fig. 1). The representation of this geologic boundary as a specified-flow boundary does not allow any water to be drawn from storage in the aquifer west of the fault zone.

This boundary is 10 miles or more from the Pojoaque River basin. After 50 years of withdrawals for irrigation development, the maximum drawdown simulated along this arbitrary boundary will be about 22 feet. Most of this drawdown is the result of continued historical withdrawals, some of which are within about 5 miles of the boundary. The 22 feet of drawdown would represent the sum of 11 feet due to the real well and 11 feet due to the image well about 5 miles across the boundary, about 10 miles from the sites of historical withdrawals, and about 15 miles from the Pojoaque River basin.

In estimating the effect of this boundary, one needs to consider that flow toward the Pojoaque River basin requires flow across the dipping anisotropic beds. It can be shown (C.V. Theis, U.S. Geological Survey, written commun., 1974) that dipping anisotropic beds produce an effective horizontal anisotropy in which

$$\frac{K_x}{K_y} = \frac{R}{1 - (1 - R)\cos^2 A} \qquad (8)$$

where

K_x = the horizontal hydraulic conductivity in the direction of the dip (L/T);

K_y = the horizontal hydraulic conductivity in the direction of the strike (L/T);

R = the ratio of cross-bed to in-bed hydraulic conductivity; and

A = the angle of dip.

Further, the anisotropic problem is reduced to an isotropic problem by the transformations

$$K' = \sqrt{K_x K_y}$$
$$S_s' = \sqrt{K_x K_y \; S_s}$$
$$x' = x/\sqrt{K_x}$$
$$y' = y/\sqrt{K_y}$$

where the variables are as defined above and the prime designates transformed values.

For the Tesuque aquifer system, the anisotropy ratio of 0.003 and a dip of 8° produce a horizontal anisotropy in which the horizontal hydraulic conductivity in the direction of the dip is 0.2 foot per day and the horizontal hydraulic conductivity in the direction of the strike is 1 foot per day. If calculations are performed on the deformed isotropic space, an image well that produces 11 feet of drawdown at the western boundary is estimated to produce less than 5 feet of drawdown near the sites of historical withdrawals and less than 2 feet of drawdown in the Pojoaque River basin.

The boundaries to the north, south, and west are estimated to have a cumulative effect of adding less than 5 feet to the drawdowns simulated for the Pojoaque River basin after 50 years of withdrawal for irrigation development. This effect will increase with time.

Simulated Changes in Water Levels

Although the model simulates response for 100 years, the simulated hydraulic-head declines are presented for the end of the 50-year project life of the irrigation development plan proposed by the U.S. Bureau of Indian Affairs. The simulated water surface in 2030 after 50 years of withdrawals is shown in figure 23. The simulated decline in hydraulic head at the water surface from 1980 to 2030 is shown in figure 24. The maximum decline of about 143 feet was simulated at row 7, column 15.

Withdrawals are primarily made not in the water surface cell, but in the underlying confined cell (fig. 21). The simulated change in hydraulic head in this production zone is shown in figure 25. The maximum decline of 334 feet was simulated at row 8, column 14. The simulated declines in hydraulic head in this production zone are presented in hydrographs for the eight locations shown in figure 25: one near each of the existing well fields at Los Alamos Canyon, Guaje Canyon, Pajarito Mesa, and Buckman; and one near each of the Pueblos of San Ildefonso, Pojoaque, Nambe, and Tesuque.

Los Alamos Canyon Well Field

In the Los Alamos Canyon well field, wells LA-1, LA-1B, LA-2, and LA-3 are represented at the cell in row 13, column 5, layer 19. The simulated decline in hydraulic head (fig. 26) is due primarily to the continuation of historical withdrawals. Without irrigation development, the simulation of continued historical withdrawals indicates a decline in hydraulic head of about 6.8 feet from 1980 through 2030. The simulation of 50 years of withdrawals with irrigation development indicates an additional decline in hydraulic head of about 6.2 feet, resulting in a total decline of about 13.0 feet.

The response is similar in the other cells in which this well field is represented. Well LA-4 is represented at row 15, column 4, layer 20. Without irrigation development, the simulation of continued historical withdrawals indicates a decline in hydraulic head of about 15.5 feet from 1980 through 2030. The simulation of 50 years of withdrawals with irrigation development indicates an additional decline in hydraulic head of about 3.4 feet, resulting in a total decline of about 18.9 feet.

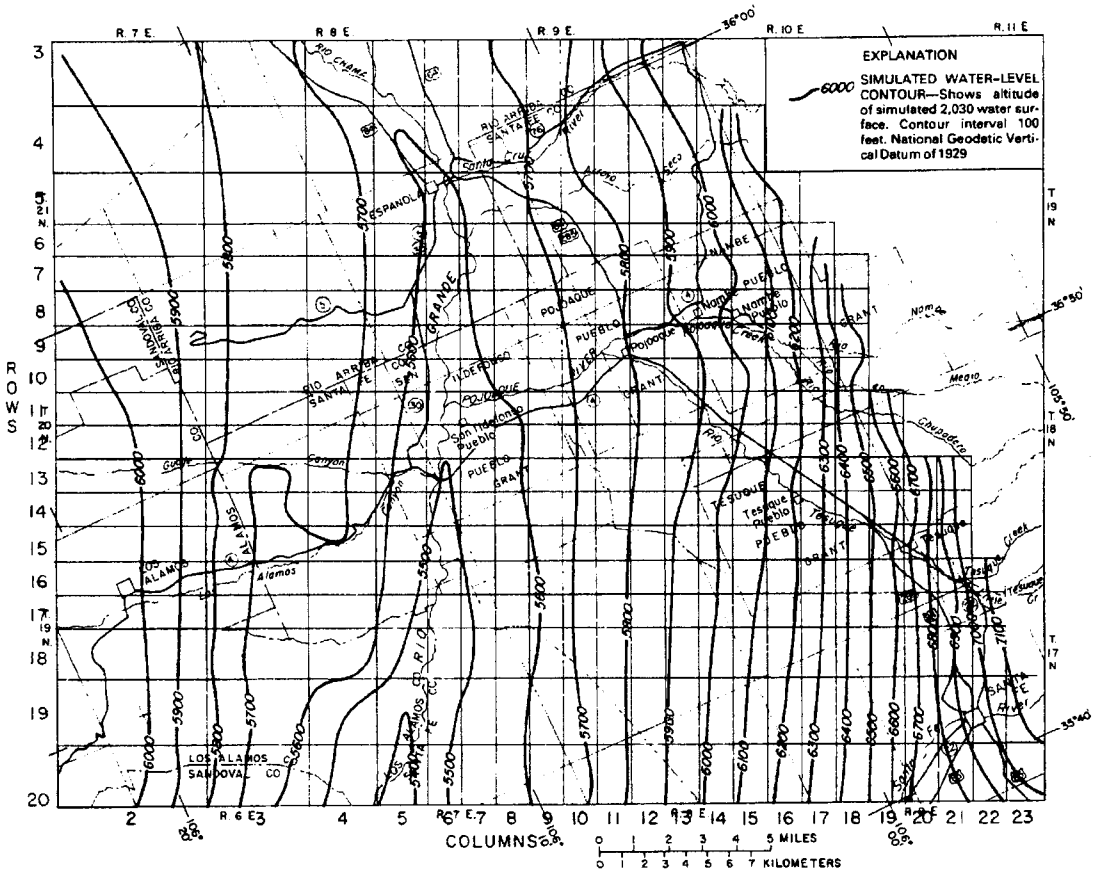

Figure 23. Contours of simulated water surface in 2030 assuming withdrawals as shown in table 12.

Well LA-5 is represented at row 14, column 4, layer 20. Without irrigation development, the simulation of continued historical withdrawals indicates a decline in hydraulic head of about 15.1 feet from 1980 through 2030. The simulation of 50 years of withdrawals with irrigation development indicates an additional decline in hydraulic head of about 3.8 feet, resulting in a total decline of about 18.9 feet.

Well LA-6 is represented at row 14, column 5, layer 19. Without irrigation development, the simulation of continued historical withdrawals indicates a decline in hydraulic head of about 7.4 feet from 1980 through 2030. The simulation of 50 years of withdrawals with irrigation development indicates an additional decline in hydraulic head of about 5.5 feet, resulting in a total decline of about 12.9 feet.

Guaje Canyon Well Field

In the Guaje Canyon well field, wells G-2, G-3, G-4, G-5, and G-6 are represented at row 13, column 3, layer 21. The simulated decline in hydraulic head (fig.27) is due almost entirely to the continuation of historical withdrawals. Without irrigation development, the simulation of continued historical withdrawals indicates a decline in hydraulic head of about 31.5 feet from 1980 through 2030. The simulation of 50 years of withdrawals with irrigation development indicates an additional decline in hydraulic head of about 0.6 foot, resulting in a total decline of about 32.1 feet.

The response is similar in the other cell in which this well field is represented. Wells G-1 and G-1A are represented at row 13, column 4, layer 20. Without irrigation

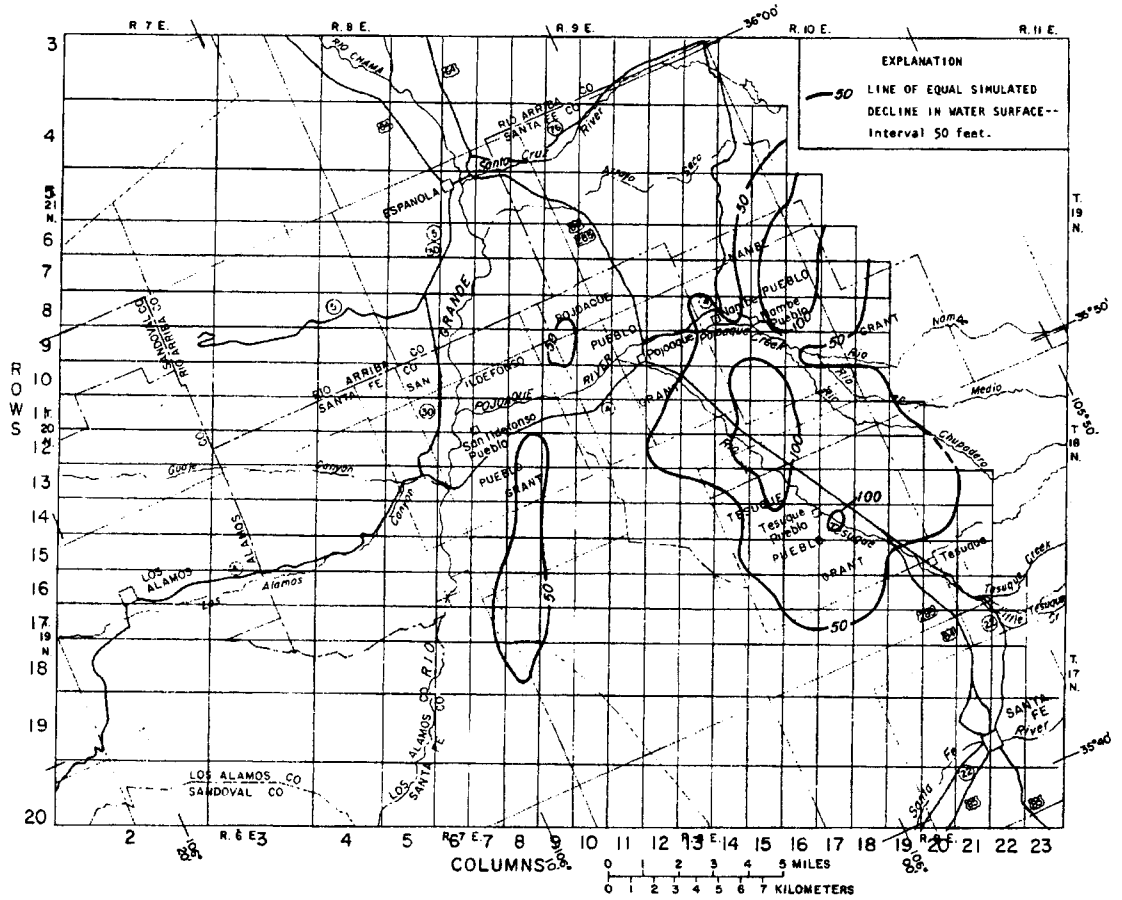

Figure 24. Lines of equal simulated decline in water surface from 1980 through 2030 assuming withdrawals as shown in table 12.

development, the simulation of continued historical withdrawals indicates a decline in hydraulic head of about 14.2 feet from 1980 through 2030. The simulation of 50 years of withdrawals with irrigation development indicates an additional decline in hydraulic head of about 4.1 feet, resulting in a total decline of about 18.3 feet.

Pajarito Mesa Well Field

In the Pajarito Mesa well field, wells PM-1 and PM-3 are represented at row 16, column 3, layer 21. The simulated decline in hydraulic head (fig. 28) is due almost entirely to the continuation of historical withdrawals. Without irrigation development, the simulation of continued historical withdrawals indicates a decline in hydraulic head of about 47.9 feet from 1980 through 2030. The simulation of 50 years of withdrawals with irrigation development indicates an additional decline in hydraulic head of about 0.5 foot, resulting in a total decline of about 48.4 feet.

The response is similar at the other cell in which this well field is represented. Well PM-2 is represented at row 18, column 3, layer 21. Without irrigation development, the simulation of continued historical withdrawals indicates a decline in hydraulic head of about 46.8 feet from 1980 through 2030. The simulation of 50 years of withdrawals with irrigation development indicates an additional decline in hydraulic head of about 0.4 foot, resulting in a total decline of about 47.2 feet.

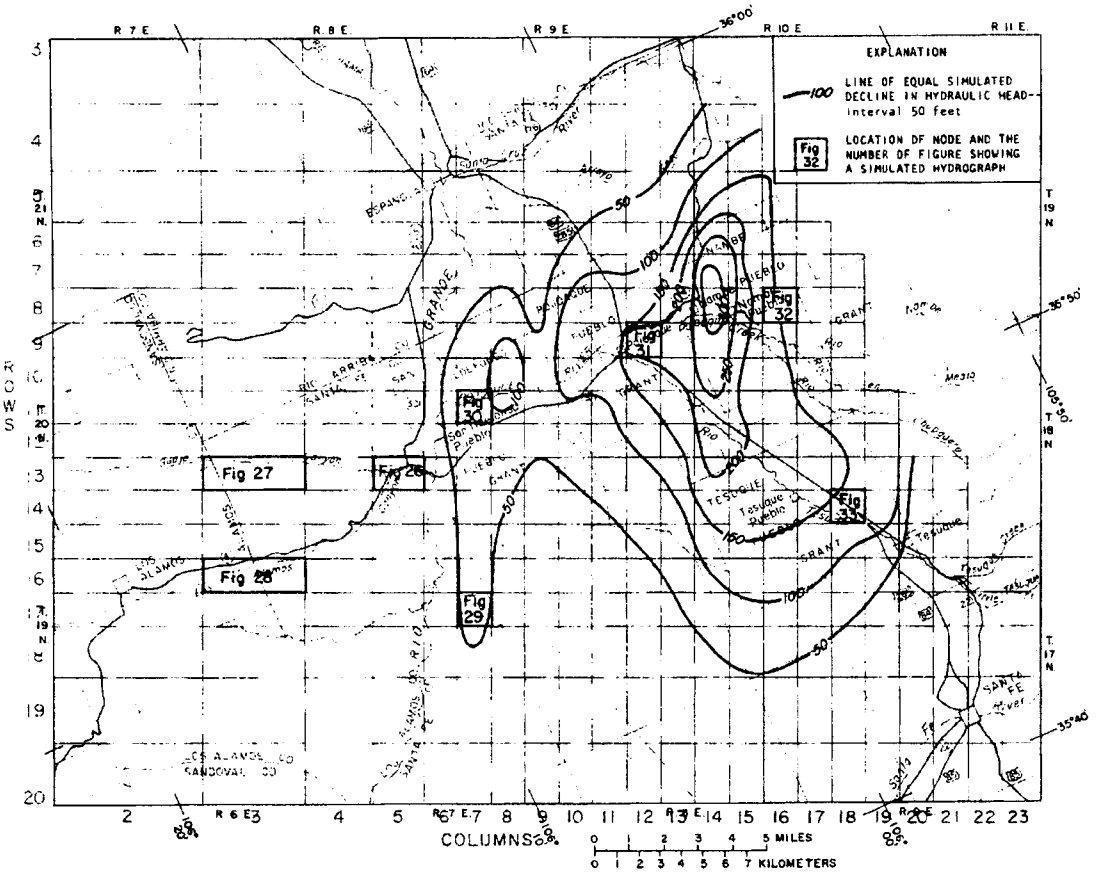

Figure 25. Lines of equal simulated decline in hydraulic head in the uppermost confined cells from 1980 through 2030 assuming withdrawals as shown in table 12.

Buckman Well Field

In the Buckman well field, production wells B-4, B-5, and B-6, and observation well B-7 are represented at row 17, column 7, layer 17. The simulated decline in hydraulic head (fig. 29) is due primarily to the continuation of historical withdrawals. Without irrigation development, the simulation of continued historical withdrawals indicates a decline in hydraulic head of about 48.7 feet from 1980 through 2030. The simulation of 50 years of withdrawals with irrigation development indicates an additional decline in hydraulic head of about 13.1 feet, resulting in a total decline of about 61.8 feet.

The response is similar at the other cell in which this well field is represented. Well B-3 is represented at row 16, column 7, layer 17. Without irrigation development, the simulation of continued historical withdrawals indicates a decline in hydraulic head of about 46.3 feet from 1980 Through 2030. The simulation of 50 years of withdrawals with irrigation development indicates an additional decline in hydraulic head of about 17.2 feet, resulting in a total decline of about 63.5 feet.

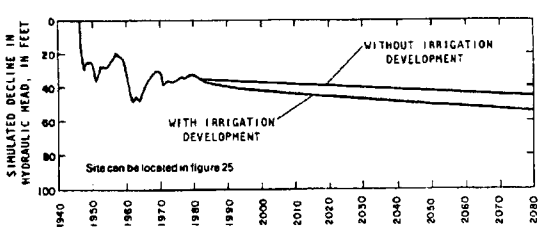

Figure 26. Simulated decline in hydraulic head near Los Alamos Canyon well field (row 13, column 5, layer 19).

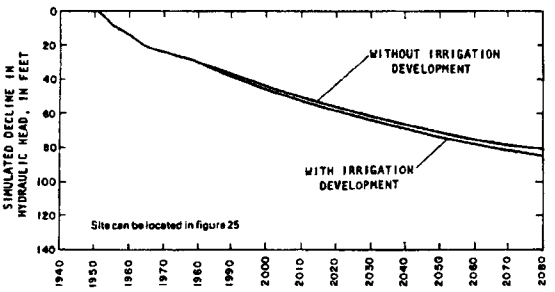

Figure 27. Simulated decline in hydraulic head near Guaje Canyon well field (row 13, column 3, layer 21).

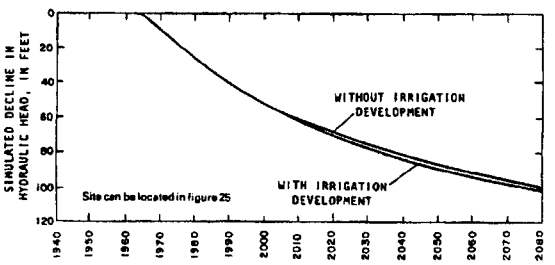

Figure 28. Simulated decline in hydraulic head near Pajarito Mesa well field (row 16, column 3, layer 21).

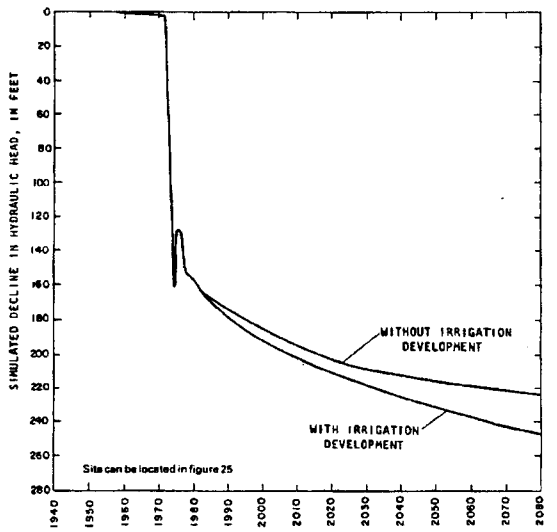

Figure 29. Simulated decline in hydraulic head near Buckman well field (row 17, column 7, layer 17).

Pojoaque River Basin

On the San Ildefonso Pueblo Grant, wells SW-07, SW-16, SW-17, SW-18, A-2A, and A-3A are represented at the cell in row 11, column 7, layer 17. The simulated decline in hydraulic head in this cell (fig. 30) is due primarily to the irrigation development. Without irrigation development, the simulation of continued historical withdrawals indicates a decline in hydraulic head of about 8.3 feet from 1980 through 2030. The simulation of 50 years of withdrawals with irrigation development indicates an additional decline in hydraulic head of about 84.0 feet, resulting in a total decline of about 92.3 feet.

On the Pojoaque Pueblo Grant, wells PW-13, PW-16, PW-17, PW-18, B-2A, B-3A, B-4A, and B-5A are represented at the cell in row 9, column 12, layer 12. The simulated decline in hydraulic head at this cell (fig. 31) is due almost entirely to the irrigation development. Without irrigation development, the simulation of continued historical withdrawals indicates a decline in hydraulic head of about 0.8 foot from 1980 through 2030. The simulation of 50 years of withdrawals with irrigation development indicates an additional decline in hydraulic head of about 210.6 feet, resulting in a total decline of about 211.4 feet.

On the Nambe Pueblo Grant, well NW-09 is represented at the cell in row 8, column 16, layer 8. The simulated decline in hydraulic head at this cell (fig. 32) is due almost entirely to the irrigation development. Without irrigation development, the simulation of continued historical withdrawals indicates a negligible decline in hydraulic head from 1980 through 2030. The simulation of 50 years of withdrawals with irrigation development indicates a decline in hydraulic head of about 160.8 feet. Nearby at row 8, column 14, layer 10, the 50-year decline in hydraulic head of about 334 feet is the maximum simulated decline.

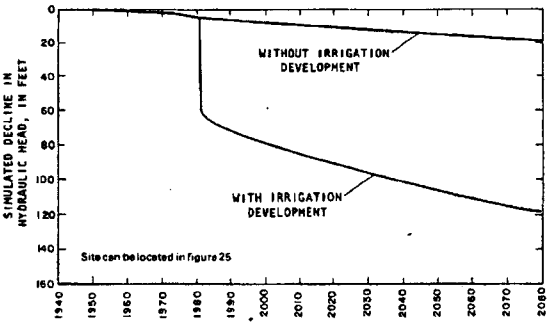

Figure 30. Simulated decline in hyraulic head near San Ildefonso Pueblo (row 11, column 7, layer 17).

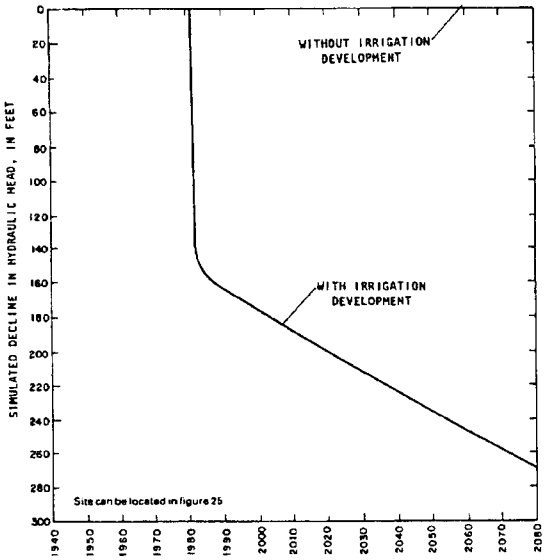

Figure 31. Simulated decline in hydraulic head near Pojoaque Pueblo (row 9, column 12, layer 12).

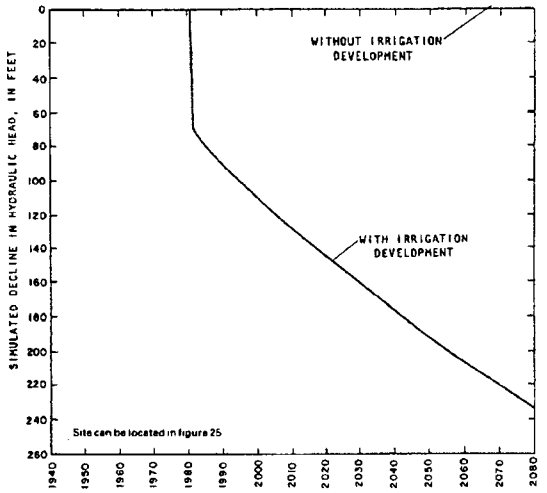

Figure 32. Simulated decline in hydraulic head near Nambe Pueblo (row 8, column 16, layer 8).

On the Tesuque Pueblo Grant, wells TW-09, TW-37, TW-38, TW-39, TW-42, and TW-43 are represented at the cell in row 14, column 18, layer 6. The simulated decline in hydraulic head at this cell (fig. 33) is due almost entirely to the irrigation development. Without irrigation development, the simulation of continued historical withdrawals indicates a negligible decline in hydraulic head from 1980 through 2030. The simulation of 50 years of withdrawals with irrigation development indicates a decline in hydraulic head of about 184.1 feet.

Simulated Changes in Flow Between Ground Water and Surface Water

As the simulated hydraulic head in areas of recharge and discharge changes, the simulated rate of recharge and discharge may change at both specified-hydraulic-head and hydraulic-head-dependent boundaries. The Rio Grande, the Santa Cruz River, and the downstream reach of the Santa Fe River are represented as specified-hydraulic-head boundaries. The Pojoaque River and its tributaries are represented as hydraulic-head-dependent boundaries.

Rio Grande, Santa Cruz, and Santa Fe Rivers

In steady state, the simulated ground-water discharge to the Rio Grande is about 22.06 cubic feet per second. In 1980 this rate is simulated to decrease by about 1.02 cubic feet per second to about 21.04 cubic feet per second. Without irrigation development, the simulation of continued historical withdrawals from 1980 through 2030 indicates a decrease of about 0.97 cubic foot per second to about 20.07 cubic feet per second. The simulation of 50 years of withdrawals with irrigation development indicates a decrease of about 0.90 cubic foot per second to about 20.14 cubic feet per second. The simulated ground-water discharge to the Rio Grande decreases less with the irrigation development than without. This is caused by

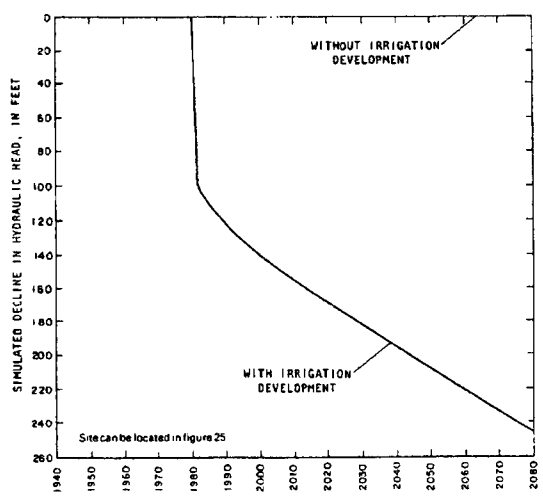

Figure 33. Simulated decline in hydraulic head near Tesuque Pueblo (row 14, column 18, layer 6).

adding return flows to the cells at the water surface; a total of 0.95 cubic foot per second of return flow is added to the cells representing the Rio Grande. The phenomenon is temporary; after 100 years the simulated decrease in discharge to the Rio Grande is 1.71 cubic feet per second for continued historical withdrawals and 2.10 cubic feet per second for irrigation development.

In steady state, the simulated Santa Cruz River recharges about 4.11 cubic feet per second to the ground water and discharges about 1.50 cubic feet per second for a net simulated flow from the Santa Cruz River of about 2.61 cubic feet per second. In 1980 this rate is simulated to increase by about 0.04 cubic foot per second to about 2.65 cubic feet per second. Without irrigation development, the simulation of continued historical withdrawals from 1980 through 2030 indicates an increase of about 0.09 cubic foot per second to about 2.74 cubic feet per second. The simulation of 50 years of withdrawals with irrigation development indicates an increase of about 1.08 cubic feet per second to about 3.73 cubic feet per second.

In steady state, the simulated ground-water discharge to the Santa Fe River is about 4.35 cubic feet per second. In 1980 this rate is simulated to decrease by about 0.01 cubic foot per second to about 4.34 cubic feet per second. Without the irrigation development the simulation of continued historical withdrawals from 1980 through 2030 indicates a decrease of about 0.06 cubic foot per second to about 4.28 cubic feet per second. The simulation of 50 years of withdrawals with irrigation development indicates a decrease of about 0.13 cubic foot per second to about 4.21 cubic feet per second.

Table 13. Projected water balances for the Pojoaque River and tributaries using the simulated flows from the digital model

Description of flow	Simulated flow, in cubic feet per second				
	1980	1981	1990	2005	2030
Tributary inflow	16.90	16.90	16.90	16.90	16.90
Consumption by vegetation[1]	−1.10	−1.10	−1.10	−1.10	−1.10
Irrigation diversion	−7.67	−13.14	−13.14	−13.14	−13.14
Net flow from (+) or to (−) ground water[2]	−0.09	0.38	−0.93	−2.29	−2.49
Pojoaque River discharge and evaporation from riverbed calculated as a residual[2]	−8.04	−3.04	−1.73	−0.37	−0.17

[1] Consumption by native vegetation is represented as specified flows from the ground-water reservoir.

[2] These values are simulated by the digital model.

Pojoaque River and Tributaries

In steady state, the simulated Pojoaque River along with its tributaries recharges about 4.25 cubic feet per second to the ground water and discharges about 4.21 cubic feet per second for a net simulated recharge from the Pojoaque River of about 0.04 cubic foot per second. In 1980 this rate is simulated to increase by about 0.05 cubic foot per second to about 0.09 cubic foot per second. Without irrigation development, the simulation of continued historical withdrawals from 1980 through 2030 indicates an increase of about 0.22 cubic foot per second to about 0.31 cubic foot per second. The simulation of 50 years of withdrawals with irrigation development indicates an increase of about 2.40 cubic feet per second to about 2.49 cubic feet per second.

Projected water balances for the Pojoaque River and its tributaries are given in table 13 for 1980 and after 1, 10, 25, and 50 years of withdrawals with irrigation development. After 25 years the model simulates most of the flow of the Pojoaque River being consumed by diversion and loss to the ground-water reservoir. Although the model does not simulate the Pojoaque River discharge to the Rio Grande as a separate item, it is reasonable to conclude that the simulated Pojoaque River discharge is negligible when the total of discharge and riverbed evaporation is less than the estimated riverbed evaporation. The riverbed evaporation is estimated in the previous section on boundaries to be about 3.32 cubic feet per second. Therefore, the simulated Pojoaque River discharge to the Rio Grande is negligible even in the first year of the irrigation development (table 13).

The simulated flow is from ground water to the Pojoaque River for the first year of irrigation development. This temporary phenomenon is caused by adding return flow to the cells at the water surface and may not occur in the prototype.

Simulated Sources of Water Withdrawn from Wells

The simulated response to the withdrawals for irrigation development as well as continued historical withdrawals is summarized by considering the sources of the water withdrawn from wells. The simulated change in flow from each of the sources is shown in figures 34 and 35 through 2080. The historical withdrawals and their continuation are shown in figure 34. The total withdrawals from the Los Alamos Canyon, Guaje Canyon, Pajarito Mesa, and Buckman well fields increased gradually from 1947 through 1977; projected withdrawals continue after 1977 at 11.24 cubic feet per second. The sources for these withdrawals are storage in the Tesuque aquifer system and capture from the Rio Grande, Santa Cruz, Santa Fe, and Pojoaque Rivers. Streamflow capture is the combination

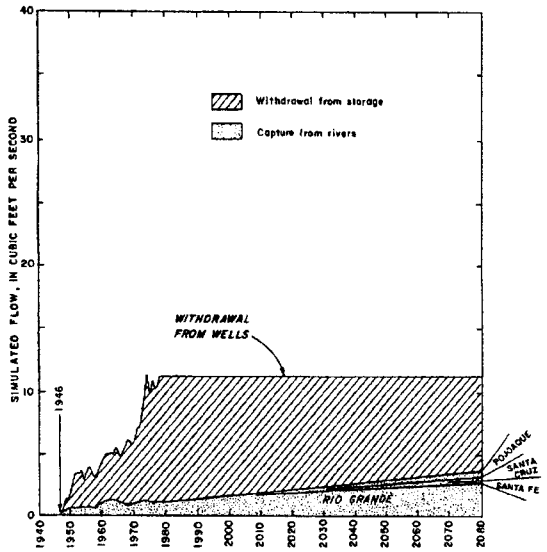

Figure 34. Simulated source of water withdrawn from Tesuque aquifer system without irrigation development.

of: (1) the reduction in the previous discharge from the aquifer to the stream; and (2) the increase in the previous recharge to the aquifer from the stream.

The rate of flow from each source is accumulated as the ordinate in figure 34. For example, in 2030 the 11.24 cubic feet per second withdrawn from wells is simulated to consist of:

- 8.79 cubic feet per second (78.1 percent) withdrawn from storage;
- 0.27 cubic foot per second (2.4 percent) capture from the Pojoaque River;
- 1.99 cubic feet per second (17.7 percent capture from the Rio Grande;
- 0.13 cubic foot per second (1.2 percent) capture from the Santa Cruz River; and
- 0.07 cubic foot per second (0.6 percent) capture from the Santa Fe River.

Superimposed on the continued historical withdrawals are the net withdrawals of 28.41 cubic feet per second for irrigation development resulting in total withdrawals of 39.65 cubic feet per second. The rate of flow from each individual source is accumulated as the ordinate in figure 35. For example, in 2030 the 39.65 cubic feet per second is simulated to consist of:

- 34.05 cubic feet per second (85.9 percent) withdrawn from storage;
- 2.45 cubic feet per second (6.1 percent) capture from the Pojoaque River;
- 1.92 cubic feet per second (4.8 percent) capture from the Rio Grande;
- 1.12 cubic feet per second (2.8 percent) capture from the Santa Cruz River; and
- 0.14 cubic foot per second (0.4 percent) capture from the Santa Fe River.

The changes in the model due to irrigation development can be seen by comparing figures 34 and 35. For example, in 2030 the 28.41 cubic feet per second withdrawn for irrigation development has resulted in an additional 25.26 cubic feet per second withdrawn from storage: additional capture of 2.18 cubic feet per second from the Pojoaque River, 0.99 cubic foot per second from the Santa Cruz River, and 0.07 cubic foot per second from the Santa Fe River, and a decrease of 0.07 cubic foot per second in capture from the Rio Grande.

Because all streams are tributary to the Rio Grande, all streamflow capture and diversion will deplete the flow of the Rio Grande downstream from the modeled area. With irrigation development, the total simulated depletion

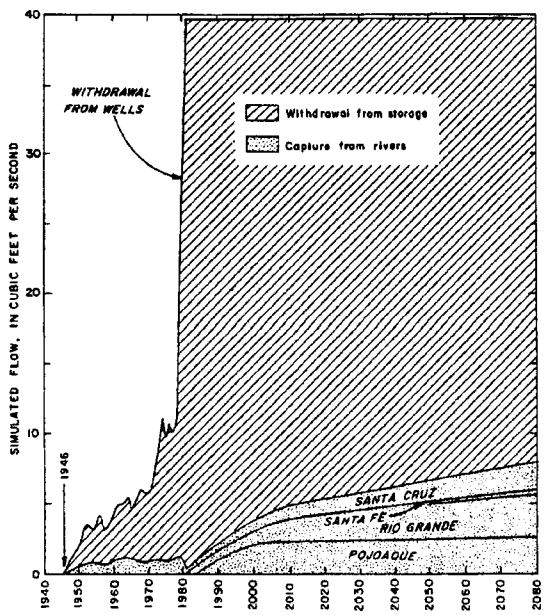

Figure 35. Simulated source of water withdrawn from Tesuque aquifer system with irrigation development.

of the Rio Grande is 18.77 cubic feet per second: streamflow capture of 5.63 cubic feet per second and diversion of 13.14 cubic feet per second. Without irrigation development, the total simulated depletion of the Rio Grande is 10.13 cubic feet per second: streamflow capture of 2.46 cubic feet per second and diversions of 7.67 cubic feet per second. The total predicted effect on the flow of the Rio Grande downstream from the modeled area in 2030 after 50 years of withdrawals is 18.77 cubic feet per second: 10.13 cubic feet per second due to the continued historical withdrawals and 8.64 cubic feet per second due to the withdrawals and increased diversions of the irrigation development.

The simulated source for most of the water withdrawn is the water in storage in the Tesuque aquifer system. The simulated capture from the Pojoaque River increases through about 2030 and is subsequently constant. The simulated capture from the Rio Grande, Santa Cruz, and Santa Fe Rivers continues to increase gradually. In 2030, simulated storage in the Tesuque aquifer system would supply 34.05 cubic feet per second of the 39.65 cubic feet per second being withdrawn (86 percent). Fifty years later, simulated storage would supply 31.80 cubic feet per second (80 percent). According to the digital model simulation, storage will probably be a significant source of water for several centuries. During this time, capture from the simulated streams will gradually increase. In general, if withdrawals are simulated to continue indefinitely, the rate of capture will approach the rate of withdrawal as heads stabilize to a new steady-state condition. In the Tesuque aquifer system, changes in head may make it impossible to continue withdrawals indefinitely at the specified locations.

If the withdrawals are simulated to stop at some future date, the simulated system will eventually return to the initial steady-state condition. The areas of figures 34 and 35 represent the volumes of water withdrawn from each source. If withdrawals cease, capture will continue until the volume of capture is equal to the volume withdrawn from storage. If withdrawals were to cease, the rate of capture would initially continue to increase. Eventually, as heads near the streams begin to recover to steady-state conditions, the rate of capture will decrease. After 100 years the rate of capture will be about 20 percent of the rate of withdrawal. If withdrawals were to cease after 100 years and the rate of capture remained at 20 percent, the system would require 500 years to return to initial steady-state conditions. Recovery would require more time because the rate of capture will decrease as the steady-state condition is approached.

MODEL SENSITIVITY

The confidence in the predicted response described in the preceding section needs to be based on a subjective appraisal of the analogy between the Tesuque aquifer system and the model. A significant part of this analogy is the assumption that the aquifer characteristics of the Tesuque aquifer system have the same or similar characteristics assumed in the model. Because the aquifer characteristics are not known with certainty, the sensitivity of the model to each of several selected characteristics was tested.

The sensitivity of the model was tested by changing the values assumed for each of five aquifer characteristics. The extent to which this variation affects the simulated response is a qualitative measure of the sensitivity of the model to uncertainty in that aquifer characteristic. Thus, if the variation produces a minor change in the predicted response, the model is not very sensitive to that aquifer characteristic.

The sensitivity of the model was tested for five aquifer characteristics: thickness, hydraulic conductivity, anisotropy ratio, specific storage, and specific yield of the Tesuque Formation. The alternative thickness of the Tesuque Formation was assumed to have a maximum thickness of about 9,000 feet as indicated by Kelley (1978). For the other characteristics, the alternative values were the lower and upper limits of the plausible range as given in table1. For each instance, the impact on both the simulated steady-state condition and the transient response is described by comparing the standard simulation (the one described thus far in the report) with an alternative simulation (one in which an aquifer characteristic had an alternative value).

The impact on the simulated steady-state condition indicates whether the value to which the aquifer characteristic was varied exceeds the uncertainty with which the value of the characteristic is known. If the steady-state condition simulated with the varied characteristic is compatible with available data, then the simulated transient response provides a measure of the uncertainty of the true transient response.

The sensitivity of the simulated steady-state condition is displayed in two figures and a table for each of the five aquifer characteristics. The first figure for each characteristic is a graph comparing historical water levels for selected sites in and near the Pojoaque River basin with those simulated by the model. The effect of characteristic variation can be seen by comparing the resultant figure with the equivalent figure (fig. 10) for the standard simulation. The second figure is a bar graph that displays the steady-state flow rates for both the standard and the varied simulations. The table presents the vertical hydraulic gradients for the same four sites given in table 5.

The sensitivity of the transient response is displayed in nine figures. Eight figures are graphs showing the change in hydraulic head at each of the eight sites shown in figure 25. In each, the change in hydraulic head for the standard simulation (as shown in figures 26-33) is accompanied by the equivalent graph for the varied simulation.

The final graph presents the source of water withdrawn from wells for both the standard and the varied simulations in 2030 after 50 years of withdrawals for the irrigation development.

In some instances the sensitivity to the aquifer characteristic is so small that the difference from the standard simulation is not demonstrated by the figure. For those instances the figures have been omitted.

Thickness of the Tesuque Formation

The predicted response was obtained by assuming that the maximum saturated thickness of the Tesuque aquifer system is about 4,000 feet (fig. 4). Because the thickness of the Tesuque Formation is not known and because some researchers (Kelley, 1978) postulate saturated thickness of as much as about 9,000 feet, the sensitivity of the model to a greater saturated thickness was tested. The alternative saturated thickness used for the sensitivity test (fig. 36) ranges from zero to almost 9,000 feet. This increase in saturated thickness provides both a greater volume in which water is stored under confined conditions and a greater cross-sectional area for flow.

Simulated Steady-State Condition

The simulated steady-state condition does respond to the variation of saturated thickness. The comparison with historical hydraulic heads is shown in figure 37 for the simulation assuming the greater saturated thickness and in figure 10 for the standard simulation. The agreement is better for the standard simulation, especially for water levels greater than about 6,400 feet. The hydraulic heads are lower for the simulation assuming a greater saturated thickness. The sensitivity of the steady- state condition to saturated thickness is significant enough that a model with the saturated thickness shown in figure 36 would require adjustments in other aquifer characteristics to provide a comparable agreement with the historical steady-state condition.

Historical vertical hydraulic gradients are compared with simulated gradients in table 14. For the sites at the Pueblo Grants of San Ildefonso and Tesuque, the gradients simulated by assuming the greater saturated thickness are closer to the historical gradients than those of the standard simulation. However, for the standard simulation the mean is 0.14, the same as that for the historical values. With the greater thickness, the simulated gradients have a mean of 0.12.

The steady-state flow through the system is greater for the simulation assuming a greater saturated thickness of the Tesuque Formation (fig. 38). The discharge to the Rio Grande is 31.04 cubic feet per second, 41 percent larger but still compatible with available data. Most of the increased recharge is from the Santa Fe River and the cells along the eastern margin of the Tesuque Formation, where the recharge has more than doubled. The net recharge from the Pojoaque River is increased about 0.22 cubic foot per second, and that along the western margin is increased about 22 percent. The Santa Cruz River has changed from a stream that recharges the ground-water system to one that receives discharge from the ground-water system.

Table 14. Effect of variations in represented saturated thickness on vertical hydraulic gradients

Site at pueblo grant (location shown in fig. 1)	Vertical hydraulic gradient		
	Historical	Simulated	
		Standard saturated thickness	Greater saturated thickness
San Ildefonso	0.12	0.09	0.13
Pojoaque	.12	.09	.14
Nambe	.20	.15	.11
Tesuque	.12	.21	.12
Mean	.14	.14	.12

Simulated Transient Response

The variation of saturated thickness affects the simulated transient response at a site. The difference can be seen both in the changes in hydraulic head and in the source of the water withdrawn from wells.

The sensitivity of the simulated declines in hydraulic head in the production zone to variation in saturated thickness is shown at five of the eight locations shown in figure 25. The simulated decline in hydraulic head after 100 years of development varies less than 2 feet from the standard simulation for the sites near Los Alamos Canyon well field (standard simulation shown in fig. 26), Guaje Canyon well field (standard simulation shown in fig. 27), and Pajarito Mesa well field (standard simulation shown in fig. 28). The difference is greater at the remaining five sites. The difference in response is shown for the sites near the Buckman well field (fig. 39), near San Ildefonso Pueblo (fig. 40), near Pojoaque Pueblo (fig. 41), near Nambe Pueblo (fig. 42), and near Tesuque Pueblo (fig. 43). In all instances the declines in hydraulic head are less for the simulation that assumes a greater saturated thickness. The maximum decline in hydraulic head at any node in the model after 50 years of development is 242 feet with the greater saturated thickness as compared to 334 feet for the standard simulation.

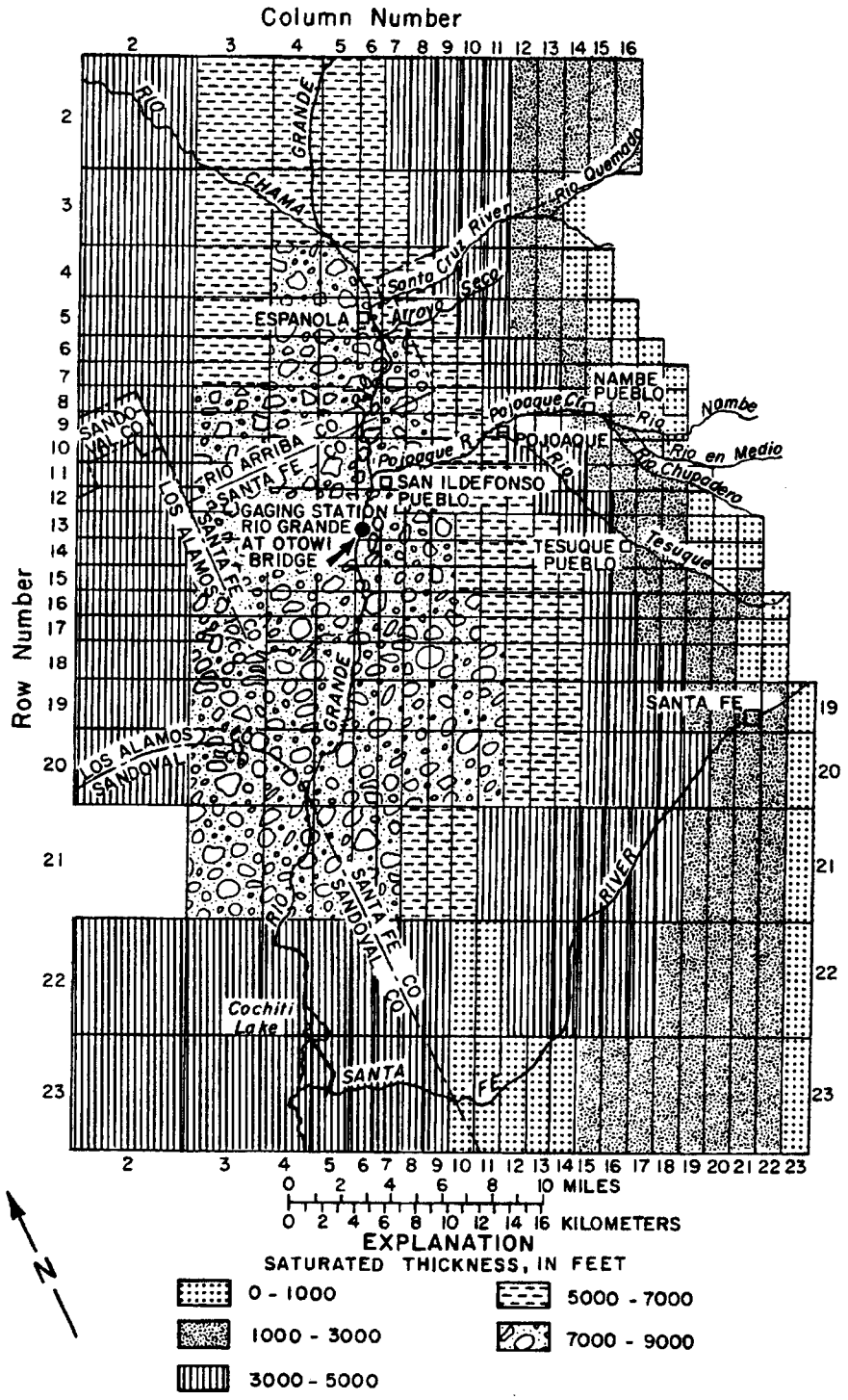

Figure 36. Alternative saturated thickness used to test sensitivity of the model to represented thickness.

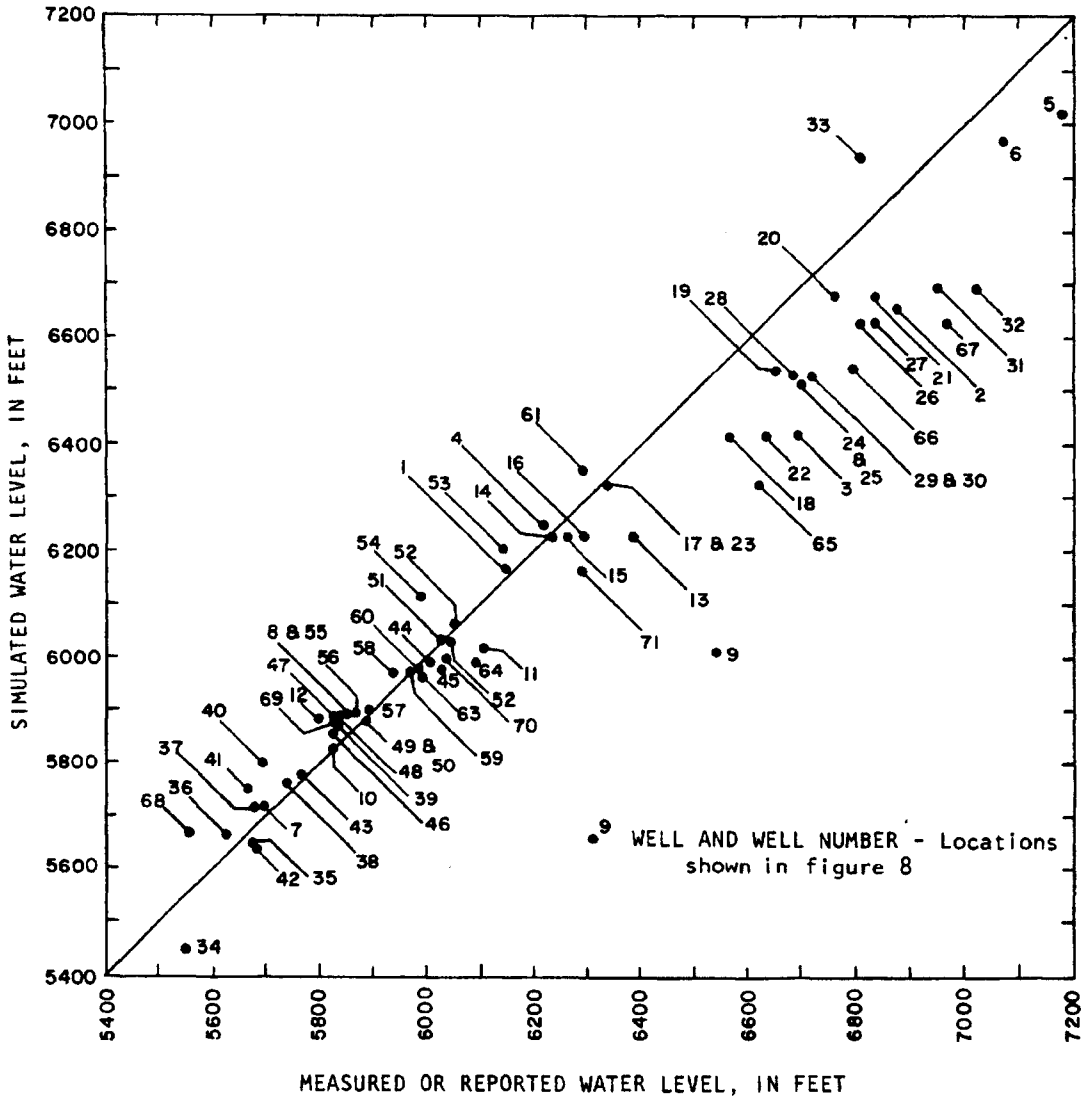

Figure 37. Comparison between measured or reported water levels for selected wells and springs and water levels simulated by assuming a greater saturated thickness.

The effect of variation in saturated thickness on the source of water withdrawn from wells is shown (fig. 44) by comparing the flow rates in 2030 after 50 years of development. With a greater saturated thickness, a larger percentage of the withdrawals comes from storage in the Tesuque Formation, and a smaller percentage comes from capture from the Pojoaque River.

A model with greater saturated thickness would respond differently if the other aquifer characteristics were adjusted to improve the comparison with the historical steady-state condition. The transient response for a calibrated model with greater saturated thickness might more closely resemble that of the standard simulation than does the response of the model with greater saturated thickness presented here.

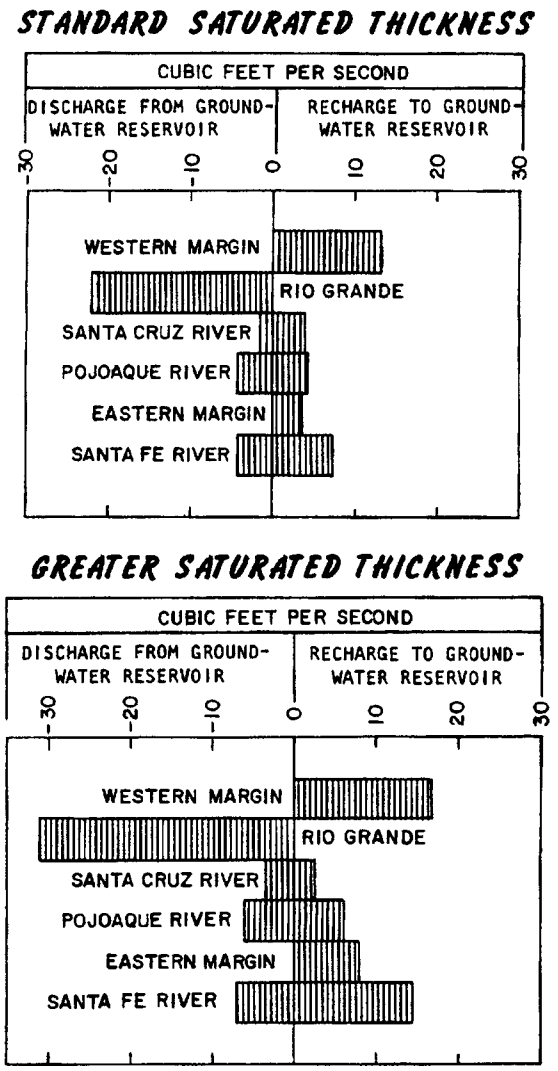

Figure 38. Effect of variations in represented saturated thickness on steady-state flow rates.

Hydraulic Conductivity

The predicted response was obtained by assuming that the hydraulic conductivity of the Tesuque aquifer system was 1.0 foot per day. The sensitivity of the model to this characteristic was tested with alternative simulations in which the hydraulic conductivity was assumed to be 0.5 and 2.0 feet per day, the lower and upper limits of the plausible range (table 1). In each instance, the constant of proportionality (leakance coefficient) for hydraulic-head-dependent boundaries was recalculated from the hydraulic conductivity. Decreasing the hydraulic conductivity reduces the ability of an aquifer to transmit water.

Simulated Steady-State Condition

Hydraulic head changes slightly with varying hydraulic conductivity. However, the comparison between historical and simulated hydraulic heads does not differ significantly from that shown in figure 10 for the standard simulation. Similarly, the vertical gradients do not differ significantly from those shown in table 5 for the standard simulation.

The steady-state flow rates are sensitive to hydraulic conductivity (fig. 45). The greater the hydraulic conductivity, the more flow through the system is required to maintain the hydraulic-head distribution. Discharge to the Rio Grande ranges from 11.02 to 44.10 cubic feet per second (fig. 45) as the hydraulic conductivity ranges from 0.5 to 2.0 feet per day. The lower rate (11.02 cubic feet per second) is about 0.2 cubic foot per second per mile, and the higher rate (44.10 cubic feet per second) is about 1.0 cubic foot per second per mile. Both are compatible with the data presented in an earlier section on "Flow Between Ground Water and Surface Water in the Prototype: Rio Grande."

Although the simulated steady-state condition is sensitive to the hydraulic conductivity, even the extremes of the plausible range (table 1) produce results that are compatible with available data.

Simulated Transient Response

The variation of hydraulic conductivity affects the simulated transient response. The difference can be seen both in the changes in hydraulic head and the source of the water withdrawn from wells.

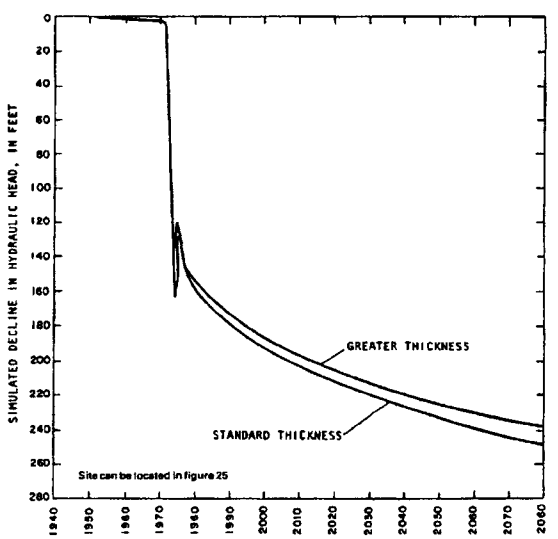

Figure 39. Effect of variations in represented saturated thickness on decline in hydraulic head near Buckman well field (row 17, column 7, layer 17).

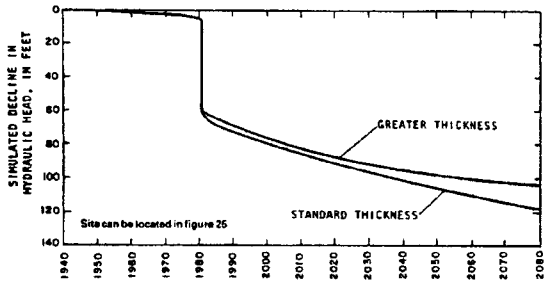

Figure 40. Effect of variations in represented satured thickness on decline in hydraulic head near San Ildefonso Pueblo (row 11, column 7, layer 17).

The sensitivity of the simulated change in hydraulic head in the production zone to hydraulic conductivity is shown at each of the eight locations shown in figure 25 (figs. 46-53). In each instance, small hydraulic conductivity is associated with large declines in hydraulic head. With the small hydraulic conductivity, less water is conducted toward the area of withdrawal from the neighboring areas, and greater declines in hydraulic head occur in the immediate vicinity of the withdrawals. The maximum decline in hydraulic head at any cell in the model after 50 years of development is 210 feet for the large hydraulic conductivity compared to 334 feet for the standard simulation and 474 feet for the small hydraulic conductivity. Because water is conducted more slowly toward the area of withdrawal from the neighboring areas, the effect on adjacent areas develops more slowly for the small hydraulic conductivity. After 50 years of development, more water is withdrawn from storage and streamflow capture is less for the small hydraulic conductivity (fig. 54). The small sensitivity of capture from the Pojoaque River is the result of the limited flow and the nearness of withdrawals to the location. In each instance, almost the entire flow is captured within 50 years.

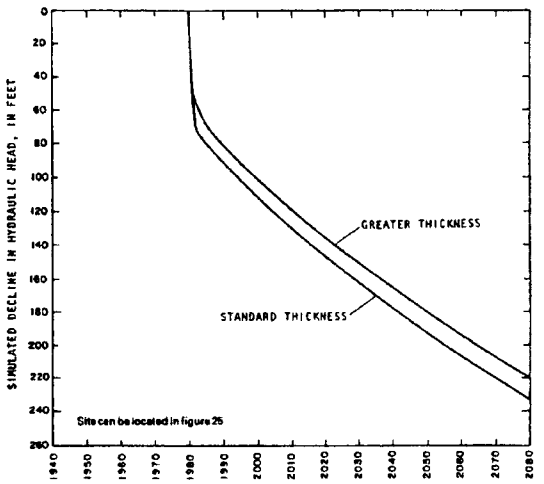

Figure 42. Effect of variations in represented saturated thickness on decline in hydraulic head near Nambe Pueblo (row 8, column 16, layer 8).

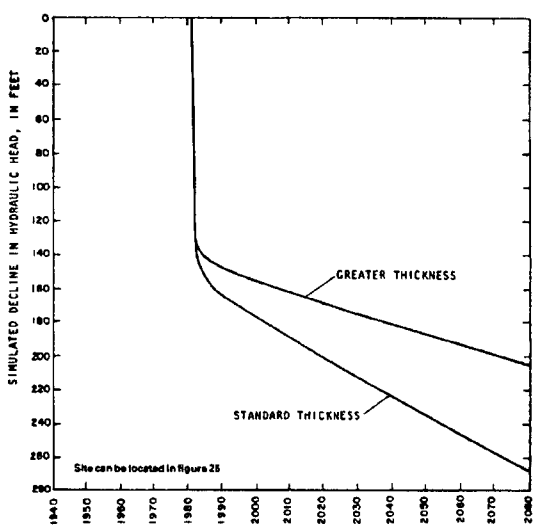

Figure 41. Effect of varations in represented saturated thickness on decline in hydraulic head near Pojoaque Pueblo (row 9, column 12, layer 12).

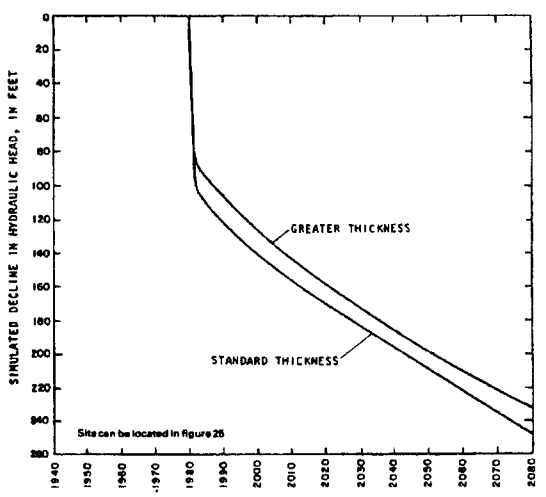

Figure 43. Effect of variations in represented saturated thickness on decline in hydraulic head near Tesuque Pueblo (row 14, column 18, layer 6).

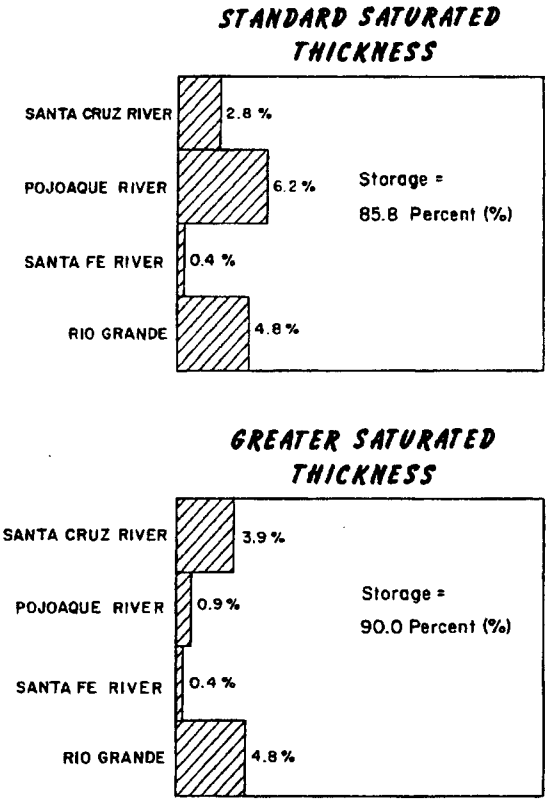

Figure 44. Effect of variations in represented saturated thickness on the source of water withdrawn from wells.

Anisotropy Ratio

The predicted response was obtained by assuming that the anisotropy ratio (the ratio of hydraulic conductivity normal to the beds to that parallel to the beds) was 0.003. The sensitivity of the model to this aquifer characteristic was tested with alternative simulations in which the hydraulic conductivity normal to the beds was assumed to be 0.001 foot per day and 0.01 foot per day. With hydraulic conductivity parallel to the beds of 1.0 foot per day, the anisotropy ratios are 0.001 and 0.01, the lower and upper limits of the plausible range (table 1). To decrease the anisotropy ratio reduces the ability of the aquifer to transmit water vertically and in the direction of the dip (both of which require flow normal to the beds) without changing the ability to transmit water in the direction of the strike.

Simulated Steady-State Condition

The simulated steady-state condition does respond to variations in anisotropy ratio. The comparison with historical hydraulic heads is shown in figure 55 for the simulation assuming a smaller anisotropy ratio and in figure 56 for the simulation assuming a larger anisotropy ratio. The changes are variable from site to site. At some sites (spring 5 and wells 22 and 23, for example) the simulated hydraulic head assuming a small ratio (fig. 55) is higher than the hydraulic head assuming a large ratio (fig. 56). At other sites (spring 7 and wells 31 and 50, for example) the hydraulic head is higher for the simulation assuming a large ratio. The general agreement between the historical and the simulated hydraulic heads is equally good in both instances.

The sensitivity of vertical hydraulic gradients (table15) reflects the increased difficulty of transmitting water vertically, which is associated with a smaller anisotropy ratio. Generally, the vertical hydraulic gradient increases as the anisotropy ratio is decreased.

The steady-state flow rates are sensitive to the anisotropy ratio (fig. 57). The smaller the anisotropy ratio, the less flow through the system is required to maintain the hydraulic-head distribution. Discharge to the Rio Grande ranges from 10.49 to 41.73 cubic feet per second as the anisotropy ratio ranges from 0.001 to 0.01. The smaller rate is about 0.2 cubic foot per second per mile, and the larger rate is about 0.9 cubic foot per second per mile. Both are compatible with the data presented in an earlier section on "Flow Between GroundWater and Surface Water in the Prototype: Rio Grande."

Therefore, although the simulated steady-state condition is sensitive to the anisotropy ratio, even the extremes of the plausible range (table 1) produce results that are compatible with available data.

Table 15. Effect of variations in represented anisotropy ratio on vertical hydraulic gradients.

Site at pueblo grant (location shown in fig.1)	Vertical hydraulic gradient			
	Historical	Simulated		
		Small anisotrophy ratio	Standard anisotrophy ratio	Large anisotrophy ratio
San Ildefonso	0.12	0.09	0.09	0.08
Pojoaque	.12	.12	.09	.05
Nambe	.20	.14	.15	.13
Tesuque	.12	.25	.21	.14
Mean	.14	.15	.14	.10

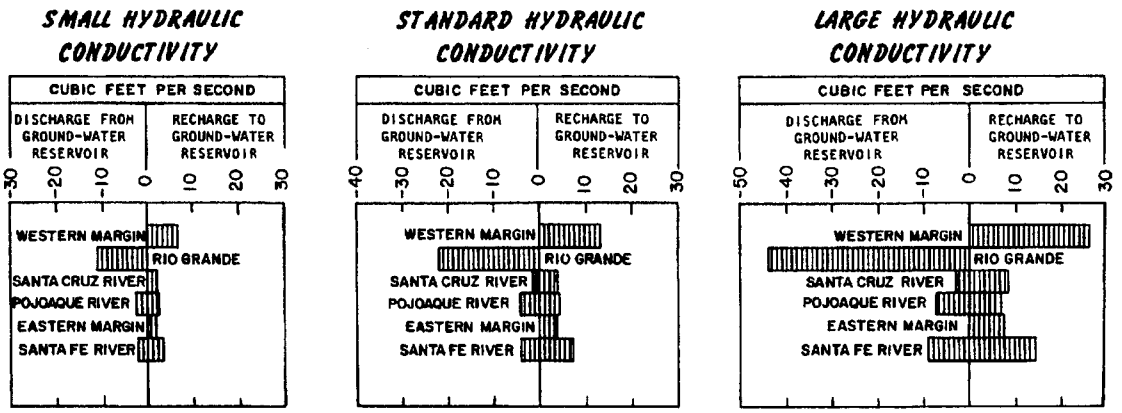

Figure 45. Effect of variations in hydraulic conductivity on steady-state flow rates.

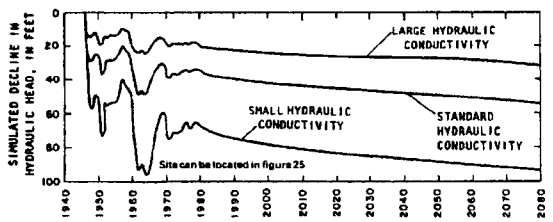

Figure 46. Effect of variations in hydraulic conductivity on decline in hydraulic head near Los Alamos Canyon well field (row 13, column 5, layer 19).

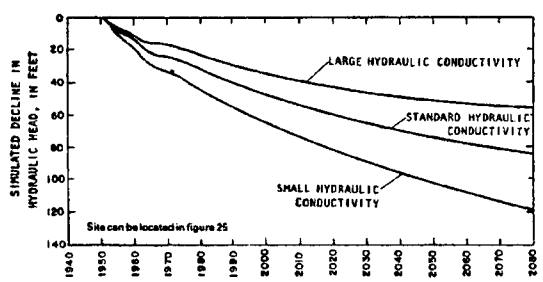

Figure 47. Effect of variations in hydraulic conductivity on decline in hydraulic head near Guaje Canyon well field (row 13, column 3, layer 21).

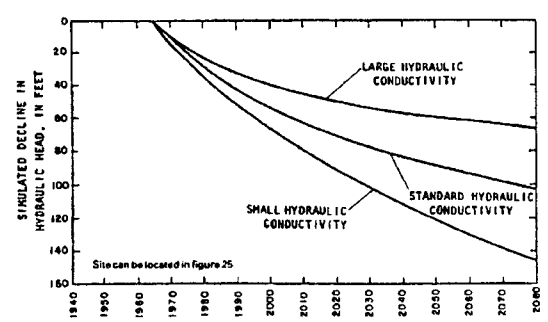

Figure 48. Effect of variations in hydraulic conductivity on decline in hydraulic head near Pajarito Mesa well field (row 16, column 3, layer 21).

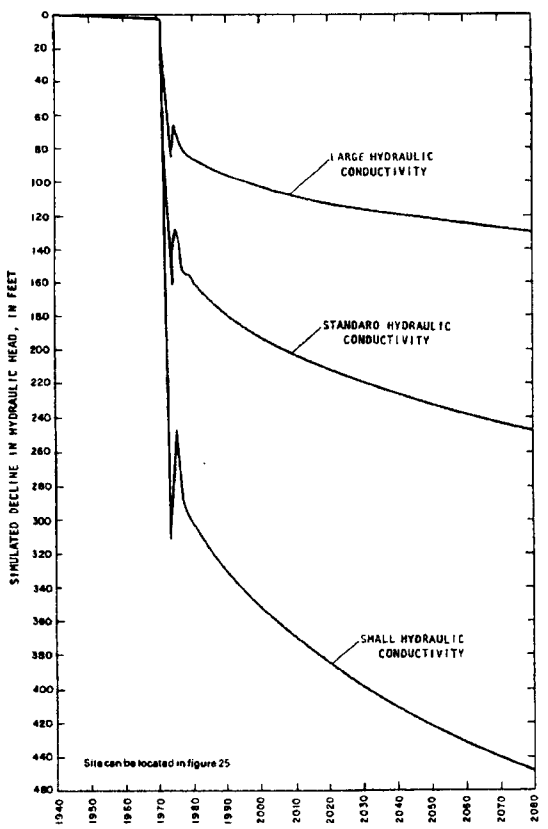

Figure 49. Effect of variations in hydraulic conductivity on decline in hydraulic head near Buckman well field (row 17, column 7, layer 17).

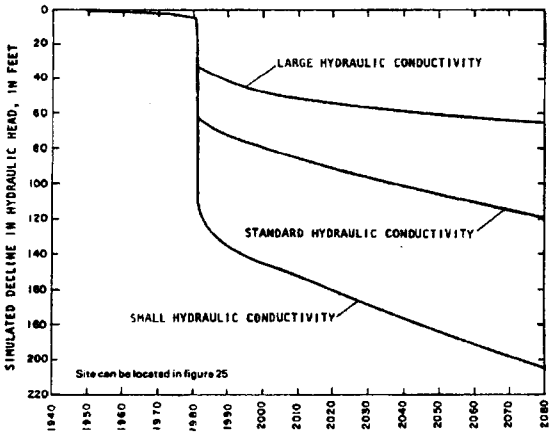

Figure 50. Effect of variations in hydraulic conductivity on decline in hydraulic head near San Ildefonso Pueblo (row 11, column 7, layer 17).

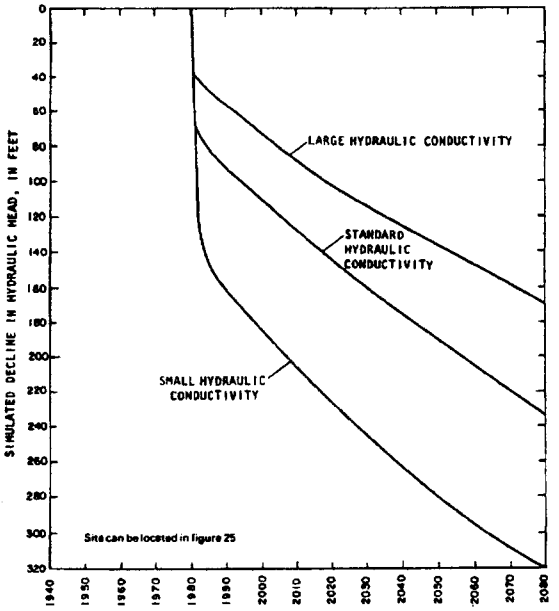

Figure 52. Effect of variations in hydraulic conductivity on decline in hydraulic head near Nambe Pueblo (row 8, column 16, layer 8).

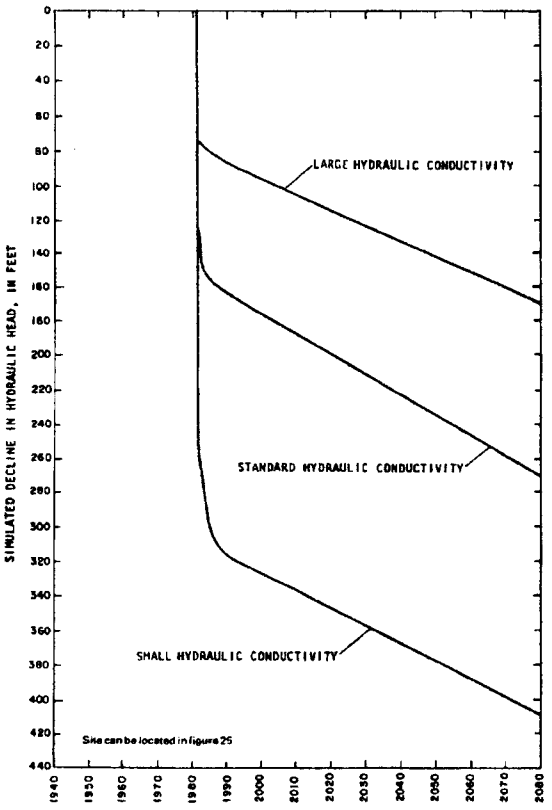

Figure 51. Effect of variations in hydraulic conductivity on decline in hydraulic head near Pojoaque Pueblo (row 9, column 12, layer 12).

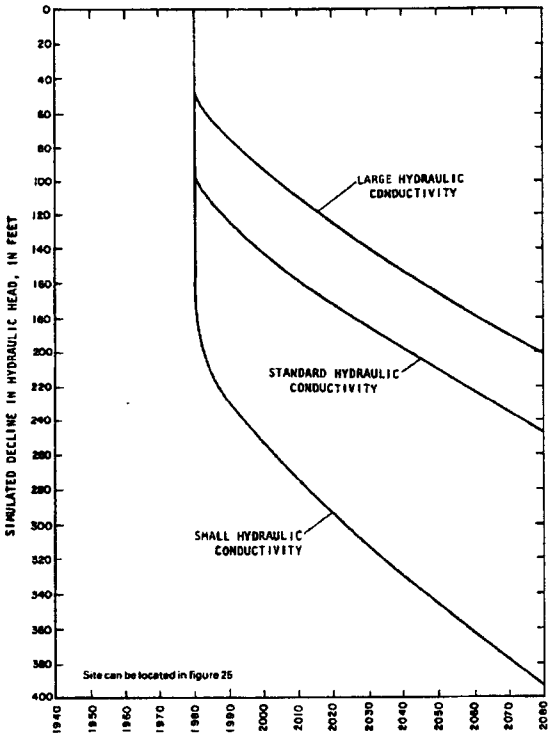

Figure 53. Effect of variations in hydraulic conductivity on decline in hydraulic head near Tesuque Pueblo (row 14, column 18, layer 6).

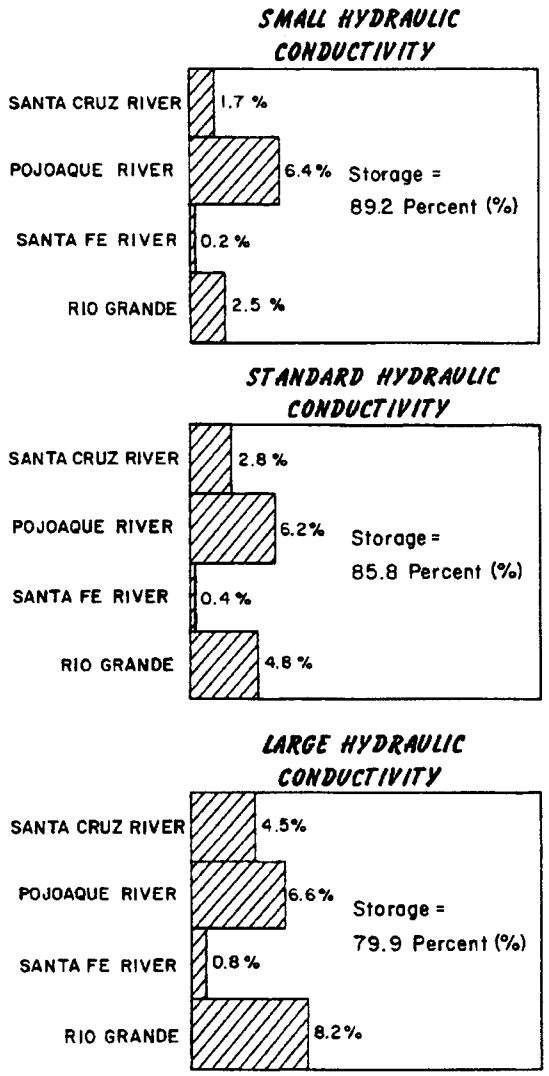

Figure 54. Effect of variations in hydraulic conductivity on the source of water withdrawn from wells.

Simulated Transient Response

The simulated transient response does differ due to the variation of anisotropy ratio. The difference can be seen both in the changes in hydraulic head and in the source of the water withdrawn from wells.

The sensitivity of the simulated change in hydraulic head in the production zone to the anisotropy ratio is shown at each of the eight locations shown in figure 25 (figs. 58-65). The variety of response can be rationalized into a consistent pattern by considering the four sites outside of the Pojoaque River basin. Near the well fields of Guaje Canyon (fig. 59), Pajarito Mesa (fig. 60), and Buckman (fig. 61), the smaller anisotropy ratio results in the greatest decline in hydraulic head. At each of these sites, the decline in hydraulic head due to withdrawals in the Pojoaque River basin is small relative to the decline in hydraulic head due to withdrawals at the site (figs. 27-29). Near Los Alamos Canyon well field, only about half the decline in hydraulic head after 1980 is due to withdrawals at the site. About half the decline in hydraulic head is due to withdrawals in the Pojoaque River basin (fig.26). Before 1980 (when the decline in hydraulic head was due mostly to withdrawals at the site), the smaller anisotropy ratio results in the larger decline in hydraulic head (fig. 58). After 1980 (when about half the decline in hydraulic head is due to withdrawals elsewhere), the smaller anisotropy ratio slows the flow of water toward the distant point of withdrawal and results in the smaller decline in hydraulic head near the Los Alamos Canyon well field (fig. 58).

The same phenomenon appears to be occurring at the sites within the Pojoaque River basin. At the sites near the pueblos of San Ildefonso (fig. 62) and Nambe (fig. 64) the smaller anisotropy ratio results in the larger decline in hydraulic head. These sites are both located near centers of maximum change in head (fig. 25). The more distal site near Tesuque Pueblo (fig. 25) responds similarly to the one near Los Alamos Canyon well field. That is, during the first fifty years of withdrawals, the smaller anisotropy ratio results in the larger decline in hydraulic head (fig. 65). Later (when a significant part of the decline in hydraulic head is due to withdrawals elsewhere), the smaller anisotropy ratio slows the flow of water toward the distant point of withdrawal and results in the smaller decline in hydraulic head near Tesuque Pueblo (fig. 65).

The site near Pojoaque Pueblo has a mixed response to the variation of the anisotropy ratio. The comparison between the standard simulation and the one assuming a large anisotropy ratio (fig. 63) is similar to that for the sites near San Ildefonso Pueblo (fig. 62) and Nambe Pueblo (fig. 64). The comparison between the standard simulation and the one assuming a small anisotropy ratio (fig. 63) is similar to that for the site near Tesuque Pueblo (fig. 65).

Because of the effect on the ability of the aquifer to transmit water toward the point of withdrawal, the source of water withdrawn from wells is sensitive to the anisotropy ratio. The rate of withdrawal from storage is about 86 percent in each instance (fig. 66). However, the streams from which flow is captured are sensitive to the anisotropy ratio. With a smaller anisotropy ratio, less flow is captured directly from the Rio Grande and more flow is captured from the Pojoaque River and other tributaries.

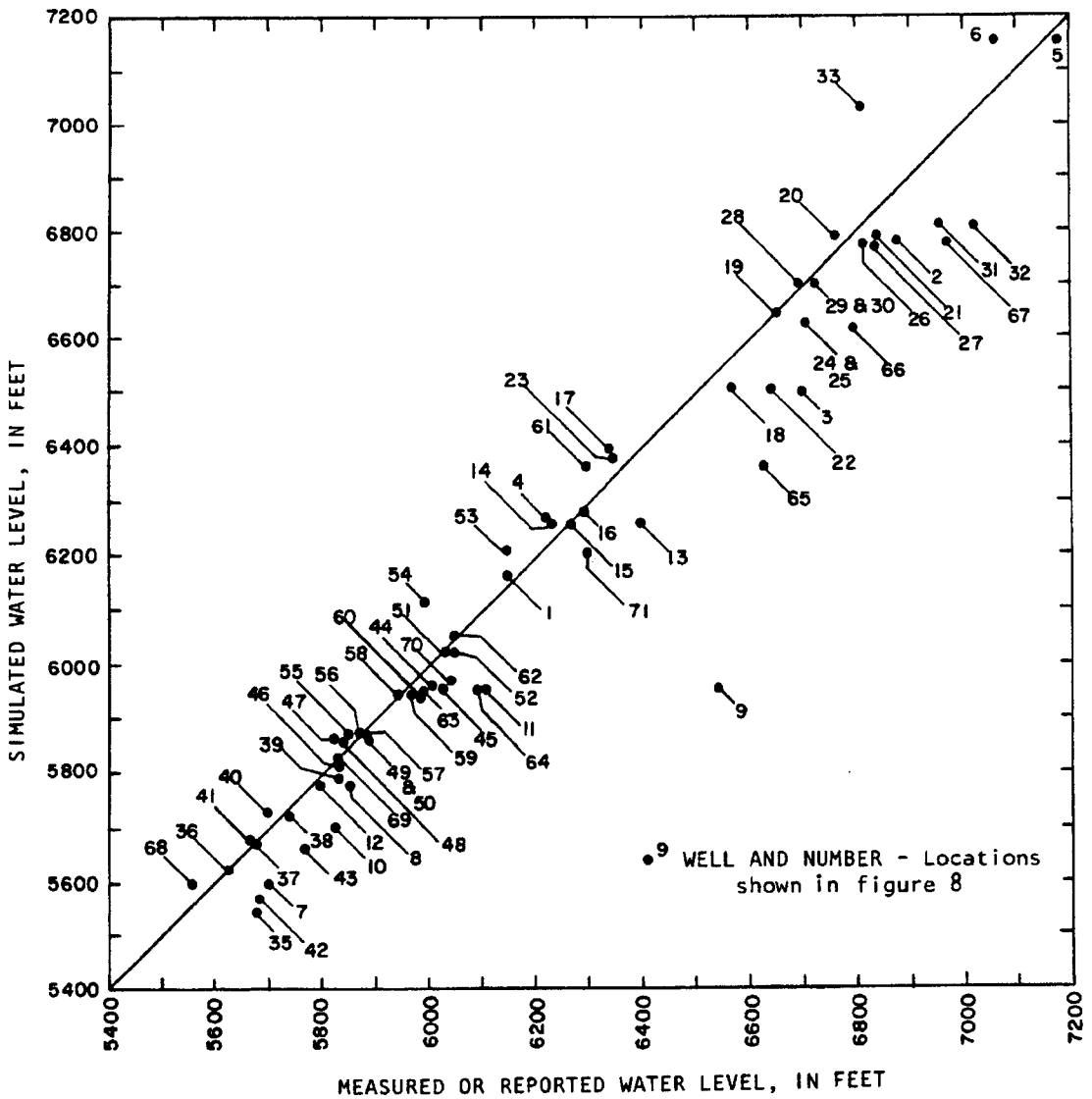

Figure 55. Comparison between measured or reported water levels for selected wells and springs and water levels simulated by assuming a smaller anisotropy ratio.

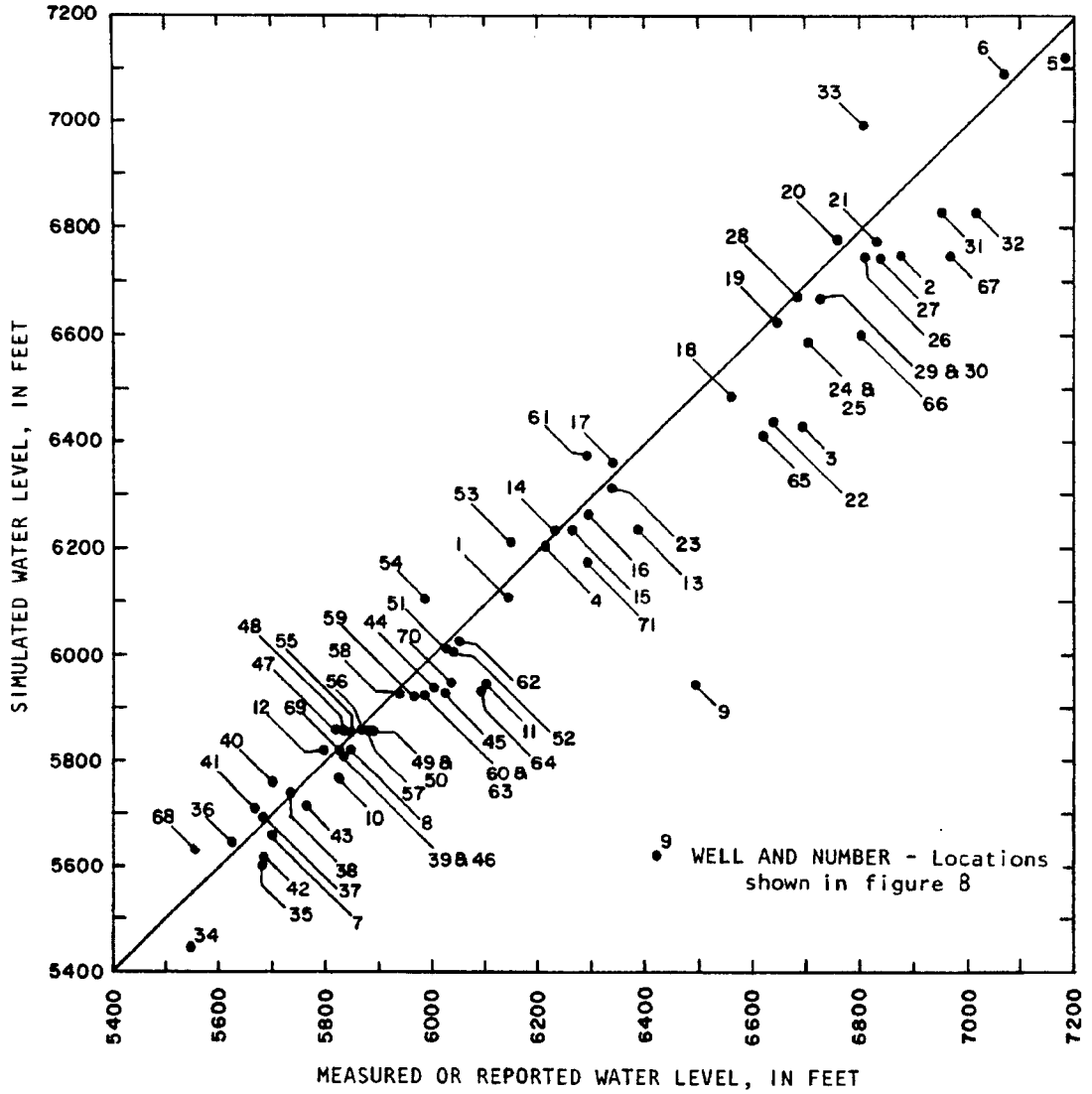

Figure 56. Comparison between measured or reported water levels for selected wells and springs and water levels simulated by assuming a larger anisotropy ratio.

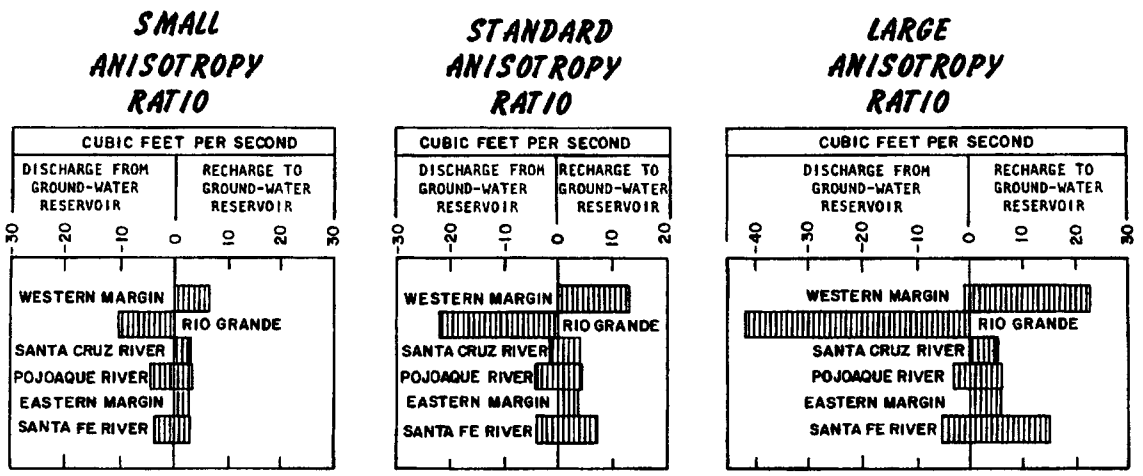

Figure 57. Effect of variations in anisotropy ratio on steady-state flow rates.

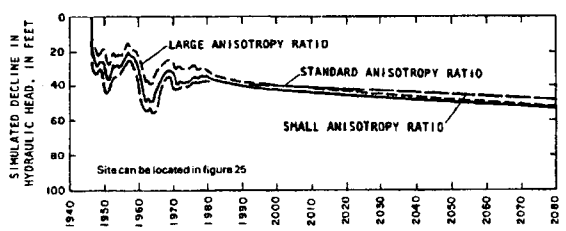

Figure 58. Effect of variations in anisotropy ratio on decline in hydraulic head near Los Alamos Canyon well field (row 13, column 5, layer 19).

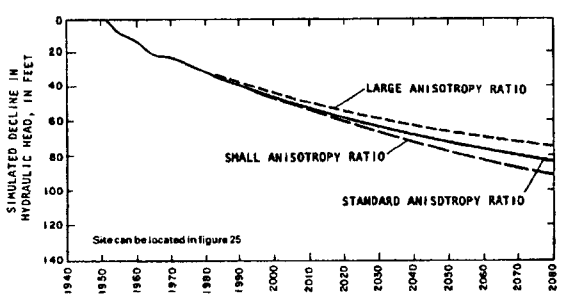

Figure 59. Effect of variations in anisotropy ratio on decline in hydraulic head near Guaje Canyon well field (row 13, column 3, layer 21).

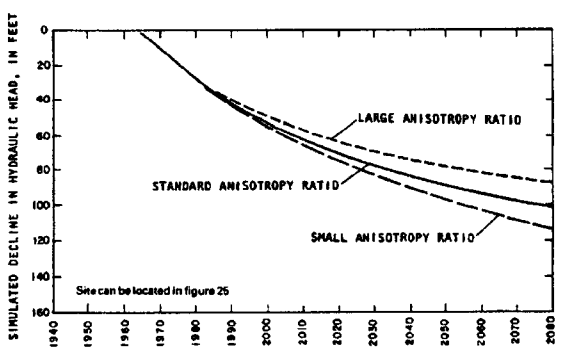

Figure 60. Effect of variations in anisotropy ratio on decline in hydraulic head near Pajarito Mesa well field (row 16, column 3, layer 21).

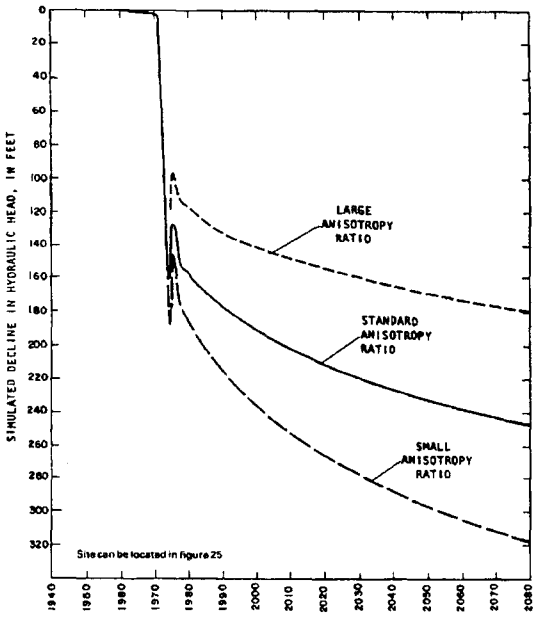

Figure 61. Effect of variations in anisotropy ratio on decline in hydraulic head near Buckman well field (row 17, column 7, layer 17).

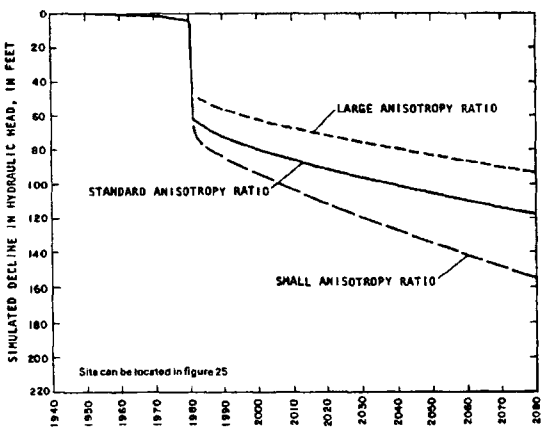

Figure 62. Effect of variations in anisotropy ratio on decline in hydraulic head near San Ildefonso Pueblo (row 11, column 7, layer 17).

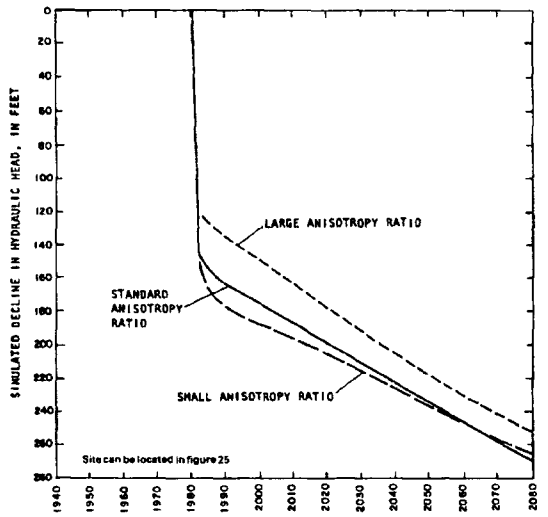

Figure 63. Effect of variations in anisotropy ratio on decline in hydraulic head near Pojoaque Pueblo (row 9, column 12, layer 12).

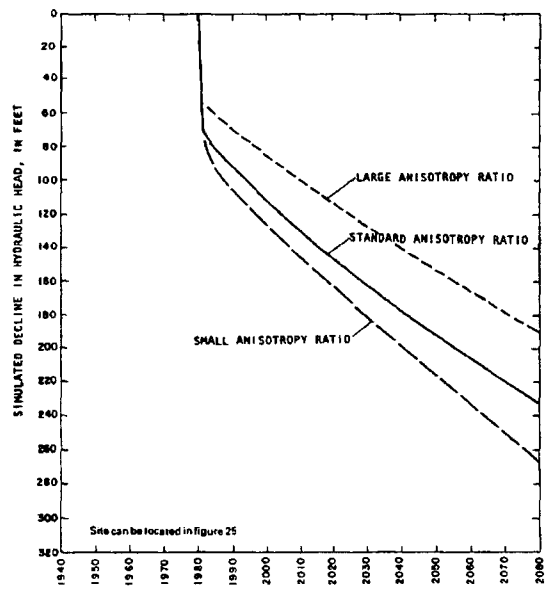

Figure 64. Effect of variations in anisotropy ratio on decline in hydraulic head near Nambe Pueblo (row 8, column 16, layer 8).

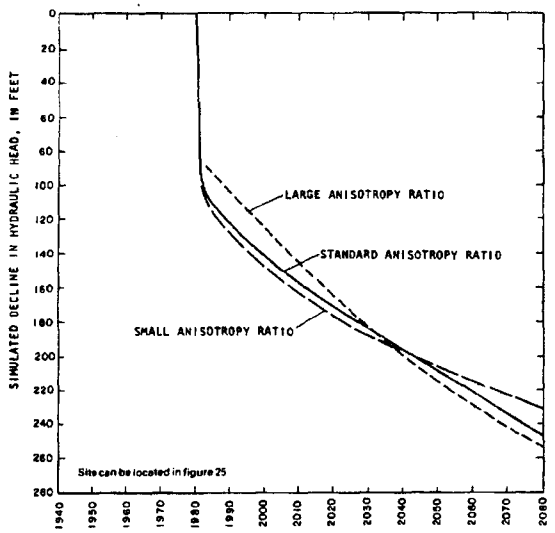

Figure 65. Effect of variations in anisotropy ratio on decline in hydraulic head near Tesuque Pueblo (row 14, column 18, layer 6).

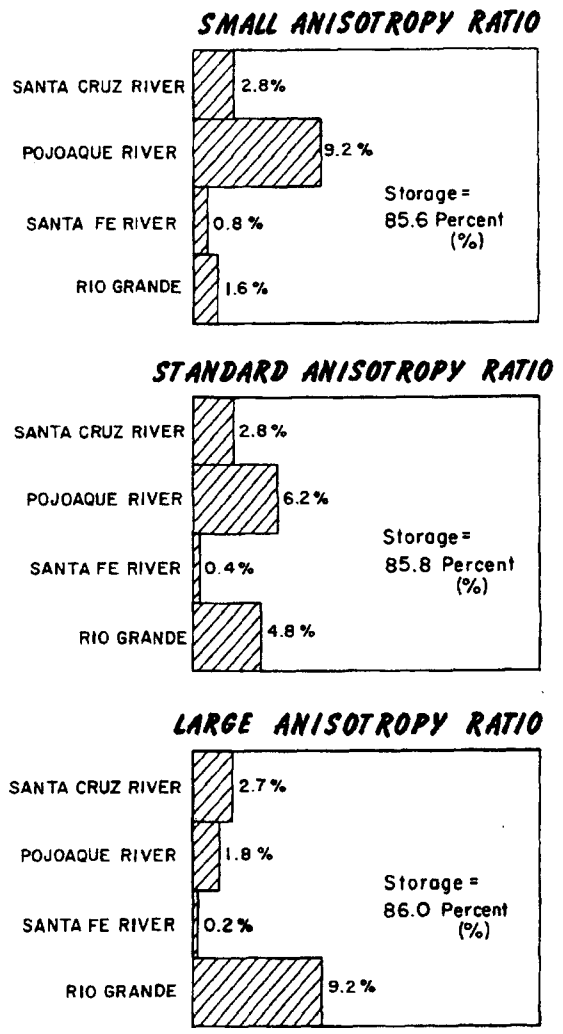

Figure 66. Effect of variations in anisotropy ratio on the source of water withdrawn from wells.

Specific Storage: Simulated Transient Response

The predicted response was obtained by assuming a specific storage of 2×10^{-6} per foot. The sensitivity of the model to this aquifer characteristic was tested with alternative simulations in which the specific storage was assumed to be 1×10^{-6} and 1×10^{-5} per foot, the lower and upper limits of the plausible range (table 1). The larger the specific storage, the more water is released from confined storage for each foot of decline in hydraulic head.

The simulated steady-state condition is independent of the variation of specific storage. The steady-state condition described in figures 10 and 11 is unchanged.

The simulated transient response does differ due to the variation of specific storage. The difference can be seen both in the declines in hydraulic head and in the source of the water withdrawn from wells. The sensitivity of the simulated declines in hydraulic head in the production zone to the specific storage is shown at five of the eight locations shown in figure 25 (figs. 67-71). The responses near the well fields of Los Alamos Canyon, Guaje Canyon, and Pajarito Mesa are insensitive to specific storage and are about the same as for the standard simulation (figs. 26-28). For the sites near Buckman well field (fig. 67), San Ildefonso Pueblo (fig. 68), Pojoaque Pueblo (fig. 69), Nambe Pueblo (fig. 70), and Tesuque Pueblo (fig. 71), the larger the specific storage, the smaller the decline in hydraulic head. Increasing specific storage by a factor of 10 (from 10^{-6} to 10^{-5} per foot) decreases the maximum 50-year drawdown at any cell in the model from 336 to 321 feet.

Although the specific storage determines the volume of water released from artesian storage, the source of water withdrawn from wells is relatively insensitive to variations in specific storage. Increasing specific storage by a factor of 10 (from 10^{-6} to 10^{-5} per foot) increases the rate of withdrawal from storage (fig. 72) from 85.5 to 88.0 percent.

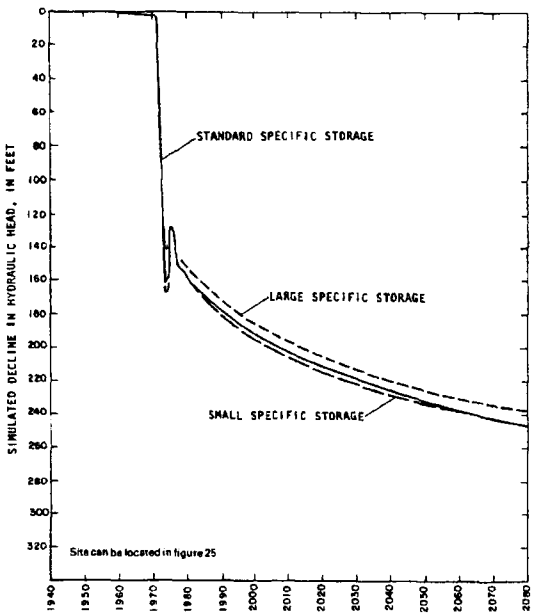

Figure 67. Effect of variations in specific storage on decline in hydraulic head near Buckman well field (row 17, column 7, layer 17).

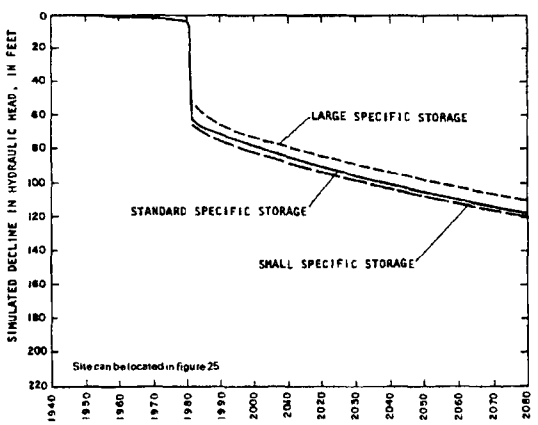

Figure 68. Effect of variations in specific storage on decline in hydraulic head near San Ildefonso Pueblo (row 11, column 7, layer 17).

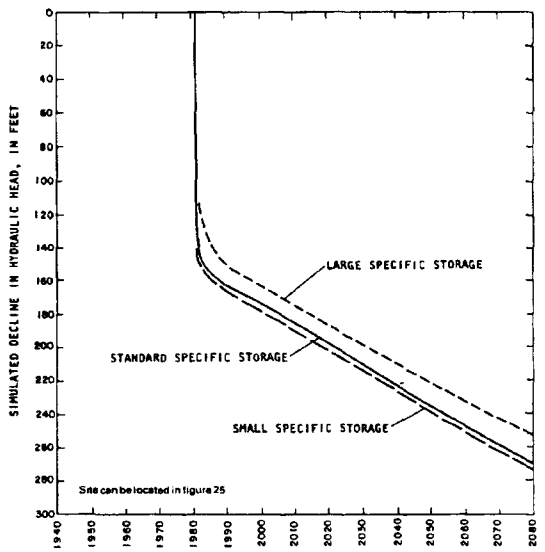

Figure 69. Effect of variations in specific storage on decline in hydraulic head near Pojoaque Pueblo (row 9, column 12, layer 12).

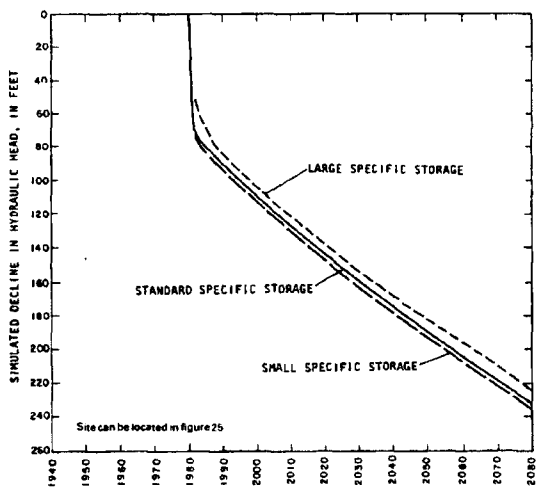

Figure 70. Effect of variations in specific storage on decline in hydraulic head near Nambe Pueblo (row 8, column 16, layer 8).

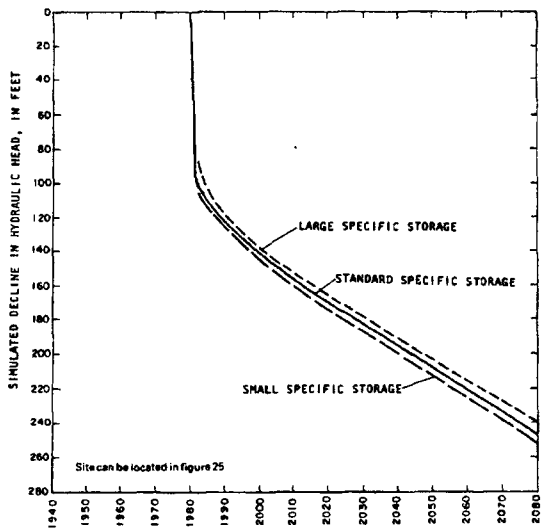

Figure 71. Effect of variations in specific storage on decline in hydraulic head near Tesuque Pueblo (row 14, column 18, layer 6).

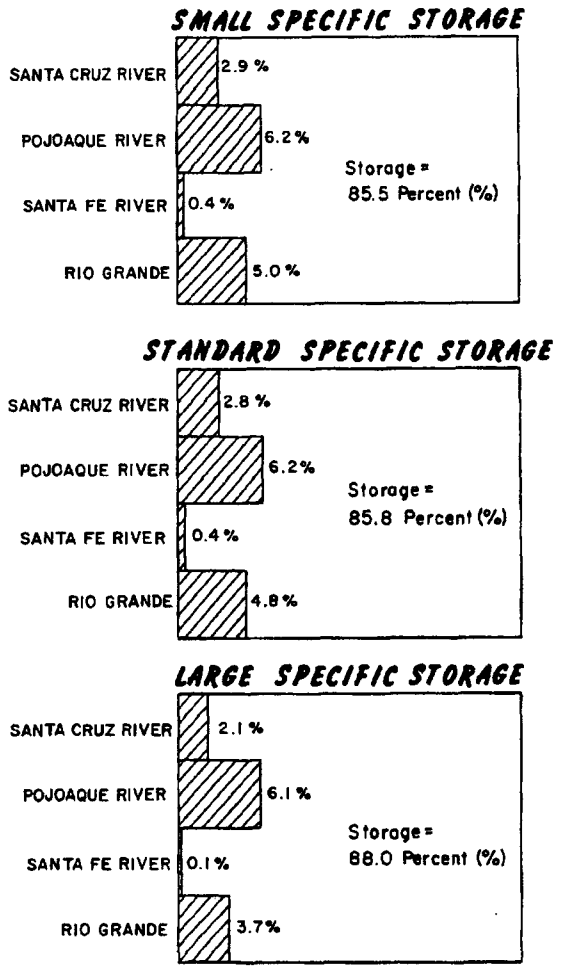

Figure 72. Effect of variations in specific storage on the source of water withdrawn from wells.

Specific Yield: Simulated Transient Response

The predicted response was obtained by assuming a specific yield of 0.15. The sensitivity of the model to this aquifer characteristic was tested with alternative simulations in which the specific yield was assumed to be 0.10 and 0.20, the lower and upper limits of the plausible range (table 1). The larger the specific yield, the more water is released from unconfined storage for each foot of decrease in hydraulic head.

The simulated steady-state condition is independent of the variations of specific yield. The steady- state condition described in figures 10 and 11 is unchanged.

The simulated transient response does differ due to variations in specific yield. The difference can be seen both in the declines in hydraulic head and in the source of water withdrawn from wells.

The sensitivity of the simulated decline in hydraulic head in the production zone to the specific yield is shown at each of the eight locations shown in figure 25 (figs. 73–80). At each site, the larger the specific yield, the smaller the decline in hydraulic head. Doubling specific yield (from 0.10 to 0.20) decreases the maximum 50-year drawdown at any cell in the model from 378 to 312 feet.

The source of water withdrawn from wells is more sensitive to variations in specific yield than to those in specific storage. Doubling specific yield (from 0.10 to 0.20) increases the rate of withdrawal from storage (fig. 81) from 82.8 to 87.5 percent.

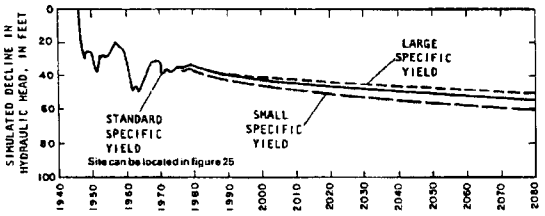

Figure 73. Effect of variations in specific yield on decline in hydraulic head near Los Alamos Canyon well field (row 13, column 5, layer 19).

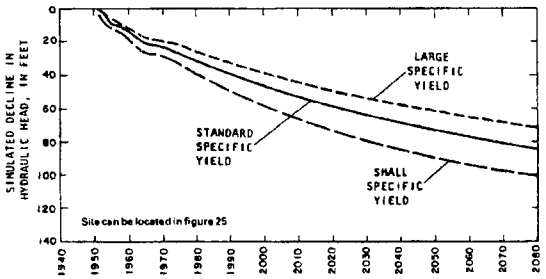

Figure 74. Effect of variations in specific yield on decline in hydraulic head near Guaje Canyon well field (row 13, column 3, layer 21).

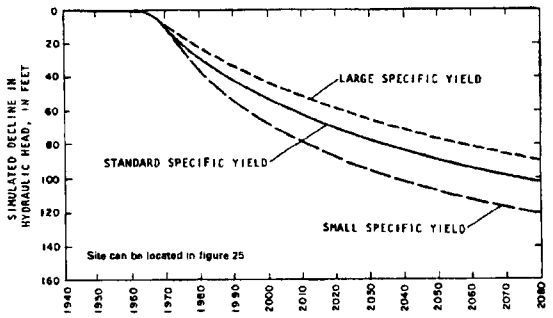

Figure 75. Effect of variations in specific yield on decline in hydraulic head near Pajarito Mesa well field (row 16, column 3, layer 21).

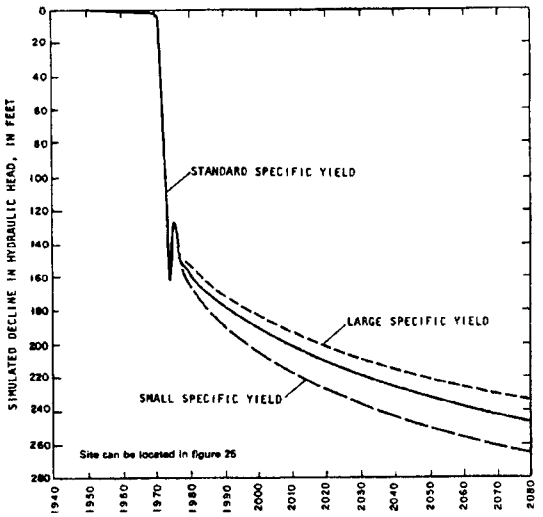

Figure 76. Effect of variations in specific yield on decline in hydraulic head near Buckman well field (row 17, column 7, layer 17).

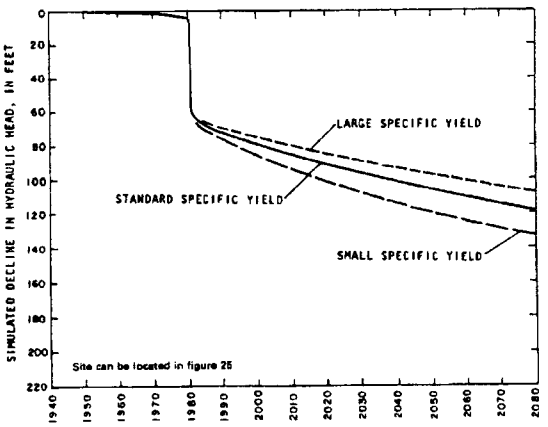

Figure 77. Effect of variations in specific yield on decline in hydraulic head near San Ildefonso Pueblo (row 11, column 7, layer 17).

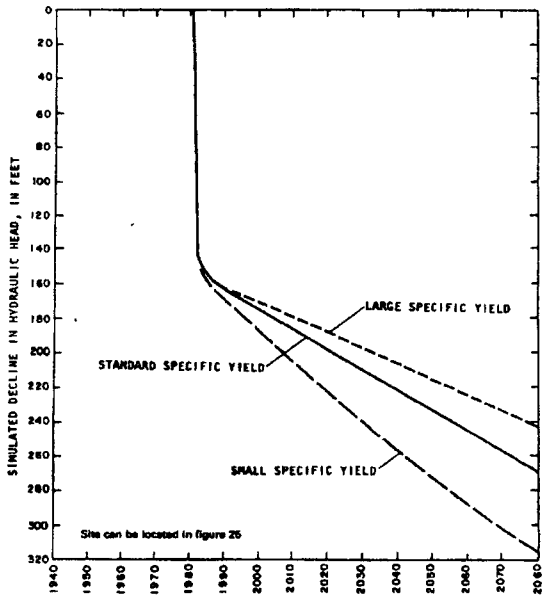

Figure 78. Effect of variations in specific yield on decline in hydraulic head near Pojoaque Pueblo (row 9, column 12, layer 12).

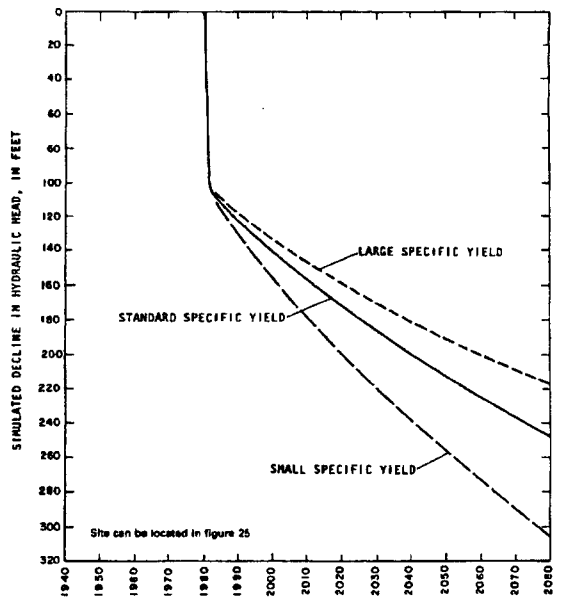

Figure 80. Effect of variations in specific yield on decline in hydraulic head near Tesuque Pueblo (row 14, column 18, layer 6).

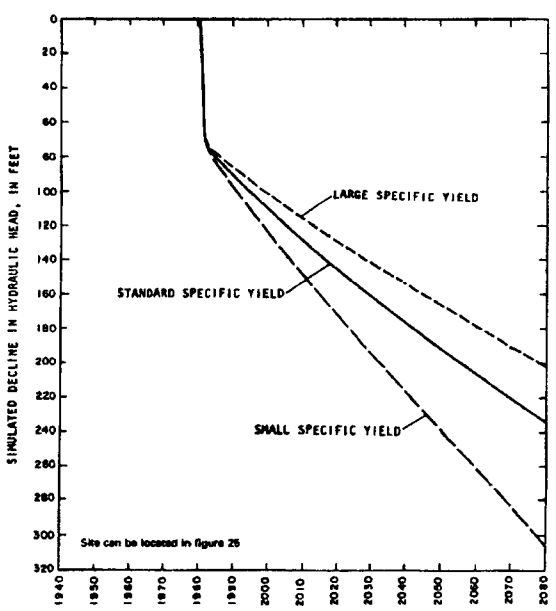

Figure 79. Effect of variations in specific yield on decline in hydraulic head near Nambe Pueblo (row 8, column 16, layer 8).

Uncertainty in Predicted Response

The preceding sensitivity tests are an aid in translating the uncertainty with which aquifer characteristics are known into uncertainty in the predicted response. The predicted response was obtained with the values of aquifer characteristics described (table 1) as the most likely average value. The uncertainty in these estimates is indicated by a range of values called the plausible range. The upper and lower limits of the plausible range were used for the sensitivity tests; therefore, the resultant uncertainty in predicted response is demonstrated by the declines in hydraulic head and the source of water withdrawn from wells, as simulated by the sensitivity tests.

Uncertainty in the predicted maximum decline in hydraulic head is shown in table 16. In the standard simulation, the maximum simulated decline in head after 50 years of withdrawals for irrigation development is 334 feet. The equivalent values from the sensitivity tests vary about 40 percent from this value due to variation of hydraulic conductivity; about 30 percent is due to the variation of saturated thickness of the Tesuque Formation, and about 20 percent or less is due to the variation of other aquifer characteristics.

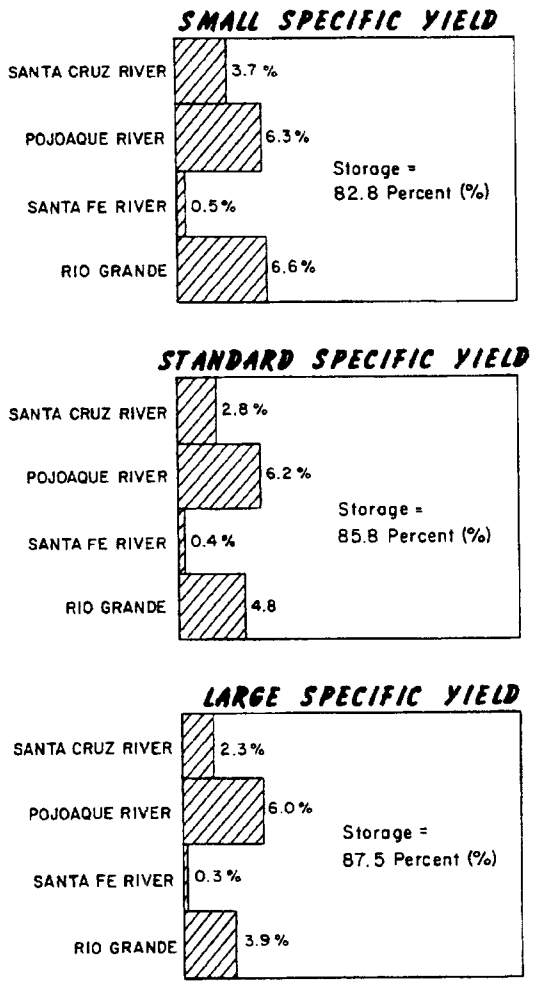

Figure 81. Effect of variations in specific yield on the source of water withdrawn from wells.

Table 16. Predicted maximum decline in hydraulic head (in feet) in 2030 after 50 years of withdrawals for irrigation development

Aquifer characteristic being varied	Lower limit of plausible range	Upper limit of plausible range
Saturated thickness of the Tesuque Formation	---	242
Hydraulic conductivity parallel to the beds	474	210
Anisotropy ratio	382	265
Specific storage	336	321
Specific yield	378	312

Simulated declines in hydraulic head are most sensitive to hydraulic conductivity. At the four sites in the Pojoaque River basin, increasing hydraulic conductivity by a factor of 4 (from 0.5 to 2.0 feet per day) decreases the declines in hydraulic head after 50 years of withdrawals by a factor of 2 or more: from 168 to 54 feet at the site near San Ildefonso Pueblo (fig. 50), from 350 to 125 feet at the site near Pojoaque Pueblo (fig. 51), from 246 to 112 feet at the site near Nambe Pueblo (fig. 52), and from 312 to 140 feet at the site near Tesuque Pueblo (fig. 53).

Uncertainty in the predicted source of water withdrawn from wells is shown in table 17. Storage within the aquifer system is the simulated source of about 80 to 90 percent of the water withdrawn from wells in 2030, after 50 years of withdrawals for irrigation development. For the standard simulation, storage accounts for 85.8 percent of the withdrawals. Variations in aquifer characteristics that make aquifer storage a more important source are greater thickness, smaller hydraulic conductivity, larger specific storage, larger specific yield, and larger anisotropy ratio. Variations in aquifer characteristics that make aquifer storage a less important source are large hydraulic conductivity, small specific yield, small specific storage, and small anisotropy ratio.

Streamflow capture is the source of the remaining 10 to 20 percent of the water withdrawn from wells in 2030 after 50 years of withdrawals. The capture from individual streams is quite variable. For example, the rate of capture from the Rio Grande ranges from 0.98 cubic foot per second (for small hydraulic conductivity) to 3.25 cubic feet per second (for large hydraulic conductivity). However, because all streams are tributary to the Rio Grande, all streamflow capture and diversion will deplete the flow of the Rio Grande downstream from the modeled area.

The predicted total streamflow capture is 5.63 cubic feet per second for the standard simulation. The sensitivity tests simulated values ranging from 3.99 cubic feet per second (for greater saturated thickness) to 7.97 cubic feet per second (for large hydraulic conductivity). Considering the diversion for irrigation of 13.14 cubic feet per second (table 13) from the tributaries of the Pojoaque River, the total predicted decrease in the flow of the Rio Grande downstream from the modeled area in 2030 after 50 years of withdrawals is 18.77 cubic feet per second (5.63 plus 13.14) for the standard simulation. Equivalent values from the sensitivity tests vary about 12 percent from this value, from 17.13 cubic feet per second (3.99 plus 13.14) to 21.11 cubic feet per second (7.97 plus 13.14).

SUMMARY

A three-dimensional model has been described that represents the Tesuque aquifer system underlying the Pojoaque

Table 17. Predicted source (in percent) of water withdrawn from wells in 2030 after 50 years of withdrawals for irrigation development.

Aquifer characteristic being varied	Limit of plausible range	Storage in Tesuque Formation	Capture from			
			Santa Cruz River	Pojoaque River	Santa Fe River	Rio Grande
Standard simulation		85.8	2.8	6.2	0.4	4.8
Saturated thickness of the Tesuque Formation	Upper	90.0	3.9	0.9	0.4	4.8
Hydraulic conductivity parallel to the beds	Upper	79.9	4.5	6.6	0.8	8.2
	Lower	89.2	1.7	6.4	0.2	2.5
Anisotropy ratio	Upper	86.0	2.7	1.8	0.2	9.2
	Lower	85.6	2.8	9.2	0.8	1.6
Specific storage	Upper	88.0	2.1	6.1	0.1	3.7
	Lower	85.5	2.9	6.2	0.4	5.0
Specific yield	Upper	87.5	2.3	6.0	0.3	3.9
	Lower	82.8	3.7	6.3	0.5	6.6

River basin and vicinity. The total simulation time is divided into three stages: steady-state, historical, and projected. Although the term calibration" is avoided because of the connotation of control over the accuracy with which aquifer characteristics are estimated, the structure and boundaries were revised until the simulated steady-state condition satisfactorily reproduced historical data. This condition was achieved with a structure in which the beds in the Pojoaque River basin dip 8° to the northwest with a strike of N. 25° E. Saturated thickness of the Tesuque aquifer system is represented as about 4,000 feet along the Rio Grande. The Rio Grande, the Santa Cruz River, and the downstream reach of the Santa Fe River are simulated as specified-hydraulic-head boundaries. The upstream reach of the Santa Fe River and recharge areas along the east and west margins of the basin are simulated as specified-flow boundaries. The Pojoaque River and its tributaries are simulated as hydraulic-head-dependent boundaries. It was not necessary to revise the initial estimates of aquifer characteristics to approximate the steady-state condition within the limits of the accuracy of available data. The hydraulic conductivity parallel to the beds is estimated to be 1.0 foot per day. The vertical-to-horizontal anisotropy ratio is estimated to be 0.003. The specific storage is estimated to be 2×10^{-6} per foot. The specific yield is estimated to be 0.15.

The simulated historical phase produced no response which forced rejection of the model based on historical data.

The projection phase simulates the withdrawal of 28.41 cubic feet per second for irrigation development in addition to 11.24 cubic feet per second of continued historical withdrawals. Storage in the Tesuque aquifer system is the primary source for the simulated withdrawals. In 2030, after 50 years of irrigation development, storage is the source for 86 percent of the total withdrawals. As withdrawals continue, the percentage of water obtained from streamflow capture will gradually increase.

The Pojoaque River is the surface-water system that is most affected by the development. The model simulates the decrease in flow of the Pojoaque River by diversion for irrigation and loss to the ground water reservoir. Simulated Pojoaque River discharge to the Rio Grande is negligible even in the first year of irrigation development.

Because all streams are tributary to the Rio Grande, all streamflow capture and diversion will deplete the flow of the Rio Grande. The total predicted decrease in the flow of the Rio Grande downstream from the modeled area in 2030 after 50 years of withdrawal is 18.77 cubic feet per second (5.63 capture plus 13.14 diverted) with irrigation development and 10.13 cubic feet per second (2.46 capture plus 7.67 diverted) without irrigation development.

The sensitivity of the model was tested by varying selected aquifer characteristics to the limits of the plausible range. In sensitivity tests the maximum simulated decline in hydraulic head after 50 years of withdrawals varies within about 40 percent of the 334 feet obtained in the standard simulation. Simulated declines in hydraulic head are most sensitive to hydraulic conductivity. If the range defined by sensitivity tests of hydraulic conductivity is not considered, the maximum simulated decline in hydraulic head after 50 years of withdrawals varies within about 30 percent of the 334 feet obtained in the standard simulation. The total simulated decrease in the flow of the Rio Grande downstream from the modeled area after 50 years of withdrawals for irrigation development varies within about 12 percent of the 18.77 cubic feet per second obtained in the standard simulation.

SELECTED REFERENCES

Borton, R. L., 1968, General geology and hydrology of north-central Santa Fe County, New Mexico: New Mexico State Engineer Open-File Report, 21 p.

Bryan, Kirk, 1928, Water supply for irrigation by artesian wells at Tesuque Pueblo, New Mexico: U.S. Geological Survey Open-File Report, 19 p.

Cabot, E. C., 1938, Fault border of the Sangre deCristo Mountains north of Santa Fe, New Mexico: Journal of Geology, v.46, no.1, p. 88-105.

Cushman, R. L., 1965, An evaluation of aquifer and well characteristics of municipal well fields in Los Alamos and Guaje Canyons, near Los Alamos, New Mexico: U.S. Geological Survey Water-Supply Paper 1809-D, 50 p.

Dane, C. H., and Bachman, G. O., 1965, Geologic map of New Mexico: U.S. Geological Survey geologic map, 2 sheets.

Denny, C. S., 1940, Santa Fe Formation in the Espanola Valley, New Mexico: Geological Society of America Bulletin, v.51, no. 5, p. 677-694.

Dinwiddie, G. A., 1964, Availability of ground water for irrigation on the Pojoaque Pueblo Grant, Santa Fe County, New Mexico: U.S. Geological Survey Open-File Report, 14 p.

Emery, M. M., 1974, Colonias de Santa Fe Subdivision well pumping test: Albuquerque, N. M., Bohannon, Westman, Huston, and Associates, Inc., 10 p., 6 app.

Galusha, Ted, and Blick, J. C., 1971, Stratigraphy of the Santa Fe Group, New Mexico: American Museum of Natural History Bulletin, v.144, 127 p.

Griggs, R. L., 1964, Geology and ground-water resources of the Los Alamos area, New Mexico: U.S. Geological Survey Water-Supply Paper1753, 107 p.

Hearne, G. A., 1980, Simulation of an aquifer test on the Tesuque Pueblo Grant, New Mexico: U.S. Geological Survey Open-File Report 80-1022, 44 p.

Johnson, A. I., 1967, Specific yield—compilation of specific yields for various materials: U.S. Geological Survey Water-Supply Paper 1662-D, 74 p.

Kelley, V. C., 1952, Tectonics of the Rio Grande depression of central New Mexico, *in* Guidebook of the Rio Grande Country: New Mexico Geological Society, p. 93-105.

———1978, Geology of Espanola Basin, New Mexico: New Mexico Bureau of Mines and Mineral Resources, Geologic Map 48.

Koopman, F. C., 1975, Estimated ground-water flow, volume of water in storage, and potential yield of wells in the Pojoaque River drainage basin, Santa Fe County, New Mexico: U.S. Geological Survey Open-File Report 74-159, 33 p.

Lohman, S. W., 1972, Ground-water hydraulics: U.S. Geological Survey Professional Paper 708, 70 p.

Manley, Kim, 1978, Structure and stratigraphy of the Espanola Basin, Rio Grande Rift, New Mexico: U.S. Geological Survey Open-File Report 78-667, 24 p.

Miller, J. P., Montgomery, Arthur, and Sutherland, P. K., 1963, Geology of part of the southern Sangre deCristo Mountains, New Mexico: New Mexico Bureau of Mines and Mineral Resources Memoir 11, 106 p.

National Resources Committee, 1938, Regional Planning Part VI.—The Rio Grande Joint Investigation in the Upper Rio Grande Basin in Colorado, New Mexico, and Texas 1936-1937: Washington, D.C., Government Printing Office, 566 p.

New Mexico State Engineer Office, 1966, Upper Rio Grande Hydrographic Survey Report; Nambe-Pojoaque-Tesuque Section, 786 p.

——— 1978, Water Rights, Nambe-Pojoaque-Tesuque adjudication suit: U.S. District Court Cause No. 6639, 69 p.

Pinder, G. F., and Bredehoeft, J. D., 1968, Application of the digital computer for aquifer evaluation: Water Resources Research, v.4, no. 5, p. 1069-93.

Posson, D. R., Hearne, G. A., Tracy, J. V., and Frenzel, P. F., 1980, Computer program for simulating geohydrologic systems in three dimensions: U.S. Geological Survey Open-File Report 80-421, 795 p.

Purtymun, W. D., 1978, Water supply at Los Alamos during 1977: Los Alamos Scientific Laboratory LA-7436-MS informal report, 38 p.

Purtymun, W. D., and Hercey, J. E., 1972, Summary of Los Alamos municipal well-field characteristics, 1947-1971: Los Alamos Scientific Laboratory LA-5040-MS, 69 p.

Purtymun, W. D., and Johansen, Steven, 1974, General geohydrology of the Pajarito Plateau, *in* Guidebook to Ghost Ranch (central-northern New Mexico): New Mexico Geological Society, 25th Field Conference, p. 347-349.

Rapp, J. R., 1960, Availability of ground water for irrigation on the San Ildefonso Pueblo Grant, Santa Fe County, New Mexico: U.S. Geological Survey Open-File Report, 21 p.

Reiland, L. J., 1975, Estimated mean-monthly and annual runoff at selected sites in the Pojoaque River drainage basin, Santa Fe County, New Mexico: U.S. Geological Survey Open-File Report 74-150, 21 p.

Reiland, L. J., and Koopman, F. C., 1975, Estimated availability of surface and ground water in the Pojoaque River drainage basin, Santa Fe County, New Mexico: U.S. Geological Survey Open-File Report 74-151, 35 p.

Spiegel, Zane, and Baldwin, Brewster, *with contributions by* F. E. Kottlowski and E. L. Barrows, *and a section on* Geophysics by H. A. Winkler, 1963, Geology and water resources of the Santa Fe area, New Mexico: U.S. Geological Survey Water-Supply Paper 1525, 258 p.

Theis, C. V., 1938, The significance and nature of the cone of depression in ground-water bodies: Economic Geology, v.33, no. 8, p. 889-902.

———1940, The source of water derived from wells: Civil Engineering, v.10, no. 5, p. 277-280.

Theis, C. V., and Conover, C. S., 1962, Pumping tests in the Los Alamos Canyon Well Field near Los Alamos, New Mexico: U.S. Geological Survey Water-Supply Paper 1619-I, 24 p.

Trauger, F. D., 1967, Hydrology and general geology of the Pojoaque area, Santa Fe County, New Mexico: U.S. Geological Survey Open-File Report, 32 p.

Trescott, P. C., 1975, Documentation of finite-difference model for simulation of three-dimensional ground-water flow: U.S. Geological Survey Open-File Report 75-438, 103 p.

Trescott, P. C., and Larson, S. P., 1976, Supplement to Open-File Report 75-438, Documentation of finite-difference model for simulation of three-dimensional ground-water flow: U.S. Geological Survey Open-File Report 76-591, 21 p.

U.S. Bureau of Reclamation, 1965, Interim report on Pojoaque unit San Juan-Chama Project: Amarillo, Texas, Bureau of Reclamation Region 5, 100 p.

U.S. Geological Survey, 1960, Compilation of records of surface waters of the United States through September 1950, part 8, Western Gulf of Mexico basins: U.S. Geological Survey Water-Supply Paper 1312, 633 p.

——— 1961, Surface water records of New Mexico, U.S. Geological Survey Water-Data Report, 211 p.

——— 1962, Surface water records of New Mexico, U.S. Geological Survey Water-Data Report, 206 p.

——— 1963, Surface water records of New Mexico, U.S. Geological Survey Water-Data Report, 228 p.

——— 1964, Surface water records of New Mexico, U.S. Geological Survey Water-Data Report, 238 p.

——— 1965, Water resources data for New Mexico, part1, Surface water records: U.S. Geological Survey Water-Data Report NM-65-1, 248 p.

——— 1966, Water resources data for New Mexico, part1, Surface water records: U.S. Geological Survey Water-Data Report NM-66-1, 262 p.

——— 1967, Water resources data for New Mexico, part 1, Surface water records: U.S. Geological Survey Water-Data Report NM-67-1, 249 p.

——— 1968, Water resources data for New Mexico, part 1, Surface water records: U.S. Geological Survey Water-Data Report NM-68-1, 271 p.

——— 1969, Water resources data for New Mexico, part 1, Surface water records: U.S. Geological Survey Water-Data Report NM-69-1, 242 p.

——— 1970, Water resources data for New Mexico, part 1, Surface water records: U.S. Geological Survey Water-Data Report NM-70-1, 254 p.

——— 1971, Water resources data for New Mexico, part 1, Surface water records: U.S. Geological Survey Water-Data Report NM-71-1, 460 p.

——— 1972, Water resources data for New Mexico, part 1, Surface water records: U.S. Geological Survey Water-Data Report NM-72-1, 248 p.

——— 1973, Water resources data for New Mexico, part 1, Surface water records: U.S. Geological Survey Water-Data Report NM-73-1, 248 p.

——— 1974, Water resources data for New Mexico, part 1, Surface water records: U.S. Geological Survey Water-Data Report NM-74-1, 238 p.

——— 1975, Water resources data for New Mexico, water year 1975: U.S. Geological Survey Water-Data Report NM-75-1, 617 p.

——— 1976, Water resources data for New Mexico, water year 1976: U.S. Geological Survey Water-Data Report NM-76-1, 666 p.

——— 1977, Water resources data for New Mexico, water year 1977: U.S. Geological Survey Water-Data Report NM-77-1, 638 p.

METRIC CONVERSION FACTORS

In this report figures for measurements are given in inch-pound units only. The following table contains factors for converting to metric units.

Multiply inch-pound units	*By*	*To obtain metric units*
foot	0.3048	meter
foot per day	0.3048	meter per day
foot per year	0.3048	meter per year
square foot	0.0929	square meter
foot squared per day	0.0929	meter squared per day
cubic foot	0.02831	cubic meter
cubic foot per second	0.02831	cubic meter per second
foot per mile	0.1894	meter per kilometer
gallon	3.785	liter
gallon per minute	0.06309	liter per second
gallon per minute per foot	0.2070	liter per second per meter
inch	25.40	millimeter
mile	1.609	kilometer
acre	0.4047	hectare
acre-foot	0.001233	cubic hectometer
acre-foot per year	0.001233	cubic hectometer per year
acre-foot per acre	0.003048	cubic hectometer per hectare

* U.S. GOVERNMENT PRINTING OFFICE: 1985-461-431:20026